University of Potsdam
Faculty of Human Sciences
Center of Excellence "Cognition Sciences"
DEPARTMENT OF SPORT AND HEALTH SCIENCES
Professorship of Sports Medicine and Sports Orthopaedics
International Master/PhD-Program "Clinical Exercise Science" (CES)

Neuromuscular adaptations of either endurance or high-intensity interval training: are there any differential adaptations in the motor unit population?

An academic thesis submitted to
The Faculty of Human Sciences of the University of Potsdam
For the degree
Doctor of Philosophy (PhD)

By

Eduardo Andrés Martínez Valdés

Born in Santiago, Chile

Potsdam, September 2016

Published online at the
Institutional Repository of the University of Potsdam:
URN urn:nbn:de:kobv:517-opus4-396383
http://nbn-resolving.de/urn:nbn:de:kobv:517-opus4-396383

Affidavits according to doctoral degree regulations (§ 4 (2), sentences No. 4 and 7) of the Faculty of Human Sciences, University of Potsdam:

Hereby, I declare that this thesis, entitled "Neuromuscular adaptations of either endurance or high-intensity interval training: are there any differential adaptations in the motor unit population?" or parts of the thesis, submitted to the Faculty of Human Sciences (Research Focus Cognition Sciences, Department of Sports and Health Sciences) of the University of Potsdam, have not yet been submitted for a doctoral degree to this or any other institution neither in identical nor in similar form. The work presented in this thesis is the original work of the author, created under guidance and mentoring of the responsible supervisors. I did not receive any help or support from commercial consultants. All parts or single sentences, which have been taken analogously or literally from other sources, are identified as citations. Additionally, significant contributions from co-authors to the articles of this cumulative dissertation are acknowledged in the author's contribution section. I am aware of the publicly accessible promotion regulation of the Faculty of Human Sciences of the University of Potsdam. In particular, I have noted the importance of § 18 and § 19. I am aware of the consequences with regard to false affidavits.

_____ _____

Place, date Eduardo Andrés Martínez Valdés

Table of content

Contents

Acknowledgements

Firstly, I would like to express my sincere gratitude to my supervisor Prof. Frank Mayer for giving me the freedom to design my own project and for his continuing support of my PhD study. His guidance helped me in all the time of research and writing of this thesis. I also very much appreciated his valuable advice during many discussions which helped me to strengthen this thesis.

I would like to thank my co-supervisors Prof. Dario Farina and Prof. Deborah Falla, for welcoming me in their department and for allowing me to borrow valuable equipment that was vital for this project. The accomplishment of this work would have been barely possible without their innumerous, valuable and inspiring discussions throughout these years. Their contributions in experimental design and implementation as well as for their constructive support in the elaboration of the manuscripts, greatly improved the quality of this project.

I would like to thank the reviewers of this thesis, in special Prof. Roger Enoka, who generously shared his knowledge throughout the years.

I also express my gratitude to my fellow colleagues of the CES program for taking the time to help me with my PhD project. In particular I would like to thank Anne Schomöller, Stephanie White and Antje Reschke for their help in this thesis, and Konrad Rossbach for nominating me for the DAAD prize.

My sincere thanks also go to my dear colleagues at the Institute of Neurorehabilitation Systems that made my stays in Göttingen a very nice experience. In particular, I would like to thank Dr. Christopher Laine and Dr. Francesco Negro for their friendship, hospitality, for always sharing their knowledge and expertise and for helping me with all the technical issues concerning the project (even at times when both were very busy).

I would also like to thank the staff of the Outpatient Clinic, especially to Daniela Schubert, Jessica Messerschmidt and Anika Schönefeld for helping me with the project logistics.

I thank the University of Potsdam for awarding me with the PhD grant that enabled my research and, the Potsdam graduate school and the FNK for providing funding for conferences, which proved to be very important for my development.

Last but not the least, I would like to thank my family, my parents Raul and Virginia, my sisters Ximena and Gabriela and my nephews Elisa, Ignacio and Magdalena. Without their support I would never be able to finish this thesis. I am incredibly grateful for their constant encouragement. Above all, I thank to my wife Pámela for her love and unconditional support throughout the period that we were 12000 km apart from each other. My love, thank you very much for joining me in this project.

This thesis is dedicated to the memory of my nephew, Nicolas Schultze. You gave me the courage, strength and perseverance to finish this project.

Abstract

During the last decade, high intensity interval training (HIIT) has been used as an alternative to endurance (END) exercise, since it requires less time to produce similar physiological adaptations. Previous literature has focused on HIIT changes in aerobic metabolism and cardiorespiratory fitness, however, there are currently no studies focusing on its neuromuscular adaptations.

Therefore, this thesis aimed to compare the neuromuscular adaptations of both HIIT and END after a two-week training intervention, by using a novel technology called high-density surface electromyography (HDEMG) motor unit decomposition. This project consisted in two experiments, where healthy young men were recruited (aged between 18 to 35 years). In experiment one, the reliability of HDEMG motor unit variables (mean discharge rate, peak-to-peak amplitude, conduction velocity and discharge rate variability) was tested (Study 1), a new method to track the same motor units longitudinally was proposed (Study 2), and the level of low (<5Hz) and high (>5Hz) frequency motor unit coherence between vastus medialis (VM) and lateralis (VL) knee extensor muscles was measured (Study 4). In experiment two, a two-week HIIT and END intervention was conducted where cardiorespiratory fitness parameters (e.g. peak oxygen uptake) and motor unit variables from the VM and VL muscles were assessed pre and post intervention (Study 3).

The results showed that HDEMG is reliable to monitor changes in motor unit activity and also allows the tracking of the same motor units across different testing sessions. As expected, both HIIT and END improved cardiorespiratory fitness parameters similarly. However, the neuromuscular adaptations of both types of training differed after the intervention, with HIIT showing a significant increase in knee extensor muscle strength that was accompanied by increased VM and VL motor unit discharge rates and HDEMG amplitude at the highest force levels [(50 and 70% of the maximum voluntary contraction force (MVC)], while END training induced a marked increase in time to task failure at lower force levels (30% MVC), without any influence on HDEMG amplitude and discharge rates. Additionally, the results showed that VM and VL muscles share most of their synaptic input since they present a large amount of low and high frequency motor unit

coherence, which can explain the findings of the training intervention where both muscles showed similar changes in HDEMG amplitude and discharge rates.

Taken together, the findings of the current thesis show that despite similar improvements in cardiopulmonary fitness, HIIT and END induced opposite adjustments in motor unit behavior. These results suggest that HIIT and END show specific neuromuscular adaptations, possibly related to their differences in exercise load intensity and training volume.

Zusammenfassung

Als Alternative zu Ausdauertraining (END) wurde während des letzten Jahrzehnts hochintensives Intervalltraining (HIIT) eingesetzt, da es weniger Zeit in Anspruch nimmt um ähnliche physiologische Anpassungen herbeizuführen. Die Literatur hat sich bislang auf Veränderungen des aeroben Stoffwechsels und der kardiorespiratorischen Fitness durch HIIT konzentriert, es fehlt jedoch an Studien, die sich mit der neuromuskulären Anpassung auseinandersetzen. Deswegen war das Ziel dieser Thesis die neuromuskulären Anpassungserscheinungen durch HIIT und END nach einer 2-wöchigen Trainingsintervention zu vergleichen.

Dafür wurde eine neuartige Technik, die sogenannte High-Density Oberflächen Elektromyographie Motoreinheiten Zersetzung (HDEMG) genutzt. Dieses Projekt bestand aus zwei Experimenten, für die junge gesunde Männer zwischen 18 und 35 Jahren rekrutiert wurden. Im Rahmen des ersten Experiments wurde die Reliabilität der HDEMG Variablen (Entladungsrate, Amplitude, Weiterleitungsgeschwindigkeit und die Variabilität der Entladungsrate) untersucht (Studie 1), eine neue Methode zur longitudinalen Verfolgung der Motoreinheiten entwickelt (Studie 2) und die Kohärenz niedriger- (<5Hz) und hoher Frequenzen (>5Hz) der Knieextensoren vastus medialis (VM) und vastus lateralis (VL) gemessen (Studie 4). Das zweite Experiment beinhaltete eine zweiwöchige HIIT und END Intervention, bei der Parameter der kardiorespiratorischen Fitness (beispielsweise die maximale Sauerstoffaufnahme) und Parameter der Motoreinheiten des VM und VL vor- und nach der Intervention erfasst wurden (Studie 3).

Die Ergebnisse bestätigen, dass HDEMG eine zuverlässige Methode zur Erkennung von Veränderungen der Motoreinheit-Aktivitäten ist, sowie zur Verfolgung der selben Motoreinheiten in verschiedenen Messungen. Wie erwartet haben HIIT und END die kardiorespiratorische Fitness gleichermaßen verbessert. Trotzdem unterscheiden sich die neuromuskulären Anpassungserscheinungen beider Trainingsinterventionen insofern, als dass durch HIIT ein signifikanter Kraftzuwachs der Knieextensoren hervorgerufen wurde, der durch eine erhöhte Entladungsrate der VM und VL Motoreinheiten und eine erhöhte HDEMG Amplitude bei größter Kraft [50 und 70% der Maximalkraft (MVC)] begleitet wurde. END hingegen bewirkte einen deutlichen Anstieg der „time to task failure“ bei

niedrigeren Kraftintensitäten (30% MVC), ohne dabei die HDEMG Amplitude oder Entladungsrate zu beeinflussen. Außerdem konnten die Ergebnisse belegen, dass VM und VL einen Großteil des synaptischen Inputs teilen, da beide Muskeln eine hohe Kohärenz bei niedrigen- (<5Hz) und höheren Frequenzen (>5Hz) zeigen. Dies könnte eine mögliche Erklärung für die Ergebnisse der Trainingsintervention sein, bei der beide Muskeln ähnliche Veränderungen in der HDEMG Amplitude und der Entladungsrate vorwiesen.

Zusammenfassend zeigen die Ergebnisse dieser Thesis, dass HIIT und END trotz ähnlicher Verbesserungen der kardiorespiratorischen Fitness unterschiedliche Anpassungen des Verhaltens der Motoreinheiten hervorrufen. Die Ergebnisse unterstreichen, dass HIIT und END spezifische Adaptionen auslösen, die möglicherweise auf den Unterschieden von Trainingsintensität und - volumen basieren.

1. Introduction

Physical inactivity has been associated with an increased risk of cardiovascular, metabolic, cognitive and musculoskeletal disorders, which can lead to higher mortality and worsened quality of life (Pedersen & Saltin, 2006; Garber *et al.*, 2011). Endurance exercise (END) has been widely regarded as a powerful preventive and treatment tool for such diseases, due to favorable physiological adaptations for health and fitness (Garber *et al.*, 2011). However, to produce any significant physiological adaptation, END must be performed for at least 150 min/week at an intensity of 3 to 6 metabolic equivalents (METS) or 50-70% of maximum heart rate (HR_{max}) (Garber *et al.*, 2011). As "lack of time" has been referred as one of the main reasons of low compliance to this type of training (Brownson *et al.*, 2001; Gibala & Little, 2010), many studies were performed in order to observe if decreasing the exercise volume, while increasing the intensity (thus, decreasing time-commitment), led to similar adaptations to those found in conventional END.

High intensity interval training (HIIT) describes physical exercise that is characterized by brief, intermittent bursts of vigorous physical activity, interspersed by periods of rest or low-intensity exercise (Gibala *et al.*, 2012). Subjects perform short periods of training (from 30 seconds to 1 minute) at intensities from 90% HR_{max} and above, interspersed with a passive or active rest, achieving an exercise volume of maximum 10 to 20 minutes/session (30-60 minutes/week). In comparison to traditional END, several authors have studied HIIT adaptations and found similar or superior changes in a range of physiological, performance and health-related markers in both healthy individuals and diseased populations (Gibala *et al.*, 2012). Moreover, as little as 6 sessions of training (2 weeks) produce significant adaptations in muscle oxidative capacity, cardiorespiratory fitness and exercise performance (e.g., increased endurance time and reduced time to complete a set amount of work) (Burgomaster *et al.*, 2005; Burgomaster *et al.*, 2006; McKay *et al.*, 2009; Little *et al.*, 2010), reduce hyperglycemia and increase muscle mitochondrial capacity in patients with type 2 diabetes (Little *et al.*, 2011). Furthermore, longer HIIT interventions (6 weeks) showed increased resting glycogen content, reduced rate of oxygen utilization and lactate production during matched-work exercise, increased

capacity for whole-body and skeletal muscle lipid oxidation and enhanced peripheral vascular structure/function (Burgomaster *et al.*, 2008; Rakobowchuk *et al.*, 2008; Gibala *et al.*, 2012). Together, the evidence supports HIIT as an attractive alternative to traditional END training, not only for those that have less time to do exercise, but also for patients who require fast metabolic and functional adaptations to improve their health and quality of life.

In relation to the fast functional adaptations seen in HIIT, no efforts have been made to clarify its neural contributions. For instance, increases in power output and endurance time are reported in as little as 6 sessions of HIIT training (Burgomaster *et al.*, 2005; Little *et al.*, 2010). Even when the increases in aerobic and metabolic capacity had been attributed to those changes, neural adaptations should play a role as well, since motor performance is enhanced by repeated exposure to exercise training (Vila-Cha *et al.*, 2010). Moreover, as those functional outcomes might have a direct impact on strength and resistance to fatigue of healthy and diseased subjects, it is indeed relevant to study the neural mechanisms involved in such fast adaptations.

Thus, the main purpose of the present thesis was to study the neuromuscular changes occurring after two weeks of either HIIT or END training by using novel methods of high-density surface electromyography (HDEMG) motor unit decomposition. This work begins with a short review of the literature pertaining to the following: (1) motor unit basic properties (2) motor units and the regulation of muscle force (3) motor unit adaptations to training and (4) methodology of motor unit decomposition. Following the review, the aims and hypothesis of this dissertation will be presented and followed by 4 complete studies showing: (1) the reliability of HDEMG to monitor changes in motor unit behavior (2) a new technique for longitudinal tracking of motor units (3) motor unit behavioral changes after HIIT and END interventions and (4) the characteristics of the neural input received by the synergistic thigh muscles studied during the training intervention.

2. Literature review

2.1. Motor Unit basic properties

Motor units are regarded as the final common pathway of the central nervous system (CNS) to the muscles (Sherrington, 1925). Therefore, the study of motor unit behavior can improve our understanding about how the CNS adapts to training. A motor unit is comprised by an alpha-motor neuron in the ventral horn of the spinal cord, its axon and the muscle fibers that the axon innervates (Sherrington, 1925). Motor units convert the neural information sent by the CNS motor centers (e.g., brain cortex, brain stem, spinal cord) into muscle forces that are ultimately responsible for the generation of movement (Heckman & Enoka, 2012).

Anatomically, muscles comprise from few tens of motor units up to several thousand. Each motor neuron innervates an average of 300 muscle fibers, however, the range also extends from tens to thousands depending on the muscle's size (Enoka & Fuglevand, 2001). The group of muscle fibers belonging to the same motor unit is called muscle unit and its territory usually extends up to the 15% of the muscle's volume (Heckman & Enoka, 2012).

Action potentials fired by the motor neuron cause the contraction of all the fibers innervated by the motor unit (muscle unit). This response is called "twitch" and corresponds to the force produced by the muscle fibers in response to a single action potential (Enoka, 2015). A twitch is regarded as the basic contractile property of a motor unit. Action potentials fired by the motor neuron produce a sharp fluctuation in voltage that can be recorded by electrodes placed on the surface of the skin or inside the muscle belly. This voltage fluctuation is called motor unit action potential or "spike".

When contractions are sustained in time, a number of motor unit action potentials (summation of spikes) are sent to the muscles in order to produce a series of overlapping twitches. The degree of overlap between successive twitches depends on the rate at which the action potentials are generated and the time-course of the twitch response (Enoka, 2015). This summation of action potentials is commonly called "spike train" or "innervation pulse train". From these spike trains motor unit behavioral properties such as mean discharge rate (frequency of discharges) and discharge rate variability (regularity of

discharges) are calculated (central properties of the motor unit).

Once an action potential arrives to the neuromuscular junction, it will propagate through the innervated muscle fibers in the longitudinal direction. The velocity of propagation of this action potential can be quantified by a group of surface electromyography (EMG) electrodes (e.g., array of at least 4 electrodes placed parallel to the muscle fibers), simply by dividing the distance between electrodes and the time it took to the action potential to travel that distance (Farina *et al.*, 2001). This measurement is called muscle fiber conduction velocity and gives information about the properties of the muscle fiber membrane (motor unit peripheral property) (Farina *et al.*, 2001). This variable has been also used to measure the size of the motor units, since action potentials from big motor units propagate faster than action potentials from smaller motor units (Farina *et al.*, 2002). **Figure 1** shows a schematic representation of motor unit central and peripheral properties.

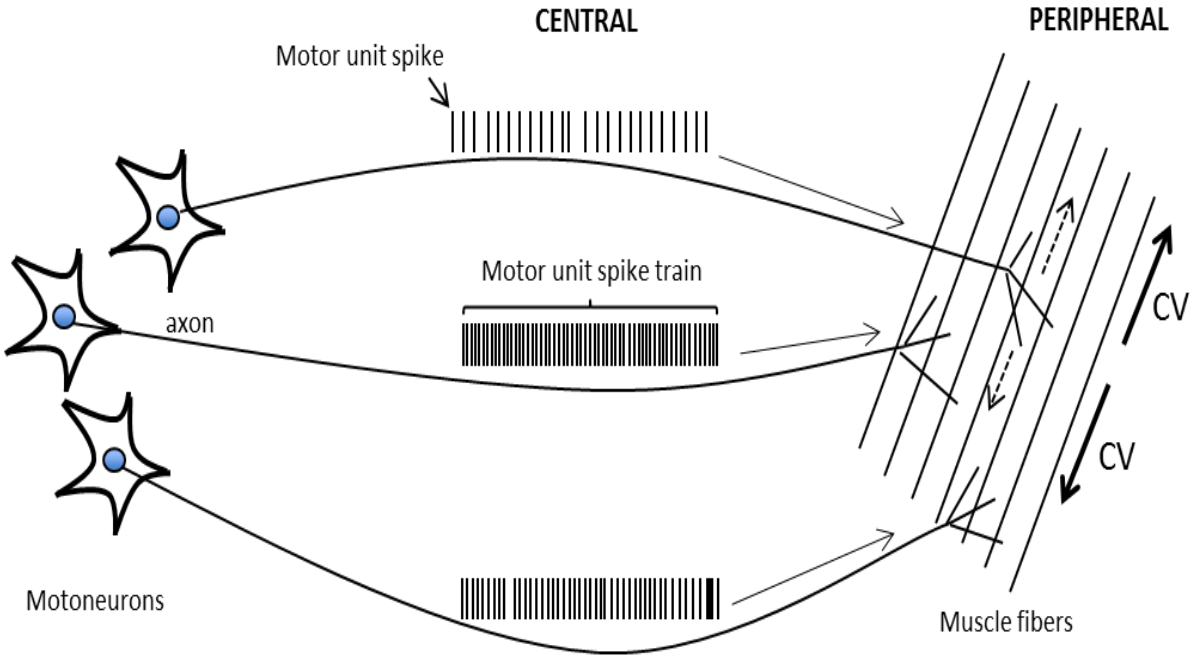

Figure 1. Schematic representation of motor units (motor neurons, their axons and muscle fibers that each axon innervates) behavior. Three motor neurons send neural information through their axons as motor unit spike trains (sum of action potentials) with different discharge rates and discharge rate variability (central motor unit properties) (left and center). Each of these axons then branch to innervate different muscle fibers (muscle unit) (right). Action potentials propagate through the muscle fiber membranes (dashed arrows) in order to produce a contraction of the muscle fibers (conduction velocity, peripheral property). CV, conduction velocity.

2.2. Motor Units and force

There are several ways in which motor units can produce/control force. For instance, the force that a muscle exerts depends on motor unit activity (Adrian & Bronk, 1929), changing with the number of motor units that are active (motor unit recruitment) and the rates at which motor neurons discharge action potentials (rate coding or discharge rate) (Duchateau *et al.*, 2006). Therefore, increases in muscle force are attributed to both increases in motor unit recruitment and discharge rate (Duchateau *et al.*, 2006). Regarding motor unit recruitment, motor units are recruited in an orderly fashion according to the size principle (motor unit size is quantified by measuring the diameter, surface area, number of dendrites, and capacitance of the cell body) (Henneman *et al.*, 1965). Thus, smaller motor units are recruited first at low force levels (low threshold motor units) while the biggest motor units are recruited last (high threshold motor units) at higher force levels. Accordingly, larger motor units typically present greater twitch tension than smaller motor units (higher force capacity) (Milner-Brown *et al.*, 1973). The size principle has been believed to have functional advantages in force production (e.g., optimization of force gradation) (Heckman & Enoka, 2012), however, this observation has been recently questioned (Dideriksen & Farina, 2013).

Finally, and regarding force control, the muscle can increase the force precision (steadiness) by regulating the number of recruited motor units (Duchateau *et al.*, 2006) and also by decreasing discharge rate variability (Moritz *et al.*, 2005), however, the latter argument has been also recently challenged (Negro *et al.*, 2009). Recent studies have documented the role of low (<5Hz) and high (>5Hz) frequency motor unit coherence (correlated oscillatory activity among motor units) for the production/control of muscle force [see (Farina & Negro, 2015) for review]. Indeed, the correlated activity between motor unit discharge rates in low frequencies (<5 Hz) has been considered to determine the effective neural drive to the muscles (Farina *et al.*, 2014). This correlated activity suggests that most of the motor units within a muscle are controlled by common synaptic input. Therefore, low-frequency correlation between motor units is needed for force control. Despite that high correlated motor unit activity has been shown in several individual muscles (within-muscle or intra-muscular motor unit coherence) (Negro *et al.*, 2009; Negro *et al.*, 2016b), the magnitude of motor unit coherence between synergistic muscles

(inter-muscular coherence) is not known.

2.3. Motor Unit adaptations to training

Previous studies about resistance (strength) training, have documented changes in motor unit features like recruitment, discharge rate, discharge rate variability, low and high frequency motor unit coherence, and conduction velocity (Semmler, 2004; Duchateau *et al.*, 2006; Vila-Cha *et al.*, 2010; Vila-Cha & Falla, 2016). For instance, changes in maximum voluntary contraction (MVC) force after resistance training have been attributed to adaptations in the force capacity of the muscle fibers and the activation characteristics of the involved motor units (Duchateau *et al.*, 2006). Therefore, it has been observed that increases in muscle strength are accompanied by increases in motor unit discharge rate (Kamen & Knight, 2004; Vila-Cha *et al.*, 2010), low and high frequency motor unit coherence (Semmler, 2004), conduction velocity (Vila-Cha *et al.*, 2010) and changes in recruitment threshold during explosive contractions (Van Cutsem *et al.*, 1998; Duchateau *et al.*, 2006). While the observed increase in force steadiness (force control) during sustained submaximal contractions after strength training has been associated with a decrease in discharge rate variability (Vila-Cha & Falla, 2016).

In contrast to resistance-training investigations, the number of studies documenting changes in motor unit behavior after END training is scarce. Most recent investigations focused on comparing changes in motor unit behavior between END and resistance training. These studies showed opposite adaptations regarding motor unit behavior (mean discharge rate and discharge rate variability) (Vila-Cha *et al.*, 2010; Vila-Cha & Falla, 2016), motor unit peripheral properties (motor unit conduction velocity) (Vila-Cha *et al.*, 2012) and functional outcomes such as MVC force (Vila-Cha *et al.*, 2010) and time to task failure (Vila-Cha *et al.*, 2012). In summary, these investigations showed that END training decreases discharge rate, does not change discharge rate variability, reduces the rate of decline in conduction velocity during fatiguing contractions and increases the time to task failure without changing the MVC force. These results are not surprising since the muscular and neural adaptations induced by each type of exercise are highly specific and may vary for different training paradigms (Hakkinen & Komi, 1986; Vila-Cha *et al.*, 2010). Indeed, and according to the principle of training specificity (Hakkinen & Komi,

1986; Morrissey *et al.*, 1995), it is very likely that training protocols analyzing different motor tasks, intensities and training volumes show different neuromuscular adaptations.

Previous investigations comparing physiological adaptations of short-term HIIT and END training (2 weeks) have used protocols with load intensities 2 to 4 times higher for HIIT, and training volumes 6 to 9 times higher for END (Gibala *et al.*, 2006; McKay *et al.*, 2009; Little *et al.*, 2010). Thus, differences in motor unit behavior between these types of training should be expected; however, this has not been investigated.

2.4. Motor unit decomposition techniques

It is not an easy task to extract information about human motor units in vivo. Many methods such as concentric needles, quadrifilar and fine wire electrodes have been developed and refined over the years. However, all of these procedures are invasive and only allow the recording of just a few motor units during low contraction levels (10-30% of the MVC) (Merletti *et al.*, 2008). Moreover, they do not allow the tracking of the same motor units longitudinally, since it is almost impossible to relocate the electrode across testing sessions (Carroll *et al.*, 2011). Since the extracted sample of motor units with these methods is small and variable, it is difficult to infer changes in motor unit behavior. Indeed, there is a large amount of studies presenting contradictory motor unit changes after training interventions. For instance, even when most of the authors have documented increases in discharge rate after resistance training (Van Cutsem *et al.*, 1998; Patten *et al.*, 2001; Kamen & Knight, 2004; Vila-Cha *et al.*, 2010), there are a number of studies not being able to find these changes, despite that the training protocols also induced large and significant increases in MVC force (Rich & Cafarelli, 2000; Pucci *et al.*, 2006).

As an alternative to address those limitations, high-density (multichannel) surface electromyography (HDEMG) techniques have been developed to study motor unit behavior non-invasively with a method called surface EMG motor unit decomposition (Merletti *et al.*, 2008; Holobar *et al.*, 2009; Farina & Holobar, 2016) **Figure 2**. With this technique, spike trains of individual motor units can be extracted from the surface EMG interference signal. In order for this method to work, the number of observation sites (EMG channels) from the surface EMG should be high enough to discriminate between different motor unit action potentials accurately (Farina *et al.*, 2008). Indeed, each motor

unit has its own spatial representation over the HDEMG electrode grid (Figure 2c) that can be identified with high precision when the number of channels is high (e.g., more than 32 EMG channels) (Farina *et al.*, 2008). Thus, the extraction of the different sources (motor units) from the surface electromyography signals can be performed with algorithms based on blind source separation, which are able to identify and discriminate between different motor unit action potential shapes, and later on extract the times that each motor unit was active (Figure 2d) (Holobar & Zazula, 2007; Farina & Holobar, 2016; Negro *et al.*, 2016a).

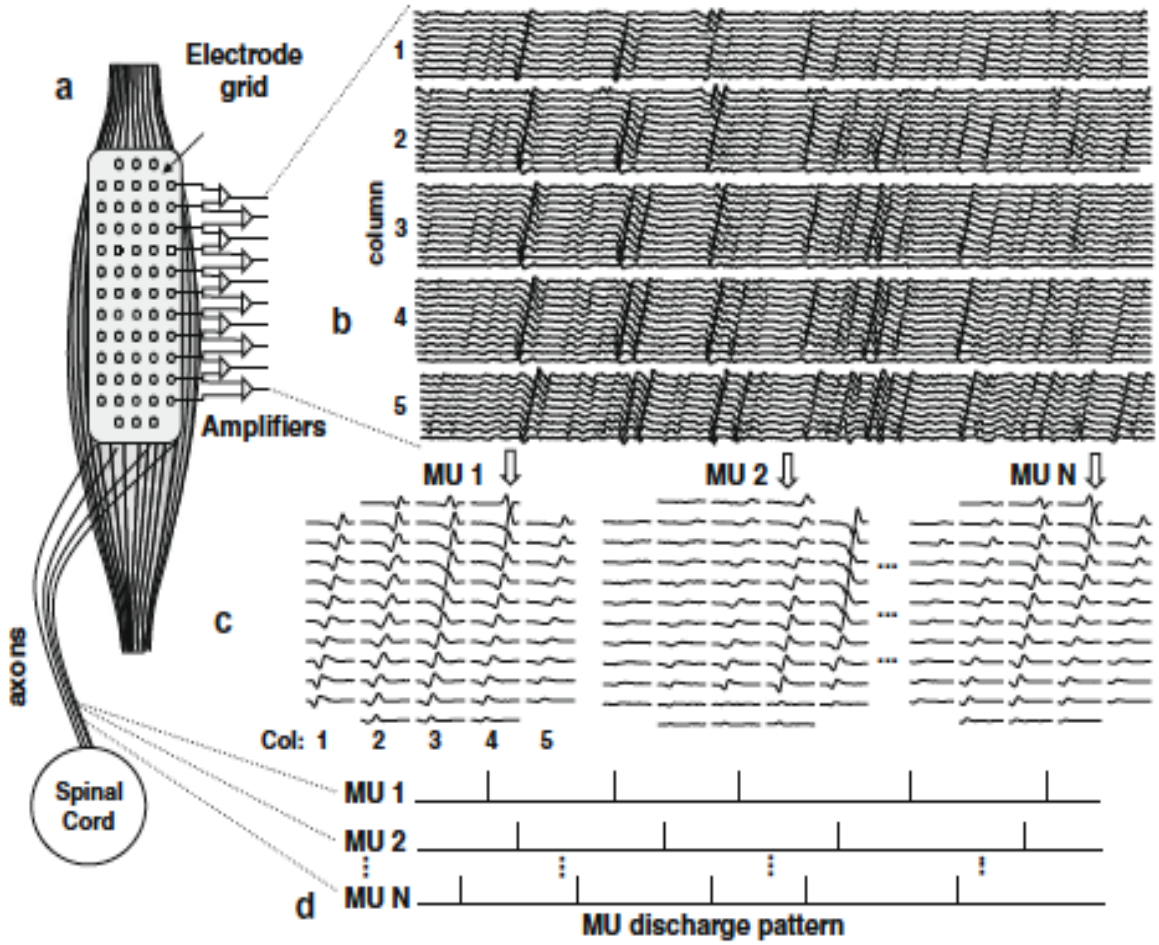

Figure 2. HDEMG motor unit decomposition procedure. (a) Surface EMG signals recorded from the biceps brachii muscle with a 13 x 5 electrode grid (corner electrodes are absent), electrode columns are parallel to fiber direction. (b) Segment of 500 ms duration of bipolar EMG detected by each column of the grid. Action potentials show propagation along the columns. (c) Multi-channel action potentials for three motor units extracted from the interference signal with the decomposition algorithm described by (Holobar & Zazula, 2007). (d) Estimated discharge patterns (motor unit spike trains) for the three motor units (horizontal bars). MU: motor unit. Figure extracted from (Merletti et al., 2008).

HDEMG presents numerous advantages compared to previous methods: first, the number of detected units is increased (Merletti *et al.*, 2008); second, a wider range of force levels can be analyzed (from 1% up to 75% of the MVC) (Holobar *et al.*, 2014); third, allows the study of the properties of the muscle fiber membrane (muscle fiber conduction velocity) (Farina *et al.*, 2001) and fourth, it might allow the tracking of the same motor units after an exercise intervention, since HDEMG electrodes can be easily repositioned across sessions (Cescon & Gazzoni, 2010).

Several study groups have been developing techniques to improve the accuracy of HDEMG to detect MU activity (Kleine *et al.*, 2007; Farina *et al.*, 2008; De Luca & Hostage, 2010; Negro *et al.*, 2016a). However, and quite surprisingly, none of these groups has measured the reliability of the variables obtained through HDEMG motor unit decomposition. This information is very important since training interventions require methods showing high reliability in order to interpret changes in motor unit behavior accurately.

2.5. Conclusion

This literature review presented the basic properties of motor units, their different adaptations to training and a new technique for the extraction of motor unit variables from HDEMG. In summary, motor units are highly sensitive to different training paradigms, showing contrasting adaptations between END and resistance training. Previous investigations about motor unit behavior following training interventions involved invasive methods of motor unit decomposition with many limitations (e.g., low number of detected motor units at low force levels). These limitations could be solved with HDEMG motor unit decomposition systems, which allow the extraction of a larger number of motor units in a wide range of force levels. However, the reliability of HDEMG for training interventions and the possibility of tracking single motor units longitudinally has not been examined. If confirmed, such advances in technology will undoubtedly help to improve our understanding of motor unit adaptations to different types of training.

3. Research objectives

High intensity interval training has been used as an alternative to END since previous research suggested that HIIT produces similar physiological adaptations but with much lower time commitment. However, there are no studies comparing the neuromuscular changes induced by these types of training. Therefore, the major aim of the present thesis is to compare the neuromuscular effects of two weeks of either HIIT or END training by the study of motor unit behavior.

For this purpose, the following four consecutive studies were conducted: first, the within and between sessions reliability of HDEMG motor unit decomposition variables (mean discharge rate, peak-to-peak amplitude, conduction velocity and discharge rate variability), extracted from motor unit population samples of VM and VL muscles, was assessed at various contraction intensities (**Study 1**); second, it was tested if HDEMG recordings would allow the tracking of the same motor units across different testing sessions (**Study 2**); third, it was examined if two weeks of conventional END exercise would produce similar neuromuscular (motor unit) adaptations to those of HIIT (**Study 3**), and fourth, the magnitude of low and high frequency motor unit coherence between VM and VL synergistic muscles were measured (**Study 4**).

Each of these studies objectives and hypothesis can be summarized as follows:

Studies 1 and 2 were planned in order to check the validity of HDEMG for training interventions since there is a total lack of knowledge about the reliability of HDEMG motor unit decomposition variables within and across different testing sessions. Furthermore, it is important to know if HDEMG would also allow the tracking of the same motor units across several days. Therefore and as a first aim, this thesis is going to address the question of whether the motor unit variables obtained from HDEMG are reliable or not, and second, it will confirm if HDEMG recordings would allow the tracking of the same motor units longitudinally. Such knowledge is extremely important for intervention studies since the amount of measurement variability obtained with HDEMG systems remains unknown. Moreover, if the possibility to track motor units across different trials is

confirmed, both the reliability and sensitivity of HDEMG to study motor unit adaptations should improve drastically and it will be possible to investigate other motor unit properties that are not possible to assess with population samples (e.g., recruitment threshold in absolute force values). Together, this would place HDEMG as the best method to study motor unit adaptations after training. In fact, there are currently no other electromyographic methods able to track the same motor units longitudinally during voluntary contractions. For study 1 it was hypothesized that motor unit variables (mean discharge rate, peak-to-peak amplitude, conduction velocity and discharge rate variability) obtained from HDEMG motor unit population samples of VM and VL muscles during isometric knee extension contractions at 10, 30, 50 and 70% of the MVC force will have a low variability within and between sessions, producing accurate and repeatable results, while for study 2 the hypothesis was that HDEMG motor unit decomposition will allow the tracking of the same VM and VL motor units across different testing sessions in a wide range of isometric force levels (from 10% up to 70% MVC force). Therefore, it is expected that the reliability and sensitivity of the variables extracted from tracked motor units (recruitment, de-recruitment threshold, mean discharge rate and conduction velocity) will be higher than the variables obtained from averaged motor unit population samples.

Study 3 aimed to investigate low and high threshold motor unit adaptations between END and HIIT as well as their possible differences in functional (motor output) outcomes such as time to task failure, force steadiness (force control), MVC force (strength) and rate of force development (ballistic contractions). The END and HIIT training programs analyzed in study 3 were specifically chosen because they previously showed similar changes in aerobic metabolism and performance, despite their differences in training intensity and volume (Gibala *et al.*, 2006; Little *et al.*, 2010). These protocols will help to elucidate if the similarities observed in metabolic and cardiopulmonary systems are also observed at a neuromuscular level. It was hypothesized that despite that both types of training will show a similar increase in cardiorespiratory fitness (peak oxygen uptake and submaximal ventilation thresholds), HIIT and END will also show opposite adaptations in motor output (MVC force, rate of force development, time to task failure and force steadiness) that will be related to different adjustments in VM and VL

motor units discharge rates. Therefore, it is expected that the short and high loads used for HIIT will induce an increase in knee extension MVC force and increased discharge rates for VM and VL high threshold motor units (at 50 and 70% of the MVC), while the long and moderate loads used for END will induce an increase in time to task failure during a sustained low-force (30% MVC) knee extension contraction without any change in knee extension MVC force and, VM and VL motor unit discharge rates

Study 4 was finally performed to understand and explain possible differences in motor unit behavior between the two synergistic knee extensor muscles (VM and VL) that were assessed during the training intervention. Synergistic muscles usually act synchronously during motor tasks, therefore, it can be expected that the motor unit activity of these muscles change similarly after training. Synchronous activity can be due to shared synaptic inputs between muscles. One way to measure if muscles are controlled by shared or independent synaptic inputs is through the study of motor unit coherence. Since the level of motor unit coherence between synergistic muscles is unknown, study 4 will aim to investigate if VM and VL muscles are controlled by a common synaptic input, or by independent inputs, with an analysis called partial coherence. This method examines and compares the amount of motor unit correlation (low and high frequency motor unit coherence) within and between synergistic muscles (intra and inter-muscular coherence). The results obtained with this study will clarify if these muscles share their neural drive, or if the CNS controls them independently. It was hypothesized that the vasti muscles would be controlled primarily by a shared neural drive with relatively little unique drive to each muscle (inter-muscular motor unit coherence will be higher than intra-muscular motor unit coherence). Therefore, it is expected that VM and VL muscles will change similarly after training.

The four studies included in this document have been accepted for publication in a peer-reviewed journal (chapters 4.1, 4.2, 4.3 and 4.4). Further details about the journals, study-design, participants and measurements performed on each of the studies can be found in table 1. Thus, the following chapters will present the full articles (introduction, methods, results and discussion) that are related to the present dissertation.

Table 1: Studies presented in the thesis

Study	Journal	Design	Participants	Measures	Chapter
1	Clin Neurophysiol (peer-reviewed)	Cross-sectional	Male (n=10)	Isom. Knee extension, HDEMG activity	4.1
2	J Physiol (peer-reviewed)	Cross-sectional & Longitudinal	CS: Male (n=10) Long: Male (n=7)	Isom. Knee extension, HEMG activity, cycling performance, gas exchange	4.2
3	Med Sci Sports Exerc (peer-reviewed)	Longitudinal	Male (n=16)	Isom. Knee extension, HDEMG activity, cycling performance, gas exchange	4.3
4	J Neurosci (peer-reviewed)	Cross-sectional	Male (n=10)	Isom. Knee extension, HDEMG activity	4.4

CS: cross sectional, Isom: isometric, Long: longitudinal

4. Studies

4.1. Study 1

HIGH-DENSITY SURFACE ELECTROMYOGRAPHY PROVIDES RELIABLE ESTIMATES OF MOTOR UNIT BEHAVIOR

E. Martinez-Valdes[1], C.M. Laine[2] , D. Falla[2,3], F. Mayer[1], D. Farina[2]

Affiliations

1. Department of Sports Medicine and Sports Orthopaedics, University of Potsdam, Potsdam, Germany.

2. Department of Neurorehabilitation Engineering,
   Bernstein Focus Neurotechnology Göttingen (BFNT),
   Bernstein Centre for Computational Neuroscience (BCCN),
   University Medical Center Göttingen,
   Georg-August University, Göttingen, Germany

3. Pain Clinic,
   Center for Anesthesiology, Emergency and Intensive Care Medicine,
   University Hospital Göttingen, Göttingen, Germany.

Reference

Martinez-Valdes E, Laine CM, Falla D, Mayer F & Farina D. (2016). High-density surface electromyography provides reliable estimates of motor unit behavior. Clinical neurophysiology : official journal of the International Federation of Clinical Neurophysiology 127, 2534-2541.

4.1.1. ABSTRACT

Objective: To assess the intra-and inter-session reliability of estimates of motor unit behaviour and muscle fiber properties derived from high-density surface electromyography (HDEMG). Methods: Ten healthy subjects performed submaximal isometric knee extensions during three recording sessions (separate days) at 10, 30, 50 and 70% of their maximum voluntary effort. The discharge timings of motor units of the vastus lateralis and medialis muscles were automatically identified from HDEMG by a decomposition algorithm. We characterized the number of detected motor units, their discharge rates, the coefficient of variation of their inter-spike intervals (CoV_{isi}), the action potential conduction velocity and peak-to-peak amplitude. Reliability was assessed for each motor unit characteristics by intra-class correlation coefficient (ICC). Additionally, a pulse-to-noise ratio (PNR) was calculated, to verify the accuracy of the decomposition. Results: Good to excellent reliability within and between sessions was found for all motor unit characteristics at all force levels (ICCs > 0.8), with the exception of CoV_{isi} that presented poor reliability (ICC < 0.6). PNR was high and similar for both muscles with values ranging between 45.1- 47.6 dB (accuracy >95%). Conclusion: Motor unit features can be assessed non-invasively and reliably within and across sessions over a wide range of force levels. Significance: These results suggest that it is possible to characterize motor units in longitudinal intervention studies.

4.1.2. INTRODUCTION

Motor neurons are the common final pathway to muscle (Sherrington, 1925) and analysis of their behavior provides a direct indication of changes occurring within the central nervous system (CNS). The assessment of the firing patterns of motor units provides the opportunity to evaluate the mechanisms of muscle control utilized by the CNS (De Luca & Erim, 1994). Classically, motor unit activities have been recorded from human muscles in-vivo via intramuscular electromyography (EMG) (e.g., concentric needle or fine wire electrodes). However, this is an invasive procedure and, because of the high selectivity, it allows the concurrent detection of only a few motor units (Merletti *et al.*, 2008), usually during low force isometric contractions. As an alternative, high-density surface EMG (HDEMG) techniques have been developed to study motor unit behavior non-invasively. Using these techniques, the number of detectable motor units has increased (Holobar et al., 2009) with respect to invasive methods, a wider range of force levels can be analyzed, and peripheral properties of the motor units, such as muscle fiber conduction velocity, can be assessed together with the motor unit behavior (Merletti *et al.*, 2008; Holobar *et al.*, 2009).

The application of HDEMG to evaluate motor unit properties may be especially relevant for monitoring changes in muscle properties and neuromuscular control following an intervention, such as training. Indeed, the relatively large motor unit sample identified may be representative enough to provide reliable information on the properties of the motor unit pool under multiple measurement sessions. For this purpose, there is the need to test whether motor unit decomposition methods are accurate (e.g., correct detection of motor unit action potentials and quantification of errors) and reliable (e.g., provide comparable results in different measurement sessions). Despite the fact that several efforts have been made to enhance the accuracy of HDEMG in detecting motor unit activity (Kleine *et al.*, 2007; Farina *et al.*, 2008; Holobar *et al.*, 2009; De Luca & Hostage, 2010; Holobar *et al.*, 2014), the reliability of the information extracted from these methods remains largely unknown. Relatively few studies have attempted to monitor changes in motor unit behavior over long time periods, as would be necessary for characterizing neuromuscular adaptations to training. While some authors have reported training-related

changes in motor units characteristics such as recruitment thresholds (Duchateau *et al.*, 2006), discharge rate (Vila-Cha *et al.*, 2010), conduction velocity (Hedayatpour *et al.*, 2009) and motor unit synchronization (Semmler, 2002), the relevance of these changes is difficult to fully assess because of the unknown measurement variability.

In this study we assessed the intra and inter-session reliability of motor unit properties estimated from the decomposition of HDEMG. Specifically, we investigated features of motor unit behavior (number of detected motor units, discharge rate, discharge rate variability) and muscle fiber properties (conduction velocity, amplitude of motor unit action potentials). Additionally, the accuracy of the decomposed set of motor unit discharge timings was determined.

4.1.3. METHODS

4.1.3.1.Participants

Ten healthy and physically active men (mean (SD) age: 27 (4) years, height: 180 (8) cm, mass: 78 (10) kg) participated in the study. All subjects were right leg dominant (determined by asking which leg they would use to naturally kick a ball). Exclusion criteria included any neuromuscular disorders, current or previous history of knee pain and age < 18 or > 35 years. Participants were asked to avoid any strenuous activity 24 h prior to the measurements. The ethics committee of the Universitaetsmedizin Goettingen approved the study (approval number 24/1/14), according to the declaration of Helsinki (2004). All participants gave written, informed consent.

4.1.3.2. Experimental Protocol

Participants attended the laboratory on three occasions. The three sessions were 7 days apart and were conducted at the same time of the day for each subject. In each experimental session, subjects were seated comfortably on an isokinetic dynamometer (Biodex System 3, Biodex Medical Systems Inc., Shirley, NY, USA) in an adjustable chair with their trunk reclined to 15° and their hip and distal thigh firmly strapped to the chair. The rotational axis of the dynamometer was aligned with the right lateral femoral epicondyle while the lower leg was secured to the dynamometer lever arm above the lateral malleolus. Maximal and submaximal isometric knee extensions were exerted with the knee flexed by 90°. Subjects performed two maximum voluntary contractions (MVC) of knee

extension each over a period of 5 s. These trials were separated by 2 min of rest. The highest MVC value was used as a reference for the definition of the submaximal force levels. In each of the three experimental sessions, the submaximal forces were expressed as a percent of the MVC measured during the same session. Five minutes of rest were provided after the MVC measurement. Then, following a few familiarization trials at low force levels, subjects performed submaximal isometric knee extension contractions at 10, 30, 50 and 70% MVC in a randomized order. The contractions at 10-30% were sustained for 20 s, while the contractions at 50 and 70% MVC lasted 15 and 10 s respectively. In each trial, the subjects received visual feedback of their knee extension force, which was displayed as a trapezoid (5 s ramps with hold-phase durations as specified above). Each contraction level was performed 3 times per session and 2, 3, 4 and 5 minutes of rest were allowed after the 10, 30, 50 and 70% MVC contractions respectively. To evaluate whether the protocol induced fatigue, one MVC was performed at the end of each testing session.

4.1.3.3. Data Acquisition

Surface EMG was recorded in monopolar derivation with two-dimensional (2D) adhesive grids (SPES Medica, Salerno, Italy) of 13 × 5 equally spaced electrodes (each of 1 mm diameter, with an inter-electrode distance of 8 mm) **(Fig. 3)**. First, the skin of the participants was marked according to the Atlas of muscle innervation zones guidelines (Barbero *et al.*, 2012). Thus, for vastus medialis (VM), a line on the distal portion of the muscle belly oriented 50º with respect to the reference line between the medial side of the patella and the anterior superior iliac spine was drawn, while for vastus lateralis (VL), a line on the distal portion of the muscle belly oriented 20º with respect to the reference line between the lateral side of the patella and the anterior superior iliac spine was marked. Furthermore, and to ensure optimal electrode placement, EMG signals were initially recorded during a brief voluntary contraction during which a linear non-adhesive electrode array was moved over the skin to detect the location of the innervation zone and tendon regions, as described previously (Masuda *et al.*, 1985; Farina *et al.*, 2001). After skin preparation (shaving, abrasion and alcohol), the electrode cavities were filled with conductive paste (SPES Medica, Salerno, Italy) and the electrode grid was positioned between the proximal and distal tendons of the VM and VL muscles with the electrode columns (comprising 13 electrodes) oriented along the muscle fibers. Reference electrodes

were positioned at the right wrist and patella. The location of the electrodes was marked on the skin of the participants using a permanent ink marker, allowing similar electrode placement across the experimental sessions.

Force and EMG signals were sampled at 2048 Hz and converted to digital data by a 12-bit analogue to digital converter (EMG-USB 2, 256-channel EMG amplifier, OT Bioelettronica, Torino, Italy, 3dB, bandwidth 10-500 Hz). EMG signals were amplified by a factor of 2000, 1000, 500 and 500 for the 10, 30, 50 and 70% MVC contractions, respectively. These gains were used to avoid EMG signal saturation, which could influence decomposition results. All data were stored on a computer hard disk and analyzed with Matlab (The Mathworks Inc., Natick, Massachusetts, USA).

4.1.3.4. Signal Analysis

The recorded EMG signals were decomposed offline with the convolution kernel compensation (CKC) method (Holobar & Zazula, 2007) which is based on a blind source separation algorithm that has been previously validated on simulated signals (Farina *et al.*, 2008; Farina *et al.*, 2009; Holobar *et al.*, 2010) as well as experimental recordings from muscles with complex architecture (Marateb *et al.*, 2011), in pathological conditions (Holobar *et al.*, 2012), and high force levels (up to 70% MVC) (Holobar *et al.*, 2014). The submaximal contractions were decomposed only from the stable plateau region of force in order to minimize the effects of force variation on motor unit discharges. The results of the decomposition were checked manually and only motor units that were active during the whole duration of the decomposition were considered for further analysis, therefore, motor units presenting pauses larger than 500 ms were excluded.

The discharge times of single motor units were used to create binary spike trains in which each data sample was assigned a value of 0 or 1, depending on whether or not the data sample marked the onset of an action potential for a given motor unit. The mean discharge rate, inter-spike interval (ISI) and coefficient of variation of inter-spike interval ($CoV_{isi,}$ standard deviation of ISI divided by the mean ISI), were calculated from the binary spike trains. Discharges that were separated from the next for <33.3 ms or >200 ms (5 and 30 Hz discharges, respectively) were excluded from the mean discharge rate calculation since such discharges are extremely rare for the vasti muscles during submaximal isometric contractions (Enoka & Fuglevand, 2001; Duchateau *et al.*, 2006) and are therefore likely to

be due to decomposition errors (Watanabe *et al.*, 2013), all motor units with a CoV_{isi} > 30% were also discarded (Holobar *et al.*, 2014; Laine *et al.*, in press). Finally, a signal-based performance metric called pulse-to-noise ratio (PNR), was used to test the accuracy of the decomposed MUs. PNR is a reliable indicator of the mean square error between the true discharge pattern of each identified motor unit and its CKC-based estimation, where motor units with PNR > 30dB, exhibit a sensitivity > 90% and a false alarm rate < 2% [see (Holobar *et al.*, 2014) for details]. Therefore, only motor units with a PNR > 30dB were included in the analysis.

The mean multi-channel surface action potential of each identified motor unit was obtained by averaging the multichannel EMG signals over 40 ms long rectangular windows, triggered by all the motor unit discharge times identified over the time in which the force was stable **(Fig. 4)**. Peak-to-peak amplitude (p2p amplitude) of multi-channel surface action potentials was then calculated for each identified motor unit and averaged over all the channels of the grid (Piitulainen *et al.*, 2012). Motor unit conduction velocity was estimated from triplets of double differential derivations of the averaged surface multi-channel action potentials in the longitudinal direction by using the maximum likelihood estimator as presented previously (Farina *et al.*, 2001). Visual selection of the channels used to estimate conduction velocity was based on the criterion of a minimal change in shape of the action potential. The criterion for acceptance of conduction velocity estimation was based on the correlation coefficient of motor unit action potential shapes (threshold set to ≥ 0.9). Additionally, values beyond the physiological range (2–6 m/s) were excluded (Andreassen & Arendt-Nielsen, 1987). Therefore, the triplet that showed the minimum change in action potential propagation and with the highest cross-correlation coefficient was selected. However, in case that the highest cross-correlated triplet presented a clearly erroneous value, the second highest cross-correlated triplet with conduction velocity between 2-6 m/s was selected. Finally, the coefficient of variation of force [(SD ÷ mean) x 100, CoV force] was calculated for the whole duration of the contractions to identify if fluctuations in knee extension force were different across contraction levels.

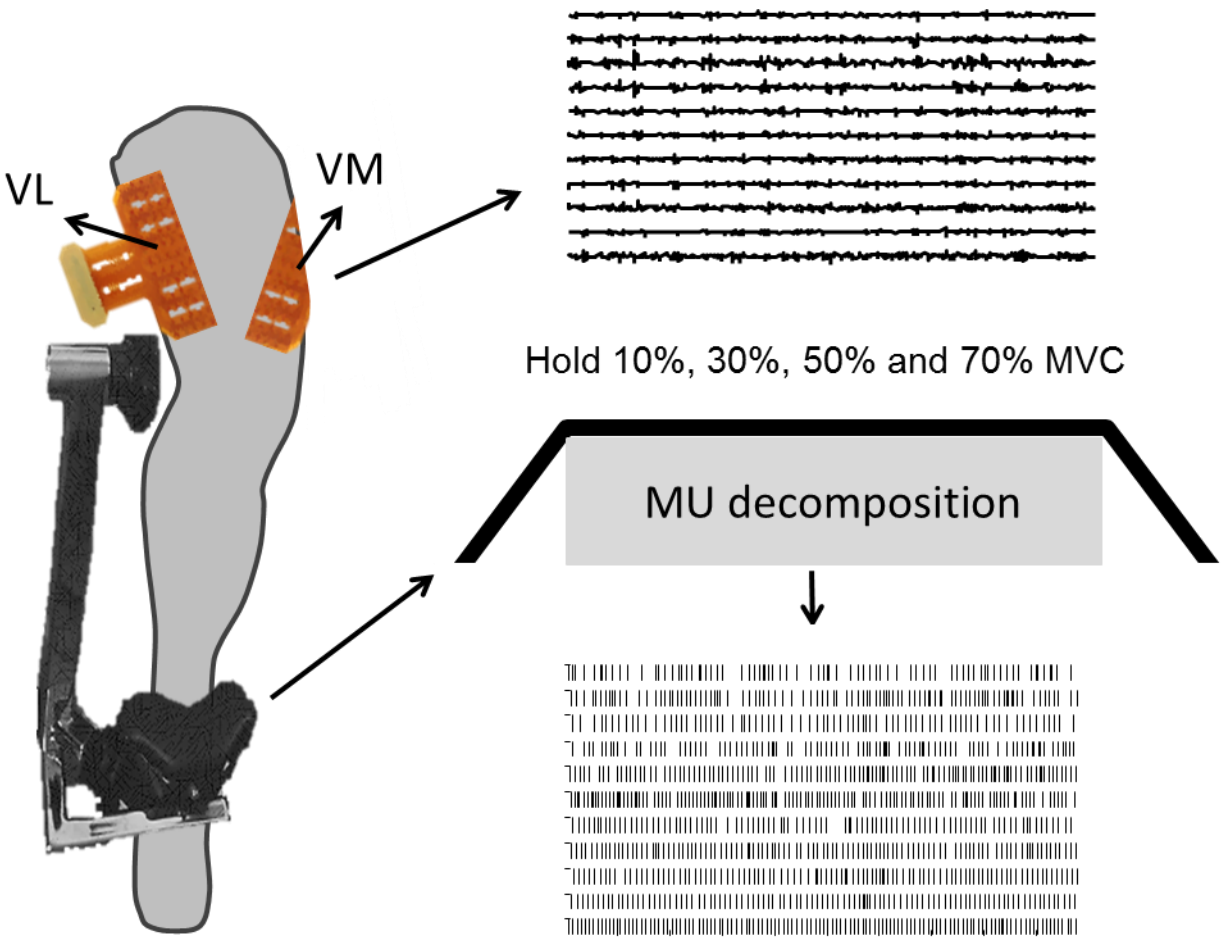

Figure 3. High-density surface EMG (HDEMG) signals (64 channels) were recorded from the vastus medialis (VM) and vastus lateralis (VL) muscles of healthy participants during the production of isometric knee extension force. A schematic representation of one participant's leg attached to the isokinetic dynamometer lever arm with the HDEMG electrodes mounted over the vasti muscles is presented on the left side of the figure. Surface EMG signals from one column of the HDEMG electrode grid (11 channels) over the VM are shown on the upper right half of the figure. Visual force feedback was displayed as a trapezoid at 10, 30, 50 and 70% of the maximum voluntary contraction (MVC). Only the hold-phase of the contractions (grey area under the trapezoid) was used to decompose the vasti motor units (lower right half of the figure).

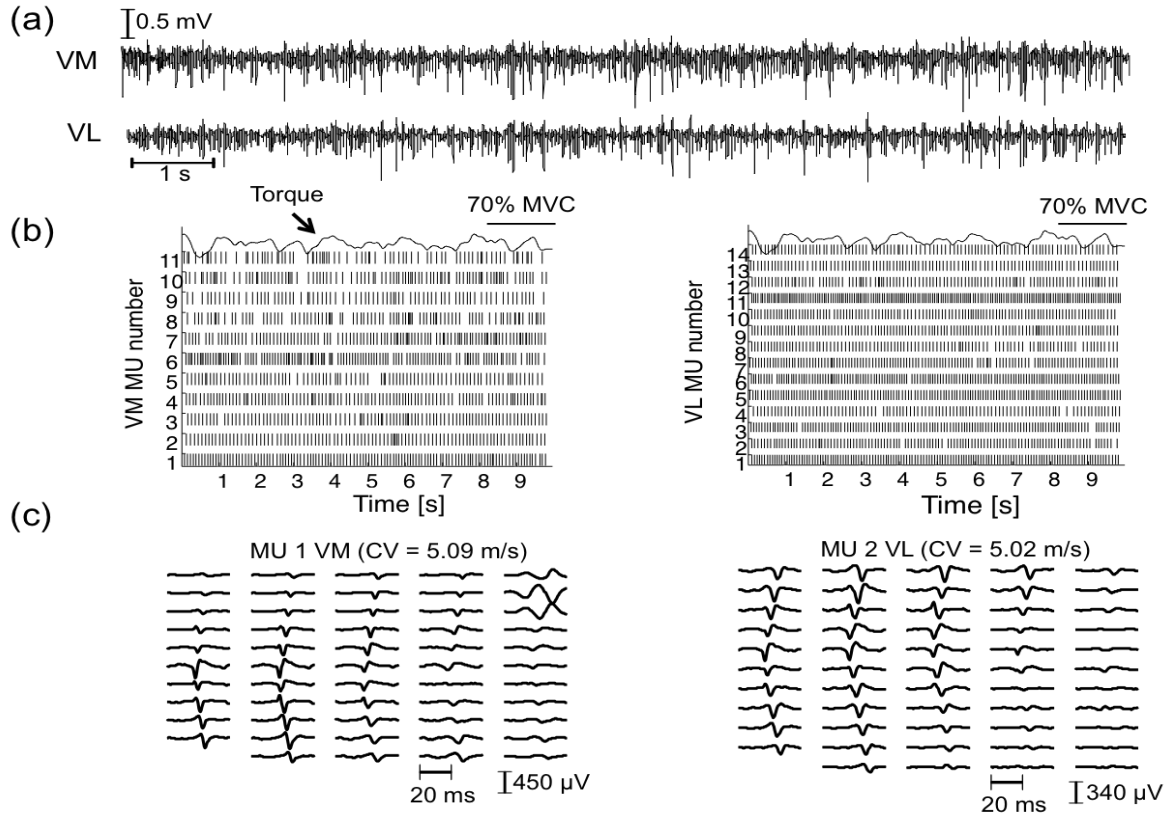

Figure 4. (a) One channel of surface EMG from the Vastus Medialis (VM) and Vastus Lateralis (VL) muscles of one subject during a steady 10 s contraction (70% of the maximum voluntary contraction (MVC)). The surface EMG was recorded with a grid of 5 x 13 electrodes (8 mm interelectrode distance). (b) Discharge times of 11 (VM) and 14 (VL) motor units that were identified from the decomposition of the surface EMG. (c) Multichannel surface action potentials of two motor units (VM left, VL right) with their mean conduction velocities (CV).

4.1.3.5. Statistical Analysis

All the results are expressed as mean and standard deviation (SD) unless stated. Before comparisons, all variables were tested for normality using the Shapiro-Wilk test. The assumption of sphericity was checked by Mauchley's test and, if violated, the Greenhouse-Geisser correction was made to the degrees of freedom. Statistical significance was set at $p < 0.05$. All decomposition variables (discharge rate, CoV_{isi}, ISI, conduction velocity, p2p amplitude and number of correctly identified motor units) were analyzed at each force level (10, 30, 50 and 70% MVC) for each muscle (VM and VL) independently. To determine the level of reliability of these variables, the intra-class correlation coefficient ($ICC_{2,1}$) was used. ICC scores between 0.8-1 were interpreted as "excellent", 0.6-0.8 as "good", and < 0.6 as "poor" (Bartko, 1966). Additionally, a one-

way repeated measures analysis of variance (ANOVA) was performed to determine if there were significant differences within a testing session or between the three sessions. Within-subject variability was calculated using the mean intra-participant coefficient of variation [(SD ÷ mean) x 100, CoV] and the standard error of the measurement [square root of the mean square error term in repeated measures ANOVA, SEM] to augment the ICC and ANOVA results (Atkinson & Nevill, 1998). ICC indicates the percentage of global variance that can be attributed to the variability between subjects (relative reliability), while CoV and SEM are measures of within-subject reliability, which provides a measure of variability of an individual's value (absolute reliability). SEM is expressed in the actual units of the measurement, and therefore, the smaller the SEM the more reliable the measurements. Typically, a change smaller than the identified SEM, is the likely result of measurement error rather than a "true" observed change (Copay *et al.*, 2007). Meanwhile for CoV, values of less than 20% were regarded as "acceptable" variability (Albertus-Kajee *et al.*, 2010).

4.1.3.6. Intra and inter-session reliability

Intra-session reliability was determined by comparing the three repetitions at each force level within a session (e.g., discharge rate from repetitions 1, 2 and 3 at 10% MVC from session 1). For the sake of clarity, intra-session reliability statistical results (ICC, SEM and CoV) were averaged for the three sessions and presented for each force level independently. For inter-session reliability, the three repetitions performed at each force level during a session were averaged and then compared between sessions (e.g., discharge rate from the three repetitions at 10% MVC from session 1 were averaged and then compared with averaged repetitions at 10% MVC from sessions 2 and 3 respectively).

4.1.3.7. Force

To check the effects of fatigue, MVCs from the beginning and end of each session were compared using a paired t-test. To examine if there was a significant difference in MVC force between sessions, all MVCs performed at the beginning of each session were compared by one-way ANOVA. Finally, CoV force values were averaged for each level (10, 30, 50, 70% MVC) and compared by two-way repeated measures ANOVA with factors: %MVC force level (4 levels: 10, 30, 50 and 70% MVC) and session (3 levels: Sessions 1, 2 and 3) followed by Bonferroni corrected t-tests if significant.

4.1.3.8. Accuracy (pulse-to-noise ratio)

To check for differences in motor unit decomposition accuracy between sessions, PNR values from the three repetitions performed at each force level during a session were averaged and then compared between sessions by one-way repeated measures ANOVA. Moreover, to test whether there was an influence of force on accuracy, PNR values from the three sessions were averaged for each force level and then compared by one-way repeated measures ANOVA followed by Bonferroni corrected t-tests if significant.

4.1.4. RESULTS

4.1.4.1. Force

Maximal voluntary knee extension force performed at the start of each session did not differ between sessions ($p = 0.099$). There was no significant change in MVC across each experimental session ($p = 0.55$, 0.13 and 0.08, for sessions 1, 2 and 3, respectively). The CoV of force significantly increased across force levels [2.0 (0.4), 2.0 (0.4), 2.4 (0.6) and 2.5 (0.5)% for 10, 30, 50 and 70% MVC respectively] ($p = 0.038$). Post-hoc analysis showed a significant difference in the CoV of force between 30 and 70% MVC ($p = 0.01$).

4.1.4.2. Motor unit decomposition accuracy (pulse-to noise ratio)

Overall, PNRs from selected motor units (motor units with $CoV_{isi} < 30\%$ and PNR > 30dB) were high for both muscles. Throughout the sessions, average PNRs were 46.1 (0.8) and 45.2 (1.7) [10% MVC], 45.5 (1.8) and 45.03 (2.3) [30% MVC], 46.4 (1.8) and 44.9 (2) [50% MVC] and 47.1 (1.6) and 45.7 (2.3) [70% MVC] for VM and VL, respectively. For both muscles, the PNRs did not significantly differ between sessions at each force level ($p= 0.26$, 0.28, 0.16, 0.8 for 10, 30, 50 and 70% MVC, respectively) and were not significantly influenced by force ($p= 0.26$, 0.93 and 0.51, in sessions 1, 2 and 3, respectively).

4.1.4.3. Motor unit characterization

The absolute values of each motor unit behavioral and peripheral properties, measured during each session are presented in **Figures 5 and 6**, respectively. Note that VM and VL showed similar results for all variables except p2p amplitude. The number of correctly identified motor units for each subject was in the range 2-13 and 3-14 (10%

MVC), 2-13 and 2-15 (30% MVC), 1-16 and 1-15 (50% MVC) and 3-14 and 1-19 (70% MVC) for VM and VL, respectively.

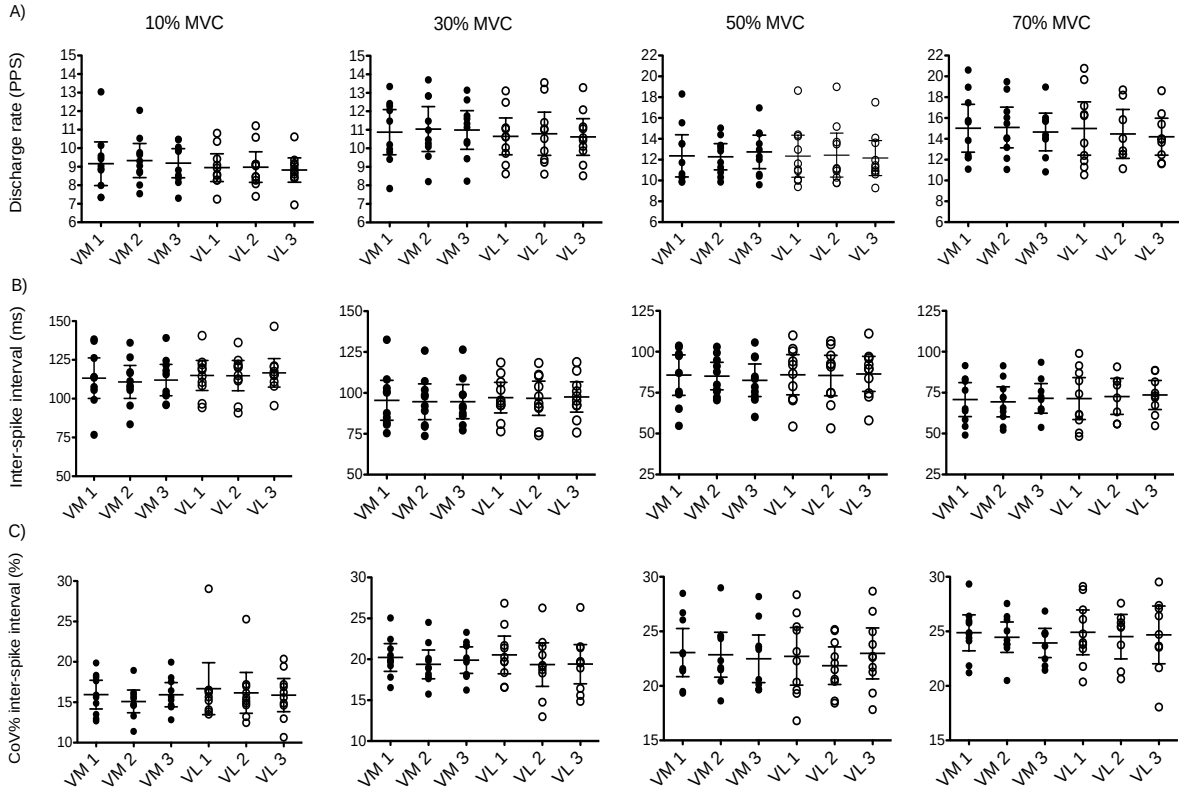

Figure 5. Individual values for motor unit (MU) behavioral properties: (A) discharge rate, (B) inter-spike interval (ISI) and (C) coefficient of variation of inter-spike interval (CoVisi). Values are presented for both muscles at all force levels [10, 30, 50 and 70% of the maximum voluntary contraction (MVC)] across the three sessions (1,2,3). Horizontal lines show the mean. Whiskers represent the 95% confidence interval. Note the change of scale between panels depicting 10-30% MVC variables and 50-70% MVC variables.

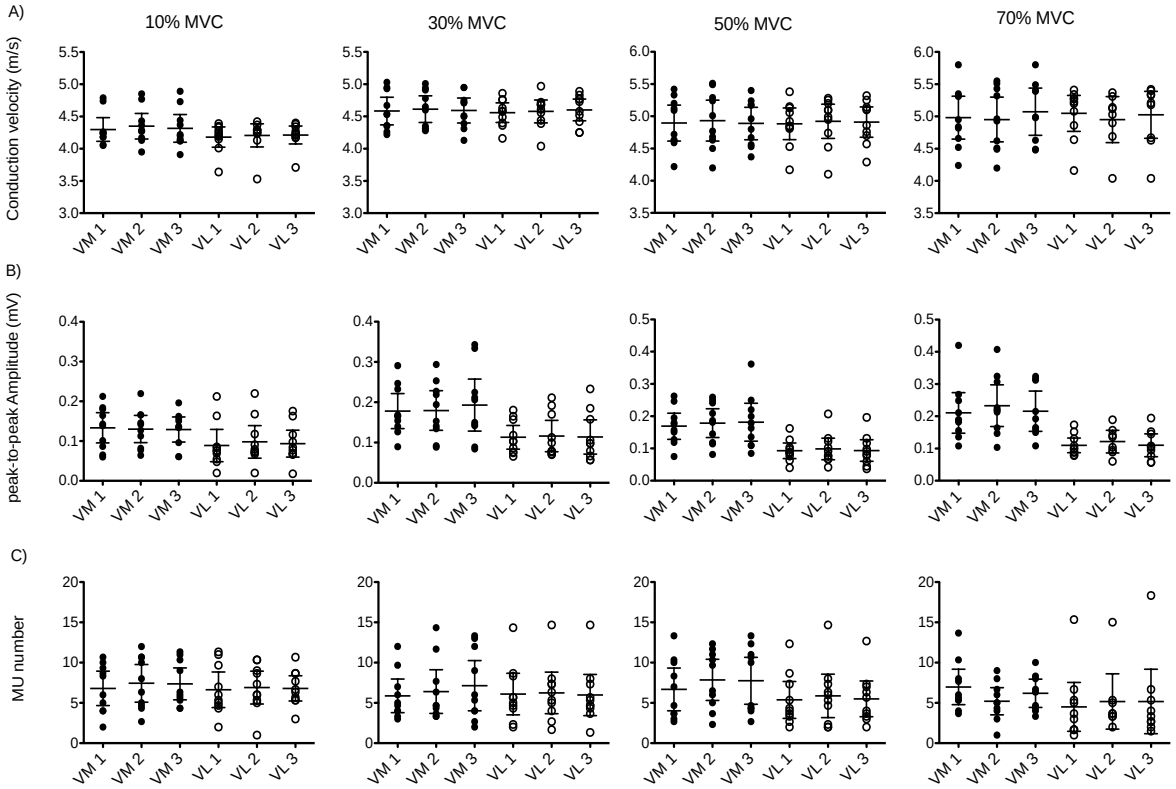

Figure 6. Individual values for motor unit (MU) peripheral properties: (A) MU conduction velocity, (B) MU peak-to-peak amplitude and (C) MU number. Values are presented for both muscles at all force levels [10, 30, 50 and 70% of the maximum voluntary contraction (MVC)] across the three sessions (1,2,3). Horizontal lines show the mean. Whiskers represent the 95% confidence interval. Note the change of scale between panels depicting 10-30% MVC variables and 50-70% MVC variables (except for MU peak-to-peak amplitude).

4.1.4.4. Intra-session Reliability

Overall, good to excellent reliability was found for motor unit discharge rate, ISI, conduction velocity, p2p amplitude, and the number of correctly identified motor units for both muscles and across all force levels, with the data extracted from VM and VL showing similar levels of reliability **(Table 2)**. However, there was a significant within-session difference for MU discharge rates and ISIs at 70% MVC in all three sessions for both muscles ($p < 0.05$). CoV_{isi} measured for VM at 70% MVC and VL at 10% MVC was the only variable with poor reliability (ICC: .517, SEM: 1.5 and ICC: .49, SEM 2.4 for VM and VL respectively). Nevertheless, good reliability and low variability of CoV_{isi} was found at the other force levels for both muscles.

Table 2. Intra-session reliability of motor units parameters. Averaged intra-session reliability values are presented for each variable, muscle (vastus medialis, vastus lateralis) and force level [10, 30, 50 and 70% of the maximum voluntary contraction, MVC]. ICC, intraclass correlation coefficient; SEM, standard error of the measurement; CoV, coefficient of variation (CoV%); pps, pulses per second; ISI, inter-spike interval. * Significant difference between repetitions ($p < 0.05$).

Variable	Force Level (% MVC)	Vastus Medialis			Vastus Lateralis		
		ICC	SEM	CoV (%)	ICC	SEM	CoV (%)
Discharge Rate (pps)	10%	.92	0.35	3.3	.92	0.29	2.8
	30%	.89	0.54	4.1	.91	0.44	3.8
	50%	.89	0.69	4.4	.93	0.59	4.4
	70%*	.85	1.05	6.2	.89	0.88	6.2
Interspike interval (ms)	10%	.92	4.41	3.3	.92	3.86	2.9
	30%	.92	4.44	4.2	.91	4.18	4.0
	50%	.90	4.24	4.7	.94	3.83	3.6
	70%*	.88	4.71	6.4	.88	4.77	6.0
Conduction Velocity (m/s)	10%	.94	0.07	1.3	.89	0.07	1.5
	30%	.88	0.09	1.9	.85	0.09	1.7
	50%	.95	0.09	1.5	.92	0.1	1.8
	70%	.97	0.09	1.5	.93	0.11	1.6
p2p Amplitude (mV)	10%	.93	0.012	8.7	.95	0.012	8.7
	30%	.84	0.031	11.7	.93	0.014	9.0
	50%	.98	0.010	5.2	.93	0.011	8.4
	70%	.96	0.018	7.6	.84	0.015	8.5
Coefficient of variation ISI (%)	10%	.71	1.26	6.9	.49	2.37	7.6
	30%	.69	1.43	6.6	.79	1.62	6.9
	50%	.78	1.51	5.5	.71	1.69	6.8
	70%	.52	1.52	5.5	.65	1.95	7.2
MU number	10%	.83	1.3	15.4	.65	1.6	16.4
	30%	.92	1.4	17.5	.89	1.2	24.4
	50%	.87	1.5	18.9	.88	1.2	22.3
	70%	.60	1.7	21.9	.94	1.2	24.8

4.1.4.5. Inter-session Reliability

Good to excellent reliability was found between sessions for measures of motor unit discharge rate, ISI, conduction velocity and p2p amplitude for both muscles and across all force levels, with similar results for both VM and VL **(Table 3).** No significant between-session difference was found for any variable ($p > 0.05$). Nevertheless, the reliability of CoV_{isi} was again poor at 10 and 70% MVC for VM and at 50 and 70% MVC for VL **(see Table 3)**.

Of the number of correctly identified motor units, poor reliability was only observed for the VM muscle at 70% MVC (ICC = .44). Nevertheless, the number of correctly identified motor units remained relatively constant across the remaining force levels of VM and all force levels of VL **(see Tables 2 and 3)**.

Table 3. Inter-session reliability of motor units parameters. Reliabiility values between the three sessions are presented for each variable, muscle (vastus medialis, vastus lateralis) and force level [10, 30, 50 and 70% of the maximum voluntary contraction, MVC]. ICC, intraclass correlation coefficient; SEM, standard error of the measurement; CoV, coefficient of variation (CoV%); pps, pulses per second; ISI, inter-spike-interval.

Variable	Force Level (% MVC)	Vastus Medialis			Vastus Lateralis		
		ICC	SEM	CoV (%)	ICC	SEM	CoV (%)
Discharge Rate (pps)	10%	.81	0.58	5.0	.86	0.38	3.7
	30%	.92	0.45	3.7	.94	0.36	2.8
	50%	.83	0.93	5.0	.91	0.8	5.4
	70%	.87	1.03	4.9	.91	0.86	6.1
Interspike interval (ms)	10%	.83	6.7	5.0	.87	4.99	3.9
	30%	.94	4.06	3.4	.96	2.99	2.8
	50%	.84	5.8	5.3	.88	6.04	5.8
	70%	.86	4.88	4.9	.83	6.13	7.1
Conduction Velocity (m/s)	10%	.95	0.06	1.3	.85	0.09	2.0
	30%	.91	0.09	1.6	.86	0,09	1.8
	50%	.96	0.08	1.4	.92	0.1	1.8
	70%	.94	0.11	1.6	.97	0.09	1.7
p2p Amplitude (mV)	10%	.93	0.013	9.7	.92	0.015	10.9
	30%	.61	0.046	16.8	.90	0.016	11.7
	50%	.75	0.034	11.1	.92	0.012	10.1
	70%	.87	0.035	10.4	.89	0.014	11.3
Coefficient variation of ISI (%)	10%	.52	1.51	9.0	.77	1.75	8.1
	30%	.70	1.29	5.6	.83	1.35	6.7
	50%	.65	1.84	6.7	.49	2.23	8.8
	70%	.49	1.47	5.6	.55	1.95	7.7
MU number	10%	.91	0.9	13.9	.82	1.2	18.2
	30%	.75	1.8	27.7	.90	1.2	18.4
	50%	.83	1.5	22.4	.82	1.5	25.8
	70%	.44	1.9	24.7	.91	1.5	30.1

4.1.5. DISCUSSION

Most variables extracted from motor unit pools estimates decomposed through HDEMG (CKC method) provide accurate, consistent, and reliable results for the VM and VL muscles across a wide range of force levels (up to 70% MVC), both within and between sessions. These variables include discharge rate, ISI, conduction velocity, p2p amplitude, and the number of identified motor units.

4.1.5.1. Motor unit accuracy

After removal of un-physiological discharges and excluding all motor units with PNRs < 30dB, accuracy of motor unit decomposition, as tested by PNR, was high for all the selected motor units (PNRs ranged from 45.1 to 47.6 dB throughout all sessions). Moreover, this parameter was not influenced by repeated measurements (different sessions) or force. As PNRs above 30 dB reveal sensitivity > 90% and false alarm rates < 2% (Holobar *et al.*, 2014), we can conclude that CKC is accurate enough to decompose motor units from the vasti muscles across a wide range of force levels (10 to 70% MVC).

4.1.5.2. Number of correctly identified motor units

Regardless of the force level, it was possible to identify 2 to 14 motor units for the VM and 2 to 16 motor units for the VL. The mean number of motor units per force level was greater compared to earlier work [(Vila-Cha *et al.*, 2010) mean of 4 motor units for VL and VM], as we were able to correctly identify a mean of 7 motor units for the VM and 6 motor units for the VL. Although the mean number of correctly identified motor units and its upper range is higher than the aforementioned study, it is important to state that the number of identified motor units varied considerably between subjects and in some participants only 2 to 3 motor units could be detected per force level. As surface EMG parameters are influenced by adipose tissue thickness and alignment of muscle fibers (Farina *et al.*, 2002), we can speculate that these factors could have influenced the decomposition algorithm. It is known, for example, that muscles covered by less adipose tissue such as tibialis anterior, usually present a higher number of correctly decomposed MUs (Holobar *et al.*, 2014). Nevertheless, as the number of correctly identified motor units presented good to excellent reliability, we can affirm that this parameter is subject specific.

4.1.5.3 Motor unit behavior

Mean discharge rates for VM and VL motor units were within the physiological range found in previous studies. For instance, Vila-Cha and colleagues (Vila-Cha *et al.*, 2010) reported mean discharge rates of approximately 9 and 11 pulses per second (pps) for VM and VL at 10 and 30% MVC contractions respectively. Moreover, Conwit et al., (Conwit *et al.*, 1998) documented mean motor unit discharge rates of approximately 15 pps for VM at 75% MVC, which is consistent with our results. Both VM and VL motor unit discharge rates showed similar consistency within and between days with ICCs revealing excellent levels of reliability at all force levels (from .813 to .941). Also, in terms of absolute reliability, SEMs and CoVs were low at all force levels, but as expected, they were higher at 50% and 70% MVC, which could be related with increased CoV of force at these levels (Moritz *et al.*, 2005) (see *Force* results). The significant differences found for discharge rate and ISI for 70% MVC for intra-session reliability (see Table 1) cannot be attributed to the effects of fatigue but rather to the difficulty of matching the target at this force level. This is confirmed by the lack of change in MVCs across each experimental session and by the fact that motor unit discharge rates increased between repetitions 1-2 but not between 2-3 at 70% MVC for all sessions [mean discharge rate of 14.1, 15.3 and 15.3 pps (for VM) and 13.9, 14.5, and 14.4 pps (for VL) for repetitions 1,2 and 3 respectively].

4.1.5.4. Muscle fiber properties

Values for motor unit conduction velocity were within the physiological range of 2-6 m/s and comparable to results reported for the vasti muscles in earlier studies at 10-30% MVC (Hedayatpour *et al.*, 2009; Vila-Cha *et al.*, 2010). As expected, motor unit conduction velocity increased with MVC. Consistent with the results for motor unit discharge rate, the ICC, SEM, and CoV revealed excellent intra and inter-session reliability for motor unit conduction velocity for both muscles. Interestingly, the variability of motor unit conduction velocity remained constant at all force levels. Excellent intra-session reliability was observed for p2p amplitudes, and good to excellent reliability was obtained for their inter-session reliability, suggesting that motor unit with similar properties were identified within and between sessions. Commonly, factors such as tissue impedance, electrode position, and contamination by volume conduction influence EMG amplitude

measures, and therefore EMG signals are typically normalized (Farina *et al.*, 2004). Due to our strict study design, we were able to place the electrodes in almost the same position in every session. Therefore, the reliability results found herein suggest that a similar population of motor units can be extracted if the electrode position remains similar throughout sessions. In addition, we found that the VM presented higher amplitude values compared to the VL. This result is in accordance with previous studies (Rainoldi *et al.*, 2008; Vila-Cha *et al.*, 2010), where a higher averaged rectified surface EMG amplitude was observed for the VM muscle. Since motor unit discharge rate and conduction velocity values were not significantly different between muscles, we can assume that other factors, such as fiber alignment and subcutaneous tissue thickness (Farina *et al.*, 2002), might have contributed to this difference. Nevertheless, we did not measure subcutaneous tissue thickness in the current study.

4.1.5.5. Motor unit CoV_{isi}

The only parameter that presented low reliability estimates within and between sessions across various force levels was motor unit CoV_{isi}. Previously, Vila-Cha and colleagues (Vila-Cha *et al.*, 2010) reported motor unit CoV_{isi} values ranging from 11.6 to 16.5% for VM and 11 to 13.4% for VL at 10-30% MVC, which is lower than the values presented herein at similar force levels (15.1 to 20.2% for VM and 15.9 to 20.5% for VL). The higher CoV_{isi} found in the present study could be attributed to two factors: first, our average number of motor units was greater than that reported by Vila-Cha et al., (26) and secondly, HDEMG motor unit decomposition methods can have lower accuracy compared to intramuscular decomposition [(Farina *et al.*, 2008) sensitivity of 92-100% compared to intramuscular EMG]. Moreover, it is important to note that CoV_{isi} is inherently a highly variable parameter that can be influenced by force fluctuations. Manual editing could solve this accuracy issue but we preferred to present only objective results obtained by fully automatic decomposition.

4.1.5.6. Data selection and limitations

Recent advances in signal processing techniques have undoubtedly increased the accuracy of HDEMG-based decomposition algorithms. Nevertheless, visual and manual checking of the decomposition results are still needed, as automatic decomposition could still contain erroneous discharges, missed firings or generally unreliable motor units. For

this reason, we used several criteria in the selection of our data (MUs with CoV_{isi} > 30% and PNR < 30dB were discarded, while firings below 5Hz and above 30Hz were filtered), which is similar to the criteria used for intramuscular motor unit decomposition (Negro *et al.*, 2009; Vila-Cha *et al.*, 2010). This helped us to find comparable results with previous literature in most of the analyzed motor unit properties. Although we did not quantify the number of corrections made, they were certainly similar across all force levels, and further, the PNRs did not significantly change with force and the number of selected motor units was similar across force levels. A similar set of criteria is essential for appropriate interpretation of any intervention study utilizing decomposed EMG data in healthy participants.

With respect to studies involving patients, a similar criterion was used in people with diabetes (Watanabe *et al.*, 2013) and post-stroke survivors (Li *et al.*, 2015). In those studies, authors filtered discharges below 4 Hz and above 30 Hz and they obtained a similar amount of motor units as in the present study. Therefore, similar levels of reliability to the ones found herein could be expected for those populations. However, it is important to acknowledge that in the case of movement disorders with high motor unit firing variability such as Parkinson or essential tremor, a more liberal approach is needed. Any removal of firings within the range presented herein would discard most of the decomposed motor units for these patients. Nevertheless, it is still important to visually inspect the motor units innervation pulse trains and use accuracy indexes such as the PNR [a PNR ≥ 26dB has been recently used in essential tremor (Gallego *et al.*, 2015) and Parkinson (Dideriksen *et al.*, 2015)] to check the accuracy of the decomposed motor units. Future studies would help to clarify if the high levels of reliability found for healthy subjects could be replicated in patients with such movement disorders.

4.1.5.7. Conclusions

This study showed that HDEMG motor unit decomposition by the CKC method provides accurate and reliable estimates of the motor unit properties in the vasti muscles, both within and across sessions, and over a wide range of forces. These findings suggest that HDEMG is appropriate for detecting changes in motor unit properties across multiple sessions, as required for longitudinal intervention studies.

4.1.6. REFERENCES

Albertus-Kajee Y, Tucker R, Derman W & Lambert M. (2010). Alternative methods of normalising EMG during cycling. *J Electromyogr Kinesiol* **20,** 1036-1043.

Andreassen S & Arendt-Nielsen L. (1987). Muscle fibre conduction velocity in motor units of the human anterior tibial muscle: a new size principle parameter. *The Journal of physiology* **391,** 561-571.

Atkinson G & Nevill AM. (1998). Statistical methods for assessing measurement error (reliability) in variables relevant to sports medicine. *Sports Med* **26,** 217-238.

Barbero M, Merletti R & Rainoldi A. (2012). *Atlas of muscle innervation zones : understanding surface electromyography and its applications*. Springer, Milan ; New York.

Bartko JJ. (1966). The intraclass correlation coefficient as a measure of reliability. *Psychol Rep* **19,** 3-11.

Conwit RA, Tracy B, Cowl A, McHugh M, Stashuk D, Brown WF & Metter EJ. (1998). Firing rate analysis using decompostion-enhanced spike triggered averaging in the quadriceps femoris. *Muscle Nerve* **21,** 1338-1340.

Copay AG, Subach BR, Glassman SD, Polly DW, Jr. & Schuler TC. (2007). Understanding the minimum clinically important difference: a review of concepts and methods. *Spine J* **7,** 541-546.

De Luca CJ & Erim Z. (1994). Common drive of motor units in regulation of muscle force. *Trends Neurosci* **17,** 299-305.

De Luca CJ & Hostage EC. (2010). Relationship between firing rate and recruitment threshold of motoneurons in voluntary isometric contractions. *J Neurophysiol* **104,** 1034-1046.

Dideriksen JL, Gallego JA, Holobar A, Rocon E, Pons JL & Farina D. (2015). One central oscillatory drive is compatible with experimental motor unit behaviour in essential and Parkinsonian tremor. *J Neural Eng* **12,** 046019.

Duchateau J, Semmler JG & Enoka RM. (2006). Training adaptations in the behavior of human motor units. *Journal of applied physiology* **101,** 1766-1775.

Enoka RM & Fuglevand AJ. (2001). Motor unit physiology: some unresolved issues. *Muscle Nerve* **24,** 4-17.

Farina D, Cescon C & Merletti R. (2002). Influence of anatomical, physical, and detection-system parameters on surface EMG. *Biol Cybern* **86,** 445-456.

Farina D, Holobar A, Gazzoni M, Zazula D, Merletti R & Enoka RM. (2009). Adjustments differ among low-threshold motor units during intermittent, isometric contractions. *Journal of neurophysiology* **101,** 350-359.

Farina D, Merletti R & Enoka RM. (2004). The extraction of neural strategies from the surface EMG. *Journal of applied physiology* **96,** 1486-1495.

Farina D, Muhammad W, Fortunato E, Meste O, Merletti R & Rix H. (2001). Estimation of single motor unit conduction velocity from surface electromyogram signals detected with linear electrode arrays. *Medical & biological engineering & computing* **39,** 225-236.

Farina D, Negro F, Gazzoni M & Enoka RM. (2008). Detecting the unique representation of motor-unit action potentials in the surface electromyogram. *J Neurophysiol* **100,** 1223-1233.

Gallego JA, Dideriksen JL, Holobar A, Ibanez J, Glaser V, Romero JP, Benito-Leon J, Pons JL, Rocon E & Farina D. (2015). The Phase Difference Between Neural Drives to Antagonist Muscles in Essential Tremor Is Associated with the Relative Strength of Supraspinal and Afferent Input. *J Neurosci* **35,** 8925-8937.

Hedayatpour N, Falla D, Arendt-Nielsen L, Vila-Cha C & Farina D. (2009). Motor unit conduction velocity during sustained contraction after eccentric exercise. *Med Sci Sports Exerc* **41,** 1927-1933.

Holobar A, Farina D, Gazzoni M, Merletti R & Zazula D. (2009). Estimating motor unit discharge patterns from high-density surface electromyogram. *Clin Neurophysiol* **120,** 551-562.

Holobar A, Glaser V, Gallego JA, Dideriksen JL & Farina D. (2012). Non-invasive characterization of motor unit behaviour in pathological tremor. *J Neural Eng* **9,** 056011.

Holobar A, Minetto MA, Botter A, Negro F & Farina D. (2010). Experimental Analysis of Accuracy in the Identification of Motor Unit Spike Trains From High-Density Surface EMG. *IEEE Trans Neural Syst Rehabil Eng* **18,** 221-229.

Holobar A, Minetto MA & Farina D. (2014). Accurate identification of motor unit discharge patterns from high-density surface EMG and validation with a novel signal-based performance metric. *J Neural Eng* **11,** 016008.

Holobar A & Zazula D. (2007). Multichannel blind source separation using convolution kernel compensation. *Ieee T Signal Proces* **55,** 4487-4496.

Kleine BU, van Dijk JP, Lapatki BG, Zwarts MJ & Stegeman DF. (2007). Using two-dimensional spatial information in decomposition of surface EMG signals. *J Electromyogr Kinesiol* **17,** 535-548.

Laine CM, Martinez-Valdes E, Falla D, Mayer F & Farina D. (in press). Motor neuron pools of synergistic thigh muscles share most of their synaptic input. *J Neurosci*.

Li X, Holobar A, Gazzoni M, Merletti R, Rymer WZ & Zhou P. (2015). Examination of Poststroke Alteration in Motor Unit Firing Behavior Using High-Density Surface EMG Decomposition. *IEEE Trans Biomed Eng* **62,** 1242-1252.

Marateb HR, McGill KC, Holobar A, Lateva ZC, Mansourian M & Merletti R. (2011). Accuracy assessment of CKC high-density surface EMG decomposition in biceps femoris muscle. *J Neural Eng* **8,** 066002.

Masuda T, Miyano H & Sadoyama T. (1985). The position of innervation zones in the biceps brachii investigated by surface electromyography. *IEEE Trans Biomed Eng* **32,** 36-42.

Merletti R, Holobar A & Farina D. (2008). Analysis of motor units with high-density surface electromyography. *J Electromyogr Kinesiol* **18,** 879-890.

Moritz CT, Barry BK, Pascoe MA & Enoka RM. (2005). Discharge rate variability influences the variation in force fluctuations across the working range of a hand muscle. *Journal of neurophysiology* **93,** 2449-2459.

Negro F, Holobar A & Farina D. (2009). Fluctuations in isometric muscle force can be described by one linear projection of low-frequency components of motor unit discharge rates. *J Physiol* **587,** 5925-5938.

Piitulainen H, Holobar A & Avela J. (2012). Changes in motor unit characteristics after eccentric elbow flexor exercise. *Scand J Med Sci Sports* **22,** 418-429.

Rainoldi A, Falla D, Mellor R, Bennell K & Hodges P. (2008). Myoelectric manifestations of fatigue in vastus lateralis, medialis obliquus and medialis longus muscles. *J Electromyogr Kinesiol* **18,** 1032-1037.

Semmler JG. (2002). Motor unit synchronization and neuromuscular performance. *Exerc Sport Sci Rev* **30,** 8-14.

Sherrington C. (1925). Remarks on some aspects of reflex inhibition *Proc R Soc Lond B Biol Sci***,** 19-45.

Vila-Cha C, Falla D & Farina D. (2010). Motor unit behavior during submaximal contractions following six weeks of either endurance or strength training. *Journal of applied physiology* **109,** 1455-1466.

Watanabe K, Gazzoni M, Holobar A, Miyamoto T, Fukuda K, Merletti R & Moritani T. (2013). Motor unit firing pattern of vastus lateralis muscle in type 2 diabetes mellitus patients. *Muscle Nerve* **48,** 806-813.

4.2. Study 2

TRACKING MOTOR UNITS LONGITUDINALLY ACROSS EXPERIMENTAL SESSIONS WITH HIGH-DENSITY SURFACE ELECTROMYOGRAPHY

E. Martinez-Valdes[1], F. Negro[2,3], C.M. Laine[3], D. Falla[4], F. Mayer[1], D. Farina[3,5]

Affiliations

1. Department of Sports Medicine and Sports Orthopaedics, University of Potsdam, Potsdam, Germany.

2. Department of Clinical and Experimental Sciences, Università degli Studi di Brescia, Brescia, Italy.

3. Institute of Neurorehabilitation Systems, Bernstein Focus Neurotechnology Göttingen (BFNT), Bernstein Centre for Computational Neuroscience (BCCN), University Medical Center Göttingen, Georg-August University, Göttingen, Germany.

4. Centre of Precision Rehabilitation for Spinal Pain (CPR Spine), School of Sport, Exercise and Rehabilitation Sciences, College of Life and Environmental Sciences, University of Birmingham, Birmingham, United Kingdom.

5. Department of Bioengineering, Imperial College London, Royal School of Mines, London, United Kingdom

Reference

Martinez-Valdes E, Negro F, Laine CM, Falla D, Mayer F & Farina D. (2017). Tracking motor units longitudinally across experimental sessions with high-density surface electromyography. The Journal of physiology 595, 1479-1496.

4.2.1. ABSTRACT

A new method is proposed for tracking individual motor units (MUs) across multiple experimental sessions in different days. The technique is based on a novel decomposition approach for high-density surface electromyography and was tested with two experimental studies for reliability and sensitivity. Experiment I (reliability): ten participants performed isometric knee extensions at 10, 30, 50 and 70% of their maximum voluntary contraction (MVC) force in three sessions, each separated by one week. Experiment II (sensitivity): seven participants performed 2 weeks of endurance training (cycling) and were tested pre-post intervention during isometric knee extensions at 10 and 30% MVC. The reliability (Experiment I) and sensitivity (Experiment II) of the measured MU properties were compared for the MUs tracked across sessions, with respect to all MUs identified in each session. In Experiment I, on average 38.3% and 40.1% of the identified MUs could be tracked across two sessions (one and two weeks apart), for the vastus medialis and vastus lateralis, respectively. Moreover, the properties of the tracked MUs were more reliable across sessions than those of the full set of identified MUs (intra-class correlation coefficients ranged between .63-.99 and .39-.95, respectively). In Experiment II, ~40% of the MUs could be tracked before and after the training intervention and training-induced changes in MU conduction velocity had an effect size of 2.1 (tracked MUs) and 1.5 (group of all identified motor units). These results show the possibility of monitoring MU properties longitudinally to document the effect of interventions or the progression of neuromuscular disorders.

4.2.2. INTRODUCTION

The neuromuscular system is highly adaptable. Improvements in motor performance can be observed after only a few training sessions (Aagaard, 2003; Selvanayagam *et al.*, 2011), while impairments in motor performance due to injury, inactivity or immobilization occur within a few days (Weibull *et al.*, 2011). Since short-term improvements in motor performance are usually not accompanied by changes in muscle structure (Aagaard, 2003), there has been wide interest to study the neural mechanisms underlying adaptations to training. For instance, the effects of strength and endurance training on motor performance reflect supraspinal and spinal adjustments (Adam & De Luca, 2005; Adkins *et al.*, 2006), which influence the neural drive to the muscles, i.e., motor unit behavior (Vila-Cha *et al.*, 2010).

Investigation of the behavior and properties of motor units provides a unique insight into the neural code underlying movements (Farina *et al.*, 2016). Yet, only a few studies have specifically analyzed motor unit adaptations to training (Duchateau *et al.*, 2006). This is mainly due to methodological limitations. Classic intramuscular fine wire or concentric needle electromyography only allows recording from few motor units concurrently. Moreover, it is not possible to follow the same motor units across experimental sessions with these classic methods (Carroll *et al.*, 2011). Therefore, the sample detected is too small and too variable across sessions to make inferences on adaptations in the motor unit pool of a muscle in longitudinal studies. The problem of a small sample, intrinsic to selective intramuscular recordings, has been addressed recently with novel multi-channel surface and intramuscular EMG systems that allow for a substantial enlargement of the number of concurrently detected motor units (Muceli *et al.*, 2015).

High-density surface electromyography (HDEMG) systems may also have the potential, not yet exploited, to track motor units across different sessions. This hypothesis is based on the observation that HDEMG provides a spatial sampling of the electrical activity of motor units over the skin plane and the large number of channels allows precise discrimination between different motor units (Farina et al., 2008). This spatial "signature" of each motor unit may be used for longitudinal tracking since it can be detected in an

almost identical manner once the electrode grid is placed in a similar location over the skin.

The likelihood of this conclusion increases for increasing number of channels since the probability that two motor units detected in different sessions present exactly the same spatial action potentials over tens of channels is negligible. The possibility of tracking motor units longitudinally with HDEMG during voluntary contractions has, however, never been verified.

In this study we aimed to track individual motor units, identified from HDEMG decomposition, across recording sessions performed in different days. For this purpose, we developed a new decomposition technique, as an extension of the convolutive blind source separation approach proposed in (Negro et al., 2016), with the introduction of the maximization of the cross-correlation of the motor unit action potential (MUAP) profiles. The approach was specifically designed to detect common sources over multiple sessions. To test the new method, we compared the motor unit action potentials and properties across days as well as pre and post two weeks of endurance training. The results revealed, for the first time, the possibility of identifying and studying the same motor units in humans over different days (separated by weeks), which opens new perspectives for studies on the neuromuscular adaptations to training and disease monitoring..

4.2.3. METHODS

4.2.3.1. Motor unit identification and tracking

The motor unit identification and tracking method is an extension of the convolutive blind source separation technique recently described in (Negro et al., 2016), derived from the convolution kernel compensation method (CKC) (Holobar & Zazula, 2007), with a different approach for convergence to the sources [see (Negro et al., 2016) for further information]. Here we adapted the convolutive blind source separation method to extract motor units with multi-channel action potential shapes maximally similar across sessions.

The convolutive mixture of HDEMG signals can be represented as a linear and instantaneous mixture of the spike trains of the individual motor units and their delayed versions (see Appendix A). Therefore, using an appropriate extension of the matrix of the

measurements (multi-channel EMG signals) and the specific properties of the sources (non-gaussianity/sparsity), it is possible to separate the activity of individual motor unit spike trains using techniques of linear instantaneous blind source separation (Negro et al., 2016). Briefly, after a de-correlation/whitening transformation applied to the extended measurements, a fixed point algorithm (Hyvarinen & Oja, 2000) is used to find a projection vector (linear filter) that maximizes the sparsity of the extracted source. The sparsity assumption is well satisfied by the spiking nature of the motor neurons. After a motor neuron spike train is correctly identified, its projection vector is removed from the solution space and the procedure is repeated to extract the next source. Since the measurement matrix is extended, the procedure extracts the original sources and their delayed versions. Therefore, the number and the order of extracted sources are not known a priori and depend on the number of iterations, the extension factor, and the spatial characteristics of the EMG signals..

In this study, a new method for the reliable extraction of common motor units in different recording sessions was implemented. After the full blind decomposition was performed on the first recording session, we applied a semi-blind separation procedure for the remaining sessions, focusing on finding only the sources that had MUAP profiles similar to the ones extracted from session 1. The decomposition procedure converged to the matched motor units first and then extracted motor units which could not be matched across sessions. In this way, it extracted a population of motor units divided in two groups. The first group consisted of the motor units that were tracked across more than one experimental session (tracked motor units); the second group included those units that were identified in only one experimental session (unmatched motor units). The group of unmatched motor units was analyzed across sessions with a sample size similar to the one used for the tracked motor units (see statistics and results). The normalized cross-correlation between the MUAP profiles was used as a measure of similarity. For each motor unit identified in session 1, we ran the semi-blind algorithm on the other sessions until a motor unit with normalized cross-correlation higher than 0.8 was found. On a limited number of trials (~15%) multiple matches with a cross correlation >0.8 were found. In such cases, the algorithm matched the highest cross-correlated sources and discarded the

other matches. Thus, the algorithm maximized the probability to find the matched motor units across different sessions and considerably reduced the computational load.

In the results presented in this study, we used an extension factor of 16 for the decomposition iteration and 50 samples for computing the similarity measures between de-whitened projection vectors (original multichannel filters or MUAP profiles). The choice of extension factor was similar to that in Negro et al., (Negro et al., 2016) for surface EMG signals sampled at 2048 Hz. The number of samples for computing similarity measures (corresponding to ~25 ms) was chosen to estimate the cross-correlation using the whole MUAP representation in each channel.

The mathematical details of the approach are provided in Appendix A.

4.2.3.2. Experimental tests

Two experiments were designed to test the proposed method and to prove its effectiveness at monitoring changes in motor unit properties compared to the classic approach of averaging results across the full population of identified units in each condition (Vila-Cha et al., 2010; Martinez-Valdes et al., 2016). From now on, the full sample of identified motor units (without matching across sessions) will be referred to as "total group of identified motor units". The first experiment (Experiment I) was designed to prove the reliability of the motor unit properties when estimated over different sessions without interventions on the subjects. This experiment was conducted by measuring motor unit properties over three sessions in two weeks. The motor units were tracked by the proposed method and their properties were estimated in each session. The reliability of these estimates was statistically analyzed when the motor units were tracked with respect to the total group of identified motor units and also to the unmatched motor units (subset of the total group of motor units that could not be tracked across sessions). The second experiment (Experiment II) was designed to test the sensitivity of motor unit tracking when measures were separated by a training intervention, which could also influence the shapes of the action potentials. Motor unit properties that were expected to change due to training were compared pre and post training, with and without tracking (total group of motor units).

The two experiments provide a strong experimental validation of the proposed method and of its effectiveness.

4.2.3.3. Subjects

Ten healthy and physically active men (mean (SD) age: 27 (4) years, height: 180 (8) cm, mass: 78 (10) kg) participated in the first experiment and seven healthy men (age: 28 (2) years, height: 177 (7) cm, mass 78 (9) kg) took part in the second longitudinal experiment (endurance training). All subjects were right leg dominant (determined by asking the subjects which leg they would use to naturally kick a ball). Exclusion criteria included any neuromuscular disorder as well as any current or previous history of knee pain and age < 18 or > 35 years. Participants were asked to avoid any strenuous activity 24 h prior to the measurements. The ethics committee of the Universitaetsmedizin Goettingen approved the first experiment (approval number 24/1/14), performed in Goettingen, and the ethics committee of the Universität Potsdam approved the training intervention (approval number 26/2015), performed in Potsdam, both in accordance with the declaration of Helsinki (2004). All participants gave written, informed consent.

4.2.3.4. Experiment I (Repeated measurements)

Participants attended the laboratory on three occasions. Consecutive sessions were 7 days apart and were conducted at the same time of the day for each subject on each occasion. In each experimental session, the participant was seated in an isokinetic dynamometer (Biodex System 3, Biodex Medical Systems Inc., Shirley, NY, USA), with the trunk reclined to 15° in an adjustable chair while the hip and distal thigh were secured to the chair. The rotational axis of the dynamometer was aligned with the right lateral femoral epicondyle and the lower leg was secured to the dynamometer lever arm above the lateral malleolus. Maximal and submaximal isometric knee extensions were exerted with the knee flexed to 90°. Subjects performed two maximal voluntary contractions (MVC) of knee extension each over a period of 5 s. These trials were separated by 2 min of rest. The highest MVC value was used as a reference for the definition of the submaximal force levels. In each of the three experimental sessions, the submaximal forces were expressed as a percent of the MVC measured during the same session. Five minutes of rest were provided after the MVC measurement. Then, following a few familiarization trials at low force levels, subjects performed submaximal ramped-isometric knee extension contractions to 10, 30, 50 and 70% MVC in a randomized order. In each trial, subjects received visual feedback of their knee extension force, which was displayed as a template that had a

triangular waveform [e.g., increased isometric leg extension force (ramp-up) from 0 to 50% MVC in 10 s and decrease of isometric extension force (ramp-down) from 50% to 0% in 10 s]. The contractions at 10% and 70% MVC lasted 14 s (ramp-up and ramp-down over 7 s, respectively) while the contractions at 30% and 50% MVC lasted 20 s (ramp-up and ramp-down over 10 s, respectively). In this study, we chose to decompose variable-force contractions, contrary to a previous study where we investigated constant force contractions (Martinez-Valdes et al., 2016). This was done to maximize the impact of tracking units on the reliability of the estimates of motor unit properties. Each force level was performed twice consecutively (with 30 s of rest between repetitions), however, only the second repetition was considered for further analysis. Rest periods of 2, 3, 4 and 5 minutes were allowed after the 10, 30, 50 and 70% MVC contractions, respectively. One additional MVC was performed at the end of each testing session to evaluate whether the protocol induced fatigue.

4.2.3.5. Experiment II (Endurance Training)

The experimental protocol consisted of a baseline session [i.e., HDEMG recordings, peak oxygen uptake (VO2peak) determination], a 2-week intervention of endurance training, and post-training session. For the baseline testing, prior to training, the subjects performed submaximal isometric knee extensions at 10 and 30% MVC (random order) on an isokinetic dynamometer (CON-TREX MJ, PHYSIOMED, Regensdorf, Switzerland), following the same procedure presented above (see Experiment I), with the only difference that visual feedback of knee extension force was displayed as a template that had a trapezoidal waveform (5 s ramps with a hold-phase duration of 20 s). Then, 24 h after the HDEMG-force measurements, the subjects performed an incremental test to exhaustion on an electronically braked cycle ergometer (Lode Excalibur Sport V2.0, Groningen, the Netherlands) to determine VO2peak using a gas analysis system (ZAN 600, Nspire Health, Oberthulba, Germany). Following a 3-min warm-up at 30 W, the test began with the workload increasing by 6 W every 12 s until volitional exhaustion. The revolutions per minute were maintained between 80 and 90, throughout the incremental test and training sessions. The value used for VO2peak corresponded to the highest value achieved over a 30 s collection period.

The training protocol commenced approximately 72 h after the incremental test and

consisted of six training sessions over 14 days. Each training session was performed on Mondays, Wednesdays, and Fridays. Training consisted of 90-120 min of continuous cycling at 65% of VO2peak (166.4 (20.1) W). The duration of exercise increased from 90 min during sessions 1 and 2 to 105 min during sessions 3 and 4, and to 120 min during sessions 5 and 6. This protocol has previously been determined to be sufficient to produce an increase in endurance performance and aerobic capacity (Gibala et al., 2006). An investigator of the study (E.M-V) supervised all training sessions. The post-training session (HDEMG recordings and incremental test) was identical to the baseline-testing procedures and was performed approximately 72 h post training to reduce the effects of post-training fatigue in all measurements (Gibala et al., 2006).

This training regime has been shown to enhance muscle fiber membrane excitability through changes in Na+ -K+ -ATPase activity (Green et al., 2004). Therefore, we hypothesized that the current protocol would also induce changes in motor unit conduction velocity of the vasti muscles, which have only been previously reported in a longer endurance training intervention (6 weeks) with much lower weekly training volume (Vila-Cha et al., 2010; Vila-Cha et al., 2012)..

4.2.3.6. Data Acquisition

Surface EMG signals were recorded in monopolar derivation with a two-dimensional (2D) adhesive grid (SPES Medica, Salerno, Italy) of 13 × 5 equally spaced electrodes (each of 1 mm diameter, with an inter-electrode distance of 8 mm), with one electrode absent from the upper right corner. First, the skin of the participants was marked according to guidelines [see (Barbero *et al.*, 2012) for details], for appropriate electrode orientation. Furthermore, to ensure optimal electrode placement, EMG signals were initially recorded during a brief voluntary contraction during which a linear non-adhesive electrode array was moved over the skin to detect the location of the innervation zone and tendon regions, as previously described (Masuda *et al.*, 1985; Farina *et al.*, 2001). After skin preparation (shaving, abrasion and alcohol), the electrode cavities of the grids were filled with conductive paste (SPES Medica, Salerno, Italy) and the grids positioned between the proximal and distal tendons of the Vastus Lateralis (VL) and Vastus Medialis (VM) muscles with the electrode columns (comprising 13 electrodes) oriented along the muscle fibers. Reference electrodes were positioned at the right ankle and patella. The

location of the electrodes was marked on the skin of the participants using a surgical pen, allowing similar electrode positioning across the experimental sessions.

Force and EMG signals were sampled at 2048 Hz and converted to digital data by a 12-bit analogue to digital converter (EMG-USB 2, 256-channel EMG amplifier, OT Bioelettronica, Torino, Italy, 3dB, bandwidth 10-500 Hz). EMG signals were amplified by a factor of 2000, 1000, 500 and 500 for the 10, 30, 50 and 70% MVC contractions, respectively. Data were stored on a computer hard disk and offline analyzed with Matlab (The Mathworks Inc., Natick, Massachusetts, USA). Finally, before decomposition, the 64-monopolar EMG channels were re-referenced offline to form 59 bipolar derivations, as the differences between adjacent electrodes in the direction of the muscle fibers.

4.2.3.7. Signal analysis

The new method for motor unit identification and maximization of the common sources across sessions described in Motor unit identification and tracking was applied to extract the MUAPs from the acquired HDEMG data. The discharge times of the identified motor units were converted in binary spike trains in which each data sample was assigned a value of 0 or 1, depending on whether or not the data sample marked the onset of an action potential for a given motor unit. Recruitment and de-recruitment thresholds for each motor unit were defined as the torque (Nm) at the times when the motor unit began and stopped repetitively discharging action potentials. Discharge times that were separated from the next by >200 ms were excluded from the estimation of recruitment and de-recruitment thresholds to avoid aligning the thresholds with noise-generated discharges (Farina et al., 2009). The mean discharge rate was defined as the average discharge rate during the interval of time of activation.

As a quality control, only motor units with a coefficient of variation for the inter-spike interval (CoVisi) <30% (Laine et al., 2015), with a silhouette (SIL) > 0.90 [see (Negro et al., 2016) for details] were considered for further analysis. SIL is the difference between the within- and between-cluster sums of point-to-centroid distances, normalized dividing by the maximum of the two values. SIL is an accuracy index for EMG decomposition similar to the pulse-to-noise ratio [see (Holobar et al., 2014) for details]. However, since SIL is a normalized measure, it can be directly associated to the accuracy of the decomposition (Negro et al., 2016). Finally, discharges that were separated from the

next by <33.3 ms or >200 ms (30 and 5 Hz, respectively) were excluded from the mean discharge rate and the coefficient of variation of inter-spike interval (CoVisi) calculations because these discharges are rare for the vasti muscles at submaximal contraction forces and therefore are likely to be due to decomposition errors (Martinez-Valdes et al., 2016).

Motor unit conduction velocity was estimated from double differential derivations of the single motor unit surface multi-channel action potentials in the longitudinal direction (Farina et al., 2001). The channels selected for conduction velocity estimates were based on the criterion of a minimal change in shape of the action potential during propagation. The acceptance criterion for conduction velocity estimates was based on the correlation coefficient of the delayed action potentials (threshold set to 90%). Since the accuracy of motor unit conduction velocity estimates increases with the number of channels used (Farina & Mesin, 2005), we selected the largest amount of channels that showed a cross-correlation >90% (3 to 8 double differential channels were used). Additionally, values beyond the physiological range (2–6 m/s) were excluded (Andreassen & Arendt-Nielsen, 1987). Finally, peak-to-peak (p2p) amplitude values were averaged across all the channels of the electrode grid, as presented previously (Martinez-Valdes et al., 2016).

4.2.3.8. Statistical Analysis: General

Results are expressed as mean and standard deviation (SD) unless otherwise stated. Before comparisons, all variables were tested for normality using the Shapiro-Wilk test. The assumption of sphericity was checked by the Mauchley's test and, if violated, the Greenhouse-Geisser correction was made to the degrees of freedom. Statistical significance was set at $p < 0.05$.

4.2.3.9. Statistical analysis: Experiment I

MVCs from the beginning and end of each session were compared using a paired t-test and the MVCs performed at the beginning of each session were compared by one-way analysis of variance (ANOVA). Paired t-tests were used to check the effect of time on the number of tracked motor units (sessions 1-2 vs. 1-3 and 2-3 vs. 1-3). Therefore, we compared the number of tracked motor units between sessions that were one (sessions 1-2 and 2-3) and two weeks apart (sessions 1-3), at each force level (10, 30, 50 and 70% MVC) and muscle (VM and VL), independently.

All motor unit variables (recruitment-de-recruitment threshold, mean discharge rate

and conduction velocity) were analyzed for reliability at each force level (10, 30, 50 and 70% MVC) and muscle (VM and VL), independently. The level of reliability of the variables extracted from matched motor units (proposed method), from the total group of identified motor units (independent decompositions using averaged motor unit population samples, including both matched and unmatched motor units), and unmatched motor units (random sample of motor units that could not be tracked across sessions, with a sample size similar to the ones used for tracked motor units) between sessions 1 and 3 was determined by the intra-class correlation coefficient (ICC 2,1). ICC scores between 0.8-1 were interpreted as "excellent", 0.6-0.8 "good" and <0.6 "poor" (Bartko, 1966). Additionally, a paired t-test was performed to detect significant differences between sessions. The absolute reliability was obtained by the standard error of the measurement (SEM=SD $\sqrt{}$(1-ICC)). The level of reliability of motor units that were matched across the three sessions was determined by ICC2,1, while a one-way repeated measures ANOVA was used to detect any significant differences between sessions. For the sake of clarity, results are presented only for motor units tracked between sessions 1-3 and 1-2-3. Reliability results (ICC and SEM) were averaged between all force levels (10, 30, 50 and 70% MVC) and presented for each variable and muscle independently.

Finally, the motor unit tracking procedure was also applied across the different force levels within each session. Motor units were tracked between 10 vs. 30, 30 vs. 50 and 50 vs. 70% MVC. The $ICC_{2,1}$ was used to evaluate the reliability of conduction velocity and p2p amplitude values of motor units that were tracked between the different force levels on each session.

4.2.3.10. Statistical analysis: Experiment II

The estimate of single motor unit conduction velocity was chosen as representative variable to compare pre and post training. The values of this variable estimated for matched and unmatched motor units, pre and post intervention, were compared by paired t-test. Additionally, the Cohen's *d* was used to estimate the effect size (ES). A Cohen's *d* less than 0.2 was classified as "trivial", 0.2-0.5 as "small", 0.5-0.8 as "moderate", and greater than 0.8 as "large" (Cohen, 1988).

4.2.4. RESULTS

4.2.4.1. Experiment I

Maximal voluntary knee extension force performed at the beginning of each session did not differ between sessions (p = 0.099). Furthermore, there was no significant change in MVC across each experimental session (p = 0.55, 0.13 and 0.08, for sessions 1, 2 and 3, respectively). The total and average number of accurately decomposed motor units from both muscles (CoV_{isi} < 30% and SIL >0.9) is presented for each session and force level in **Table 4**.

Table 4. Total of accurately decomposed motor units.

	Force Level (% MVC)	Vastus Medialis			Vastus Lateralis		
		Session 1	Session 2	Session 3	Session 1	Session 2	Session 3
Total MUs	10%	50	57	49	66	67	72
	30%	74	83	69	67	75	73
	50%	62	56	59	62	58	59
	70%	31	35	42	23	26	25
Average MU p/subject	10%	5.0 (1.3)	5.7 (2.3)	5.4 (1.5)	7.2 (3.5)	7.4 (3.4)	7.2 (3.0)
	30%	7.4 (2.7)	8.3 (3.1)	6.8 (2.7)	6.7 (3.1)	7.5 (3.9)	7.3 (4.1)
	50%	6.0 (3.1)	5.5 (2.7)	6.3 (3.7)	6.0 (3.7)	5.7 (3.1)	6.2 (3.1)
	70%	3.4 (1.7)	3.6 (2.1)	4.9 (2.9)	3.3 (2.2)	3.3 (2)	3.3 (2.3)

Total and average number of accurately decomposed motor units (MU) [mean (SD)]. Results are presented for each muscle (vastus medialis, vastus lateralis), session (1,2 and 3) and force level [10, 30, 50 and 70% of the maximum voluntary contraction (MVC)], independently.

Figure 7 shows an example of the motor unit decomposition and tracking procedure for VM and VL during ramped isometric contractions at 50% of MVC (Fig. 1a). The MUAPs shown in Figure 1 [which correspond to a motor unit identified in session 1 (blue) and 3 (red)] had a similarity measure (cross-correlation coefficient) greater than 90% (Fig 7b), and therefore, they were associated to the same unit. The visual inspection of the action potential shapes confirms the correct automatic identification of the same motor unit. Following the automatic procedure, the number of tracked motor units across two sessions varied between [mean (range)] 21 (6 - 34) and 23 (6 – 40), while for three sessions it was possible to track 11 (8 -17) and 11 (1-16) motor units for VM and VL, respectively, across all force levels (from 10 to 70% MVC), in the 10 subjects (mean number of tracked motor units per subject was 2.2 (0.1) and 1.4 (0.5) for VM, and 2.3 (0.4)

and 1.3 (0.1) for VL, across two and three sessions, respectively). Therefore, a mean (range) of 38.3 (16.5 – 46.5)% and 40.1 (24.5 – 54.1)% of motor units from those identified by decomposition could be tracked across two sessions, while 21.0 (13.6 – 25.0)% and 16.3 (4.1 – 23.4)% could be tracked across the three sessions for VM and VL, respectively. Overall, the number of tracked motor units remained relatively constant at 10, 30 and 50% MVC between all sessions comparisons; however, it decreased at 70% MVC **(Table 5)**, where only 1 motor unit could be tracked across the three sessions for VL. Finally, the number of tracked motor units remained consistent in time since there were no significant differences in the number of tracked motor units between sessions separated by one (1-2 and 2-3) or two weeks (1-3), in both muscles and at all force levels ($p > 0.05$) (**Table 5**). Further details regarding the total number of matched motor units, the cross correlation coefficients between tracked and unmatched motor units (average cross correlation coefficient was calculated from the maximum cross correlation coefficient obtained from all possible unmatched motor unit comparisons) and the percentage of tracked motor units from the total across 2 and 3 sessions comparisons are shown in **Table 5**.

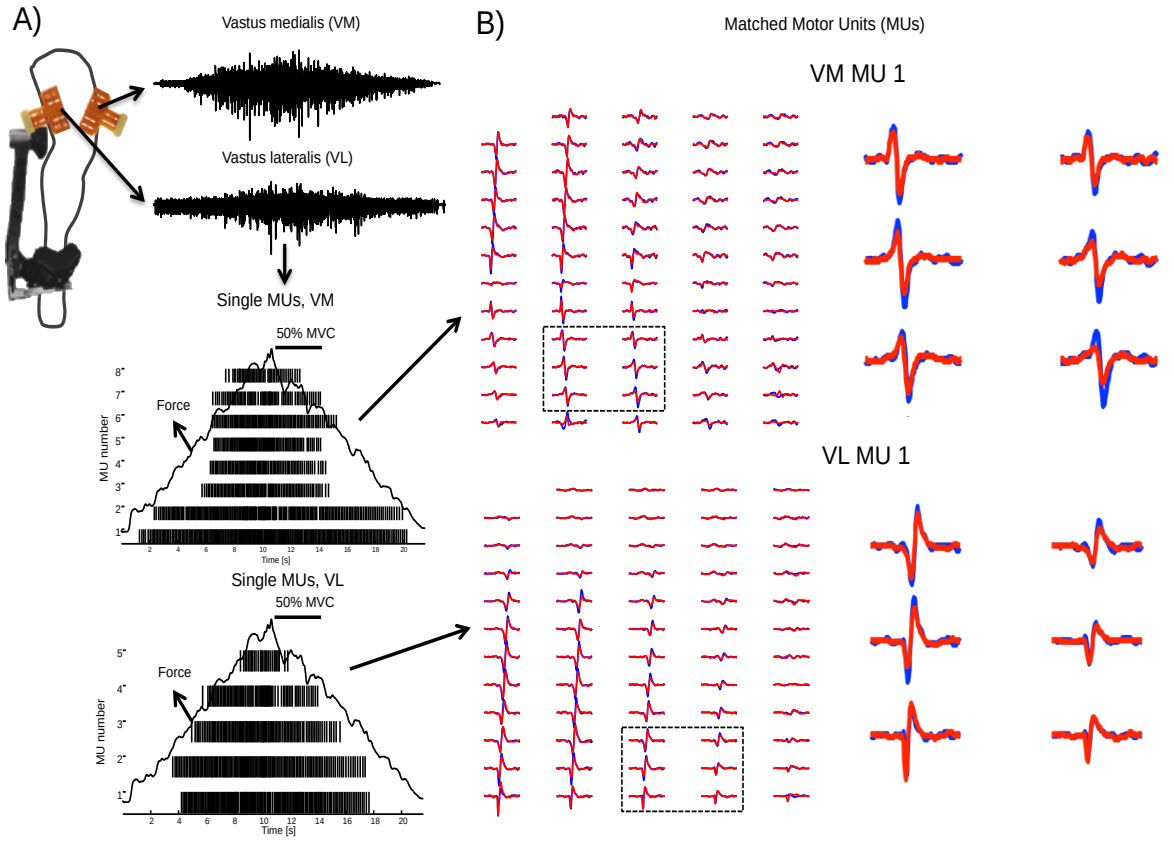

Figure 7. A) High-density surface EMG signals (64 channels) were recorded from the vastus medialis (VM) and vastus lateralis (VL) muscles during a ramp isometric knee extension [50% of the maximum voluntary contraction (MVC)]. The EMG signals were decomposed to reveal the firing activities of single motor units. A schematic representation of the task and motor unit (MU) recording methodology is shown in the left half of the figure. B) The procedure developed in the study was then used to identify two matched MUs between the first and the last session of experiment I. The cross-correlation between the projecting vectors of the identified MUs was higher than 90%. Multichannel action potentials (59 bipolar channels) of the original (blue) and matched (red) MUs are shown to confirm their similar MU action potential shapes. Two matched MUs are being shown on the right side of the figure (1 for VM, up and 1 for VL, down). For clarity, MU action potentials inside the dashed boxes are zoomed in the right half of the figure. Those matched MUs had cross correlation coefficients > 0.9.

Table 5. Number, percentage of tracked motor units and cross correlation coefficients from tracked and unmatched motor units across sessions.

	Force Level (% MVC)	Vastus Medialis				Vastus Lateralis			
		Sessions 1-2	Sessions 2-3	Sessions 1-3	Sessions 1,2,3	Sessions 1-2	Sessions 2-3	Sessions 1-3	Sessions 1,2,3
Tracked MU (N, %)	10%	23 (43%)	22 (42%)	23 (47%)	11 (21%)	22 (33%)	30 (43%)	26 (38%)	16 (23%)
	30%	34 (45%)	31 (41%)	25 (35%)	17 (23%)	28 (39%)	40 (54%)	31 (44%)	16 (22%)
	50%	19 (32%)	22 (38%)	20 (33%)	8 (14%)	25 (42%)	24 (41%)	16 (26%)	9 (15%)
	70%	15 (46%)	16 (42%)	9 (17%)	9 (25%)	6 (25%)	15 (58%)	9 (38%)	1 (4%)
CCC Tracked (%)	10%	88.3 (3.9)	87.4 (3.2)	83.2 (3.1)	87.9 (2.6)	84.8 (3.7)	86 (4.1)	84.4 (6)	86 (2.4)
	30%	84.8 (3.8)	84.4 (4.6)	83.3 (3.3)	86.8 (3.4)	86.2 (4.6)	86.4 (3)	81 (3.7)	87.4 (3.6)
	50%	84.2 (3.5)	83.9 (4.5)	83.6 (5.8)	85.1 (3.7)	85.1 (4.9)	86.9 (3.3)	81 (3.9)	85.4 (4.5)
	70%	83.2 (4.2)	85.6 (2.5)	81 (3.9)	85.6 (1.4)	83.3 (4.2)	85.6 (2.5)	81 (3.9)	80
CCC Unmatched (%)	10%	58.7 (4.7)	59.3 (3.7)	59.9 (4.6)	59.3 (4.2)	53.6 (5.7)	55.1 (4.2)	55.9 (4.8)	54.9 (4.7)
	30%	65.6 (6.7)	64.5 (7.3)	64.4 (6.9)	64.8 (6.7)	59.6 (6.1)	59.4 (5.2)	57.2 (5.5)	58.7 (4.3)
	50%	68.5 (2.6)	68.4 (2.8)	68.2 (3.9)	68.9 (2.5)	62.3 (5.2)	66.5 (4.8)	62.8 (6.5)	63.9 (3.7)
	70%	68.6 (4.4)	68.7 (4.9)	63.7 (7.9)	67.1 (4.3)	63.6 (8.4)	66.9 (8.3)	62.6 (7.4)	63.9 (7.4)

Total number (N) and percentage of tracked motor units (MUs). Cross correlation coefficients (CCC) [mean (SD)] are presented for each session comparisons at each force level for matched and unmatched motor units (sample of units that could not be tracked across sessions). The number of tracked MUs (%) represents the percentage of MUs that could be tracked from the total number of accurately identified MUs between sessions. Percentages of tracked MUs from sessions 1,2,3 were obtained by averaging the total number of decomposed MUs across the 3 sessions (Table1). Note that (SD) for vastus lateralis at 70% MVC (Sessions 1,2,3) is not shown, as only 1 MU could be matched across the 3 sessions.

The absolute values of the variables extracted from the motor units that were matched between the three sessions are presented in **Table 6**. Overall, mean discharge rates and conduction velocity increased with force and presented values within physiological range, while the recruitment thresholds were similar to the de-recruitment thresholds **(Table 6)**. A representative example of MUAPs corresponding to three different VM motor units (identified from session 1) that could be tracked across the three sessions with a high similarity measure (cross-correlation coefficients > 80%) is shown in **Figure 8a**. The discharge timings of each matched motor unit, with their corresponding recruitment and de-recruitment thresholds (expressed as Nm torque) for each session are shown in **Fig. 8b**. Across sessions, the estimates of recruitment and de-recruitment thresholds for these matched motor units were stable, as expected. These results were confirmed by the good to excellent levels of reliability (ICCs > .60) found for the recruitment-de-recruitment thresholds, mean discharge rate and conduction velocity of all the tracked motor units in both muscles and across all force levels (see **Tables 7 and 8**). These results were consistent when variables were compared between two **(**session 1 vs. 3, **Table 7**) or three sessions (sessions 1,2,3, **Table 8**). These reliability indexes were substantially greater than those computed from the total group of identified motor units and

from the unmatched motor units (see Tables 4 and 5), strongly supporting (together with the shape similarity over all channels) the matching performed by the proposed method. None of the variables (from matched, total and unmatched motor units) changed significantly across sessions ($p > 0.05$).

Finally, for VM and VL, an average of 14 (3) motor units could be tracked between the different force levels within each session (10 vs. 30, 30 vs. 50 and 50 vs. 70% MVC). This represented 24 (6) % of the motor units identified between those force levels. As expected, the tracked motor units showed high cross correlation coefficients (average 91.1 (1.1) %) and good to excellent levels (ICCs>0.60) of reliability for conduction velocity and p2p amplitude (**Table 9**).

Table 6. Motor unit variables in absolute values

	Force	Vastus Medialis			Vastus Lateralis		
	(% MVC)	Session 1	Session 2	Session 3	Session 1	Session 2	Session 3
Recruitment threshold (Nm)	10%	14.8 (3.9)	14.9 (5.4)	14.2 (5.6)	9.5 (5.2)	9.8 (5.4)	10.3 (5.6)
	30%	32.0 (15.2)	32.6 (14.4)	32.6 (13.0)	23.6 (16.9)	23.9 (15.0)	24.1 (16.4)
	50%	71.6 (33.3)	72.7 (36.3)	69.5 (29.1)	70.0 (29.5)	71.6 (34.8)	70.2 (28.2)
	70%	105.0 (22.9)	104.7(30.8)	110.3(33.6)	77.1	81.1	78.7
De-recruitment threshold (Nm)	10%	11.2 (4.9)	12.0 (3.9)	11.4 (4.5)	9.0 (4.2)	9.0 (4.8)	10.0 (4.1)
	30%	35.4 (12.4)	37.6 (12.3)	37.3 (10.4)	24.9 (15.6)	25.2 (16.3)	25.1 (14.1)
	50%	75.9 (33.2)	76.4 (27.5)	75.5 (36.5)	73.9 (27.1)	79.6 (29.8)	76.9 (32.2)
	70%	117.9 (32.6)	120.7(37.3)	120.7(39.8)	113.0	110.7	115.6
Mean discharge rate (Hz)	10%	9.4 (1.3)	9.3 (1.3)	9.2 (1.4)	9.7 (1.6)	9.7 (1.8)	9.6 (1.7)
	30%	10.5 (1.0)	10.7 (1.1)	10.3 (0.7)	10.6 (1.1)	10.7 (1.2)	10.7 (1.1)
	50%	12.0 (2.3)	12.0 (2.3)	11.9 (2.0)	10.8 (1.4)	11.2 (1.9)	11 (1.6)
	70%	15.0 (3.1)	14.9 (2.8)	14.7 (2.1)	11.1	11.7	11.6
Conduction velocity (m/s)	10%	4.4 (0.4)	4.4 (0.4)	4.3 (0.3)	4.2 (0.3)	4.2 (0.3)	4.3 (0.3)
	30%	4.5 (0.2)	4.5 (0.2)	4.5 (0.3)	4.3 (0.2)	4.4 (0.3)	4.4 (0.2)
	50%	4.8 (0.6)	4.8 (0.5)	4.7 (0.3)	4.7 (0.4)	4.7 (0.4)	4.7 (0.4)
	70%	4.9 (0.5)	4.9 (0.4)	4.7 (0.4)	4.3	4.4	4.4

Motor unit (MU) variables results [mean (SD)] for MUs matched between sessions 1-2-3. Results are presented for each muscle (vastus medialis, vastus lateralis) and force level [10, 30, 50 and 70% of the maximum voluntary contraction (MVC)], independently. Note that (SD) for vastus lateralis variables at 70% MVC is not shown, as only 1 MU could be matched across the 3 sessions.

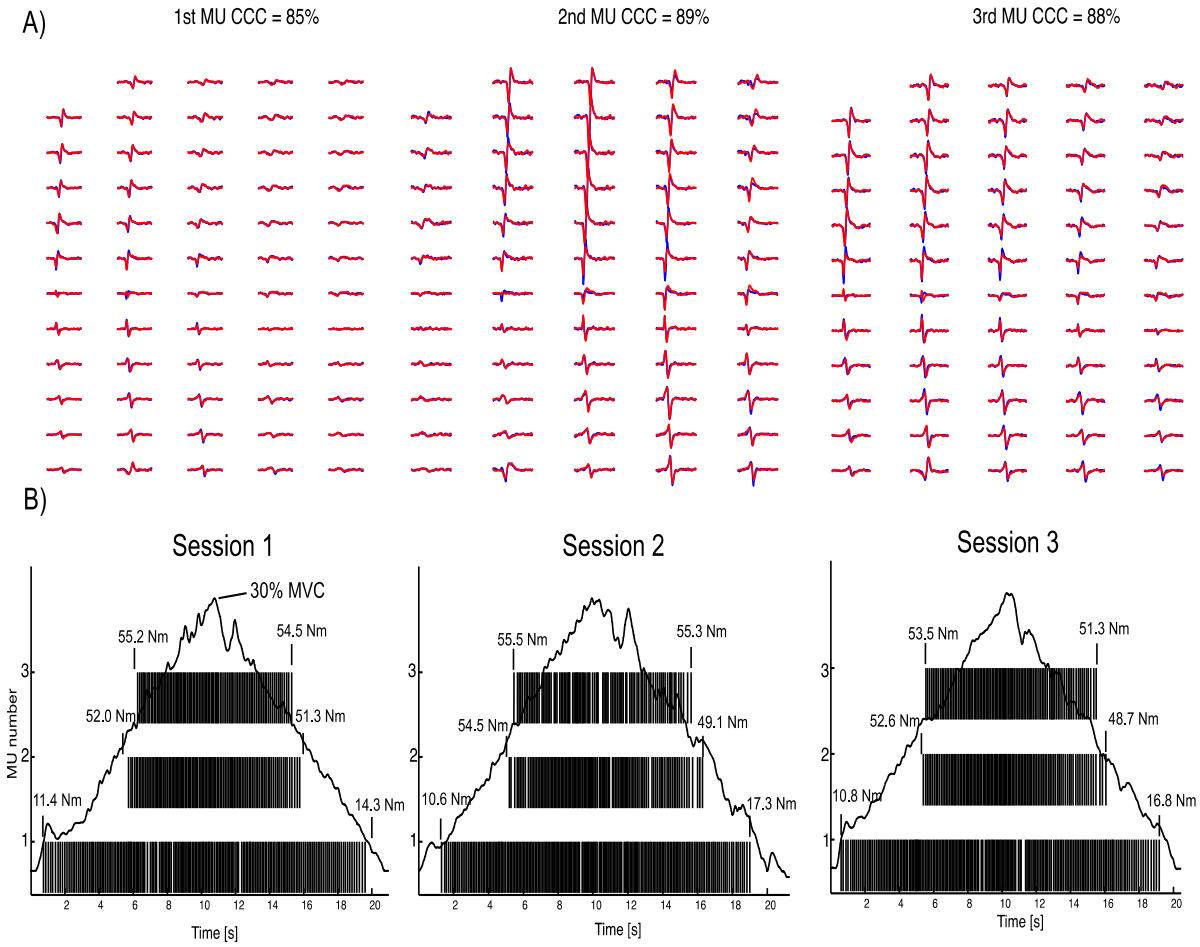

Figure 8. A) Multichannel surface action potentials of 3 different vastus medialis motor units (MUs) that were tracked across the three sessions. The cross correlation coefficients (CCCs) of the MU action potential projecting vectors between the three sessions can be seen above. For sake of clarity MU action potential matching is presented between two sessions only. MU action potentials extracted from the first session are presented in blue while matched action potentials from the second session are presented in red. B) Discharge times of each matched MU during ramped contractions at 30% MVC during the 3 sessions, note the similarity of their recruitment and de-recruitment thresholds.

Table 7. Reliability of tracked, total and unmatched motor units from sessions 1 and 3

	Matched MUs				Total MUs				Unmatched MUs			
	Vastus Medialis		Vastus Lateralis		Vastus Medialis		Vastus Lateralis		Vastus Medialis		Vastus Lateralis	
	ICC	SEM	ICC	SEM	ICC	SEM	ICC	SEM	ICC	SEM	ICC	SEM
Recruitment Threshold (Nm)	.92 (.89 - .96)	5.1 (1.8 - 8.5)	.92 (.88 - .94)	4.5 (1.5 - 6.3)	.75 (.54 - .95)	5.8 (1.6 – 10.2)	.63 (0.41 - .92)	7.0 (1.5 – 11.5)	.29 (.15 - .73)	14 (4.2 -21.3)	.44 (.34 - .49)	14.5 (3.4 - 22.7
De-recruitment Threshold (Nm)	.86 (.71 - .95)	6.3 (2.4 - 8.8)	.87 (.82 - .92)	6.6 (2.0 - 12.4)	.57 (.43 - .70)	10.1 (2.2 - 14.4)	.66 (.52 - .93)	7.1 (2.7 – 13.7)	.36 (.21 - .50)	16.3 (4.2 – 24.1)	.46 (.41 - .60)	15.3 (4.7 – 24.8)
Mean discharge rate (Hz)	.77 (.72 - .83)	0.8 (0.6 – 0.9)	.87 (.78 - .91)	0.6 (0.6 – 0.7)	.56 (.39 - .73)	1.1 (0.8 – 1.4)	.61 (.42 - .89)	1.0 (0.7 – 1.5)	.31 (-.11 - .59)	1.6 (1.1 – 2.3)	.38 (.21 - .54)	1.5 (1.0 – 2.5)
Conduction Velocity (m/s)	.84 (.83 - .87)	0.18 (0.16 – 0.21)	.88 (.84 - .99)	0.12 (0.07 – 0.12)	.66 (.43 - .86)	0.21 (0.16 – 0.25)	.56 (.51 - .67)	0.22 (0.14 - 0.27)	.25 (.05 - .45)	0.35 (0.3 – 0.39)	.30 (.15 - .57)	0.64 (0.44 – 0.95)

Reliability values are averaged across all contraction levels (10, 30, 50 and 70% of the maximum voluntary contraction) and presented as mean (range) for each variable and muscle (vastus medialis, vastus lateralis). Between sessions comparisons were non- statistically significant for all variables at all force levels, for both muscles ($p > 0.05$). ICC, intra-class correlation coefficient; SEM, standard error of the measurement.

Table 8. Reliability of tracked, total and unmatched motor units from all sessions

	Matched MUs				Total MUs				Unmatched MUs			
	Vastus Medialis		Vastus Lateralis		Vastus Medialis		Vastus Lateralis		Vastus Medialis		Vastus Lateralis	
	ICC	SEM	ICC	SEM	ICC	SEM	ICC	SEM	ICC	SEM	ICC	SEM
Recruitment Threshold (Nm)	.92 (.89 - .97)	5.2 (1.7 - 9.6)	.93 (.91 - .96)	4.8 (1.4 - 9.7)	.81 (.73 - .94)	6.4 (1.9 – 9.6)	.73 (.65 - .74)	6.2 (2.0 – 9.7)	.29 (.16 - .39)	14.5 (5.2 – 19.8)	.42 (.13 - .66)	14.6 (3.6 – 22.4)
De-recruitment Threshold (Nm)	.81 (.75 - .92)	7.1 (2.2 - 17.6)	.89 (.83 - .93)	4.8 (1.7 - 8.4)	.70 (.67 - .82)	9.3 (3.9 – 14.4)	.73 (.62 - .88)	7.2 (1.6 – 13.5)	.38 (.27 - .49)	16.2 (3.9 – 25.8)	.47 (.27 - .59)	15.5 (3.8 – 25.2)
Mean discharge rate (Hz)	.83 (.63 - .94)	0.6 (0.6 – 0.7)	.84 (.74 - .90)	0.6 (0.5 – 0.6)	.70 (.58 - .82)	0.9 (0.6 – 1.1)	.76 (.64 - .87)	0.8 (0.5 – 1.1)	.30 (.07 - .59)	1.5 (1.1 – 2.4)	.48 (.26 - .62)	1.4 (0.8 – 2.0)
Conduction Velocity (m/s)	.83 (.78 - .87)	0.16 (0.12 – 0.21)	.88 (.83 - .94)	0.10 (0.10 – 0.11)	.73 (.61 - .85)	0.32 (0.17 – 0.21)	.66 (.57 - .77)	0.2 (0.13 – 0.28)	.16 (-.29 - .36)	0.4 (0.35 - 0.58)	.39 (.32 - .46)	0.44 (0.35 – 0.56)

Reliability values are averaged across all contraction levels (10, 30, 50 and 70% of the maximum voluntary contraction) and presented as mean (range) for each variable and muscle (vastus medialis, vastus lateralis). Between sessions comparisons were non-statistically significant at all force force levels, for both muscles ($p > 0.05$). ICC, intra-class correlation coefficient; SEM, standard error of the measurement. Note that reliability for VL at 70% MVC was not calculated (for matched motor units results), since only one motor unit could be tracked across the three sessions.

Table 9. Number, percentage and reliability of tracked motor units across the different force levels within a session

Force levels MVC%	Vastus Medialis				Vastus Lateralis			
	Motor Units (N,%)	CCC (%)	CV ICC	p2p amp. ICC	Motor Units (N,%)	CCC (%)	CV ICC	p2p amp. ICC
10 vs. 30	13 (21%)	90.7 (0.3)	.88 (.81-.93)	.82 (.78-.84)	12 (17%)	93.2 (0.7)	.94 (.89-.95)	.82 (.69-.93)
30 vs. 50	13 (19%)	90.2 (0.8)	.72 (.60-.95)	.73 (.59-.84)	19 (29%)	91.4 (0.1)	.88 (.80-.92)	.93 (.91-.94)
50 vs. 70	15 (31%)	90.0 (0.4)	.91 (.88-.94)	.77 (.64-.96)	11 (26%)	91.0 (0.1)	.92 (.83-.97)	.87 (.74-.96)

Total number (N) and percentage (extracted from the total number of motor units identified between force levels) of tracked motor units across the different force levels (10 vs. 30, 30 vs. 50 and 50 vs. 70% MVC) within each session. The cross correlation coefficients (CCC) [mean (SD)] and intra-class correlation coefficients [mean (range)] for conduction velocity (CV) and peak-to-peak (p2p) amplitude are also presented. For sake of clarity, results are averaged across all sessions.

4.2.4.2. Endurance training

After the intervention, incremental cycling peak power output significantly increased from 347.4 (63.2) W to 370.3 (56.9) W, p=0.0004, ES=2.6. VO2peak also increased significantly after intervention from 45.1 (6.7) ml/kg/min to 48.4 (4.6) ml/kg/min, p=0.031, ES=1.1. Peak torque did not differ pre and post intervention (pre: 249.4 (71.6) Nm vs. post: 245.7 (59.6) Nm, p=0.5008, ES=0.3).

For VM, a total of 57 and 77 motor units could be decomposed (CoVisi < 30% and SIL >0.9), while for VL a total of 59 and 52 units were decomposed at 10% and 30% MVC, respectively. From these units, 44.1% and 41.4% could be tracked post-training for VM and, 66.7% and 42.5% could be tracked for VL at 10% and 30% MVC, respectively (average cross-correlation coefficient of 87.0%). Figure 9 shows the motor unit tracking procedure from a representative subject at 30% MVC pre and post intervention. Even though both VM (fig. 9a) and VL (fig. 9b) showed a large increase in conduction velocity (10.2% and 11.5% increase, respectively), the shape of their MUAPs remained consistent between pre and post testing sessions as confirmed by the large cross correlation coefficients between MUAPs (91.0% and 90.3% for VM and VL, respectively).

Finally, conduction velocity was compared pre-post training to check for the sensitivity of the proposed motor unit tracking method to changes induced by training. For VM, motor unit conduction velocity increased significantly with training when computed for the matched motor units at both 10% (pre: 4.19 (0.27) vs. post: 4.37 (0.28) m/s, p=

0.013, ES=1.3) and 30% MVC (pre: 4.51 (0.32) vs. post: 4.71 (0.25) m/s, p=0.003, ES=1.9). These differences were smaller for the total group of identified motor units at both 10% (pre: 4.22 (0.28) vs. post: 4.31 (0.22) m/s, p=0.0585, ES=0.9) and 30% MVC (pre: 4.54 (0.31) vs. post: 4.65 (0.24) m/s, p=0.0514, ES=0.9), for which significant differences were not found. To explain the difference in the results for the matched and total group of identified motor units, Figure 10 shows individual motor unit conduction velocity results (pre and post training) of the 7 participants when using matched (Figure 10a, left) and total group of identified units (Figure 10a, right) at 30% MVC (VM). The data from all subjects presented in Figure 10a (left) show a clear intervention effect when tracking the same motor units that was masked when the motor units were not matched [Figure 10a (right)], with 2 subjects showing no effect of the intervention without tracking. One of these subjects is highlighted in red (Fig. 10a and 10b). The results for the highlighted subject can be seen in Figure 4b. The twelve matched motor units (Fig. 10b, left) of this subject showed a clear intervention effect with a large effect size (p=0.004, ES=1.0). However, this difference could no longer be observed when using all motor units [p=0.595 (unpaired t-test), ES=0.1, Fig. 10b, right]. Similarly, for VL, conduction velocity increased significantly at 10% (pre: 4.14 (0.22) vs. 4.35 (0.19) m/s, p=0.0006, ES=2.5) and 30% MVC (pre: 4.37 (0.27) vs. 4.59 (0.28) m/s, p=0.0004, ES=2.7) for the matched motor units as well as for the total group of motor units at 10% (pre: 4.17 (0.21) vs. post: 4.34 (0.19) m/s, p=0.0008, ES=2.3) and 30% MVC (pre: 4.39 (0.27) vs. post: 4.58 (0.26) m/s, p=0.0018, ES=2.0).

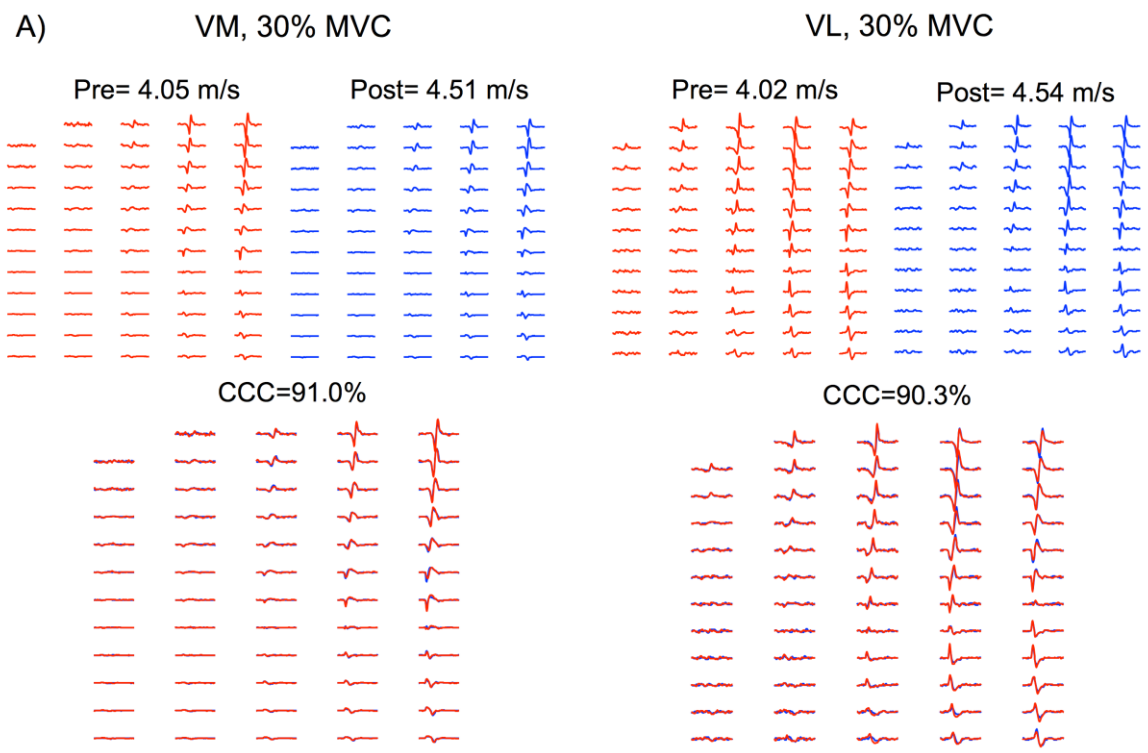

Figure 9. A) Motor unit conduction velocity (CV) values from the vastus medialis (VM) at 30% of the maximum voluntary contraction (MVC) from n=7 subjects, previously (PRE) and after (POST) an endurance training intervention. Left graph shows results obtained with tracked motor units, while right graph shows the results obtained using unmatched motor units (CV values were averaged per subject and compared PRE and POST intervention). The effect size and p-values of the two procedures are shown in the lower right corner of all graphs. The dashed line depicts an example of one subject that showed an increase in CV of matched motor units (left), which is masked when using unmatched motor units (right). B) Matched (left) and unmatched (right) motor units (mean and 95% confidence interval), from the same subject depicted in A (dashed line). The 12 matched motor units from this subject show a clear intervention effect (left graph), which is not possible to distinguish when using all decomposed motor units [CV values are extracted from all the motor units decomposed pre and post intervention (two repetitions per session)].

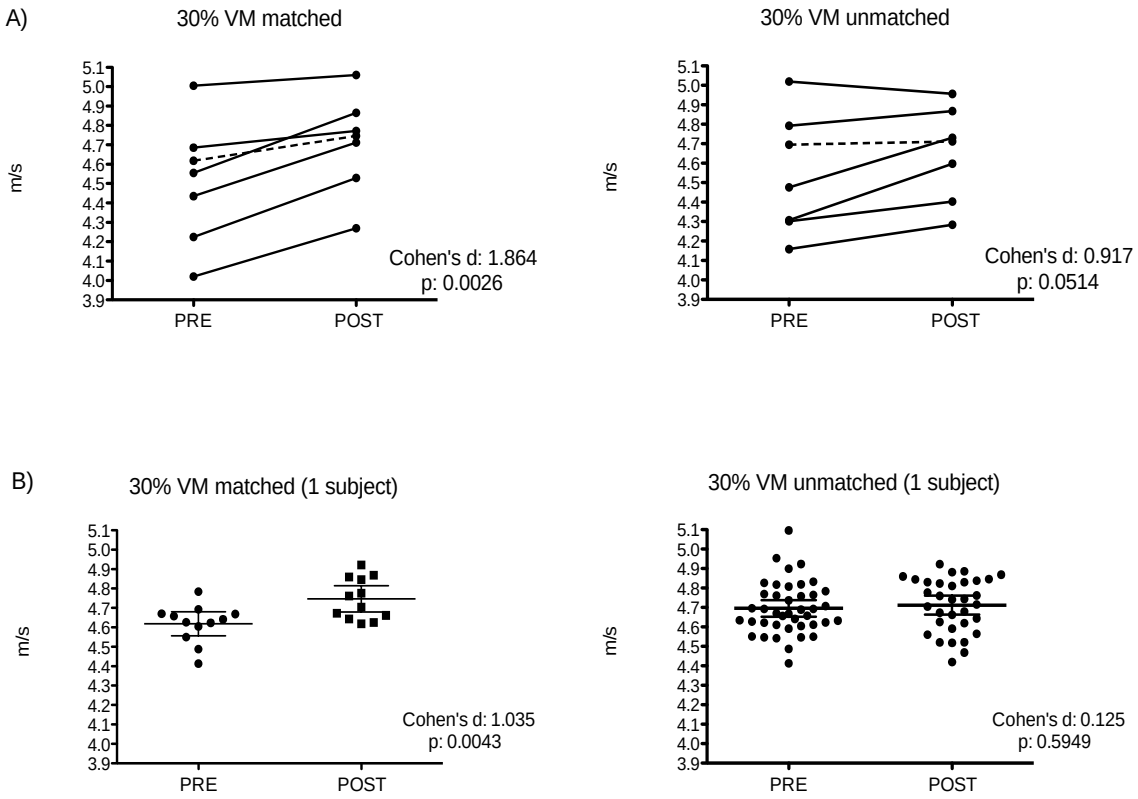

Figure 10. A) Motor unit conduction velocity (CV) values from the vastus medialis (VM) at 30% of the maximum voluntary contraction (MVC) from n=7 subjects, previously (PRE) and after (POST) an endurance training intervention. Left graph shows results obtained with tracked motor units, while right graph shows the results obtained using the total group of identified motor units (CV values were averaged per subject and compared PRE and POST intervention). The effect size and p-values of the two procedures are shown in the lower right corner of all graphs. The red line depicts an example of one subject that showed an increase in CV of matched motor units (left), which is masked when using unmatched motor units (right). B) Matched (left) and unmatched (right) motor units (mean and 95% confidence interval), from the same subject depicted in A (red line). The 12 matched motor units from this subject show a clear intervention effect (left graph), which is not possible to distinguish when using all decomposed motor units [CV values are extracted from all the motor units decomposed pre and post intervention (two repetitions per session)].

4.2.5. DISCUSSION

This study demonstrates the possibility of tracking individual motor units across different days, in humans during voluntary contractions with HDEMG. In Experiment I, without intervention, we were able to effectively track 38.3 % and 40.1 % of the identified motor units across two sessions and 21 (4.9)% and 16.3 (8.9)% across three sessions in the VM and VL, respectively. Moreover, the reliability indexes obtained from tracked motor units were larger than those calculated from the total group of identified motor units and

from the unmatched motor units, which strongly confirms a correct tracking. Additionally, the results showed that tracking motor units improved the sensitivity to changes in motor unit conduction velocity following an endurance training intervention, since the changes of conduction velocity of the matched motor units showed a larger effect size compared to the total group of motor units. Taken together, these findings are the first to demonstrate successful tracking of individual motor units recruited during voluntary contractions across several days.

Previous methods have focused on identifying groups of motor units across sessions by using percutaneous electrical stimulation of motor axons (Doherty and Brown 1994, Maathuis et al., 2008). This method involves the application of a low-intensity transcutaneous electrical impulse to the efferent nerve fibers, producing a compound MUAP that can be followed longitudinally. This method has been successfully employed for motor unit number estimation (MUNE) during the progression of neuromuscular disorders, such as amyotrophic lateral sclerosis (Gooch & Harati, 1997). However, this technique does not provide information about central (e.g., discharge behavior) or peripheral properties (e.g., conduction velocity) of the recorded motor units activated during voluntary contractions (Carroll *et al.*, 2011). Thus, the stimulation method is not appropriate for the study of motor unit adjustments during training or other interventions.

The alternative to tracking individual motor units across recordings is to extract a representative sample of motor units and infer population-behavior from them (Duchateau *et al.*, 2006; Vila-Cha *et al.*, 2010). However, this approach requires a sample large enough to provide reliable information about the properties and behavior of the motor unit pool (Martinez-Valdes *et al.*, 2016). Moreover, with this approach, a large number of subjects are needed to reach high sensitivity. The method proposed in the current study, conversely, showed the possibility of detecting and monitoring the same motor units across days (up to two weeks) with high reliability and sensitivity, which opens new possibilities and opportunities for longitudinal studies.

In comparison to previous single-channel or intramuscular recordings, HDEMG has the advantage that it provides spatial information as well as time varying aspects of the EMG signal (Blok *et al.*, 2002). The likelihood for different motor units to have the same spatial action potential representation decreases fast with the number of recording channels

(Farina *et al.*, 2008). Cescon and Gazzoni (Cescon & Gazzoni, 2010) attempted to track motor units during voluntary contractions using EMG recordings before and after a short-term bed rest period. The authors analyzed motor unit conduction velocity and used a distance measure to discriminate among the different motor units found between trials. However, due to the small number of EMG channels used (7 in the longitudinal direction) and the incomplete decomposition, it was not possible to assure that matched MUAPs corresponded to the same motor unit, as the authors acknowledged.

In this study, we used a large number of channels in order to exclude the possibility that, due to the volume conductor properties, different motor units showed MUAPs of identical shape (Farina *et al.*, 2008). In fact, placing the EMG arrays accurately in the same position for each session and using a relatively large number of channels, it is extremely unlikely that the MUAPs for the decomposition identified in different sessions would show high similarity if they do not correspond to the same motor unit. This property was strongly verified by the reliability and sensitivity analysis which were found both superior for the tracked motor units with respect to the average of all identified motor units, despite the greater sample size of all units. If the motor units were not tracked correctly, the probability of improving reliability and sensitivity of their estimated properties by choosing a smaller subsample of all units would have indeed been negligible. To prove this point further, we also conducted a reliability analysis between random samples of unmatched motor units (the sample size used was similar to the one used for tracked motor units). As expected, the reliability indices decreased even more than those found for the total group of identified motor units, which strongly confirms the accuracy of the tracking.

With our new analysis we were able to identify highly correlated MUAPs for approximately 40-50% of the motor units identified in two sessions and 15-25% of the motor units identified across 3 sessions, when no intervention was applied. The time-gap between the different measurement sessions did not influence the number of tracked motor units since the number remained consistent between all two-sessions comparisons (1-2, 1-3 and 2-3), regardless if they were conducted one or two weeks apart (See Results and Table 5). This highlights the applicability of the current method for training interventions, since training studies typically last several weeks. However, the number of matched motor units decreased when the procedure was conducted including more than two sessions (e.g.

sessions 1-2-3). Finally, we also checked the possibility of tracking motor units across different force levels within a session. Approximately 25% of the motor units identified at each force level (10, 30, 50 and 70% MVC) could be identified at a force level 20% higher (e.g., 10 vs. 30% MVC), despite large differences in motor unit recruitment. This shows that the current approach is robust to monitor the properties of the same motor units at different activation levels within a session. Consequently, it is expected that the current approach would still be able to follow motor units when MVC force changes ~20%.

In terms of reliability, both VM and VL recruitment/de-recruitment thresholds, mean discharge rates, and conduction velocities showed greater consistency across sessions for the matched motor units compared to the total group of identified motor units. Specifically, ICCs from matched motor units for all variables were substantially greater compared to the ICCs of the total group of identified motor units and unmatched motor units (see Tables 7 and 8), in accordance with the results on SEM (Tables 7 and 8). These observations can be confirmed further by the fact that these reliability indices were as large (or even larger) than the reliability indices obtained from a population of motor units during a sustained isometric contraction (Martinez-Valdes *et al.*, 2016). It is important to note that during ramped contractions, as analyzed in this study, motor unit firing behavior is inherently more variable across the population than during constant-force isometric contractions (Enoka, 1995). For example, discharge rates of motor units (within a subject) are less correlated during ramped contractions than during constant force contractions (Tenan *et al.*, 2014). Therefore, the fact that we still found high cross-session reliability in the present study would be extremely difficult to explain unless matched MUAPs belonged to the same motor units. In fact, there would be no reason for an increase in reliability of measures of motor unit properties when selecting a subset of these units unless they are correctly tracked across sessions, as confirmed by the low reliability levels observed for unmatched motor units.

To show a potential application of the method as well as its sensitivity, we conducted a short-term high volume endurance training intervention (Experiment II), using a protocol that previously showed an increase of endurance performance, vasti muscle oxidative capacity (Gibala *et al.*, 2006) and Na^+-K^+-ATPase activity (Green *et al.*, 2004), in just two weeks. Since changes in oxidative capacity and Na^+-K^+-ATPase activity have

been suggested as one of the main factors influencing motor unit conduction velocity during submaximal isometric contractions following endurance training (Vila-Cha *et al.*, 2012), it was hypothesized that our protocol would result in an increase in motor unit conduction velocity. Indeed, motor unit conduction velocity increased for both muscles (VM and VL) after the training intervention. However, the magnitude and significance of the detected change differed according to the approach used to assess the motor units. For instance, when matched motor units were used, all the subjects showed a systematic and clear increase in motor unit conduction velocity at 10% and 30% MVC for VM, with high statistical significance and a large effect size (Fig. 10a). However, no statistical difference was observed when using the total group of motor units (Fig. 10a and 10b), with one subject even showing an effect in the opposite direction (Fig. 10a, right). Even though the total group of identified motor unit results for VM were close to reaching statistical significance, it is worth to note that the results for the matched motor units presented an effect size which was almost double than that of the total motor units (matched units ES: 1.8 and 2.4, averaged units ES: 1.2 and 1.1, at 10% and 30% MVC, respectively). Taken together, these results show the impact of the proposed tracking method in sensitivity to track longitudinal changes in motor unit properties. The large number of identified and tracked motor units made available by our technique is critical for obtaining the statistical power needed to support conclusions about motor unit adaptations to training, rehabilitation, or disease (Carroll *et al.*, 2011; Button *et al.*, 2013; Heroux & Gandevia, 2013).

As representatively shown in the present study, the current method can be applied to the study of motor unit adaptations to training interventions (e.g., resistance or endurance training), but could also be extended to monitor different stages of rehabilitation within the context of injury or disease. For example, the tracking of individual motor unit properties (from low to high threshold motor units) could be of great benefit in characterizing discharge characteristics and muscle-fiber membrane properties during the progression of neuromuscular disorders (which has not yet been possible with any of the currently available methods). Furthermore, our tracking procedure allows the absolute recruitment threshold force to be measured across sessions without the need of normalizing it to %MVC force, providing accurate information about the force capacity of each motor

unit. Regarding resistance training, many authors have used surface EMG recordings to attribute early strength gains to neuromuscular adaptations (Folland & Williams, 2007). However, due to the many factors influencing surface EMG amplitude measures [see (Farina *et al.*, 2004) for review], the evidence is equivocal (Folland & Williams, 2007). Although there are some studies reporting changes in motor unit behavior following training, demonstrated through intramuscular EMG recordings, the results are not in agreement between studies (Rich & Cafarelli, 2000; Kamen & Knight, 2004; Pucci *et al.*, 2006; Vila-Cha *et al.*, 2010), probably due to the small number of motor units that can be identified with this technique and the impossibility to track them. Conversely, the current approach could provide clearer evidence of motor unit changes occurring after training interventions since the same motor units can be followed across the intervention. A number of studies have successfully used HDEMG to accurately extract motor unit activity in a number of neuromuscular disorders in single experimental sessions (Holobar *et al.*, 2012; Dideriksen *et al.*, 2015; Li *et al.*, 2015). Our study suggests that these investigations can be extended to include longitudinal characterization of individual motor unit properties in clinical populations.

Some limitations of the proposed approach need to be discussed. In the current study, the motor unit tracking procedure was only applied across sessions that were 2-2.5 weeks apart, during which changes in muscle morphology were not expected. Since changes in muscle morphology (e.g., muscle architecture and cross-sectional area) influence MUAP shapes, the number of motor units tracked by the algorithm would presumably decrease if the muscle structure changes considerably. However, muscle structural changes, i.e., following resistance exercise (Narici *et al.*, 1996; Aagaard *et al.*, 2001; McCarthy *et al.*, 2002)] may not always impact the MUAP shape substantially. As shown in Figure 3, the present method can successfully track motor units showing large changes in conduction velocity (>10%). Moreover, the algorithm can also track motor units between force levels that differ by ~20% (Table 9). Since motor unit conduction velocity adjustments >10% and increases in MVC force >20% are only expected after approximately 6-8 weeks of resistance training (McCarthy *et al.*, 2002; Aagaard, 2003; Vila-Cha *et al.*, 2010), it is very likely that the present method can successfully track motor units during longer training interventions than the one shown in this study. A direct

evaluation of the method for longer interventions is however needed. Similarly, future tests should analyze the possibility of tracking motor units in pathological conditions, such as during the progression of amyotrophic lateral sclerosis (ALS) over long periods of time (van Dijk *et al.*, 2010).

The lower number of motor units identified for the vasti muscles with respect to other muscles [e.g., tibialis anterior (Castronovo *et al.*, 2015)] has been reported previously with a similar blind source separation decomposition method (Watanabe *et al.*, 2013; Martinez-Valdes *et al.*, 2016). Differences in muscle fiber architecture across muscles may explain the variability of the identified motor unit sample size across muscles. For example, the tibialis anterior and the gastrocnemius muscles have signal characteristics (Barbero *et al.*, 2012) that positively influence the decomposition (less spatially correlated recordings), with respect to muscles such as the vasti or biceps bracchi (Piitulainen *et al.*, 2012) that present EMG signals with a higher spatial correlation.

Finally, although occasional, there were a small number of trials (~15%) where motor units presented multiple matches with a cross correlation coefficient >0.8. As commented above, this can be due to the high spatial correlation that the vasti muscles present. However, the algorithm always selected the highest cross-correlated source, which prevented the chance of having double matches. The observation of this high correlation between multiple pairs of identified MUAPs indicated the occasional similarity of MUAPs belonging to different motor units. Some degree of similarity is expected and decreases consistently with the number of channels, being negligible for a large number of channels and/or for muscles resulting in low spatial correlation in EMG recordings (Farina *et al.*, 2008).

4.2.5.1. Conclusion

This study presents and validates, for the first time, a method for processing HDEMG in humans that allows the tracking of the same motor units longitudinally during voluntary contractions performed in different sessions, separated by weeks. This method provides new opportunities to track adaptations of the same motor units over time in vivo, as it would be required in longitudinal interventions or during the progression of neuromuscular disorders.

4.2.6. APPENDIX A

Multichannel EMG signals can be described mathematically as convolutive mixtures with finite impulse response filters (motor unit action potentials). They can be represented as a linear and an instantaneous mixture of an extended vector of sources (motor unit spike trains) that include the original sources and their *L*-1 delayed versions, where *L* is the length of the filters (Negro et al. 2016). This leads to the following extended observation vector for channel *i*:

$$\tilde{x}_i(k) = [x_i(k)x_i(k-1),...,x_i(k-R)] \qquad i = 1,...,m$$

After the extension of the observations, we also have:

$$\tilde{s}_j(k) = [s_j(k), s_j(k-1),...,s_j(k-L-R+1)] \qquad j = 1,...,n$$

and

$$\tilde{n}_i(k) = [n_i(k), n_i(k-1),...,n_i(k-R)] \qquad i = 1,...,m$$

Where k is the discrete time, x_i is the EMG signal recorded at channel *i*, $s_j(k)$ the *j*-th source (motor unit spike train) and n_i the additive noise at channel *i*-th. Therefore, the extended model becomes:

$$x(k) = [Hs(k) + n(k)] \qquad k = 0,...,D_R \qquad (3)$$

with

$$s(k) = [s_1(k), s_2(k), \ldots, s_n(k)]^T$$

$$x(k) = [x_1(k), x_2(k), \ldots, x_m(k)]^T$$

$$n(k) = [n_1(k), n_2(k), \ldots, n_m(k)]^T$$

$$H_{ij} = \begin{bmatrix} h_{ij}[0] & \cdots & h_{ij}[L-1] & 0 & \cdots & 0 \\ 0 & \ddots & \ddots & \ddots & \ddots & \vdots \\ \vdots & \ddots & \ddots & \ddots & \ddots & 0 \\ 0 & \cdots & 0 & h_{ij}[0] & \cdots & h_{ij}[L-1] \end{bmatrix}$$

$$\underline{\underline{\tilde{H}}} = \begin{bmatrix} \tilde{h}_{11} & \cdots & \tilde{h}_{1n} \\ \vdots & \ddots & \vdots \\ \tilde{h}_{m1} & \cdots & \tilde{h}_{mn} \end{bmatrix}$$

Where D_r is the duration of the recording and h_{ij} the action potential of the *j*-th motor unit recorded at the channel *i*. In order to solve the inverse problem, the number of extended measurements *R* should be higher than the number of sources *n* multiplied by the length of the filters *L* (MUAP shapes).

The instantaneous model described by Eq. 3 can be inverted to recover the matrix of the extended sources using the fixed point optimization procedure and an appropriate cost function following the spatial whitening procedure [Negro et al. 2016]. Since the inverse of Eq. 3 may have a relatively large space of possible solutions, the procedure aims to find the sources $w_i^T z$, where $\boldsymbol{z}$ are the whitened extended measurements and w_i the projection vector (filter) of the *i*-th source, that maximize the non-Gaussianity measure employed by the selected cost function. In this study, this method, that we call here "full decomposition", was applied to the first (A) recording session. In the following sessions, we modified the algorithm to identify projection vectors w_i that would maximize both the non-gaussianity of the extracted *i*-th source and the similarity with the previously identified motor units in the first session. The similarity was estimated by cross-correlation between the de-whitened projecting vectors with a threshold of 0.8. Each time the threshold was crossed, the discharge times of the identified source were removed from the following iterations. The approach is called Sparse Deflation (Natora & Obermayer, 2011) and provides an optimal extraction scheme for sparse signals (e.g., motor unit spike trains) that avoids the convergence to the same solution multiple times. In the tracking application, indeed, the subtraction of the sources in the spike train space resulted more efficient. Among all matched sources, we selected those with the highest similarity measures.

4.2.7. REFERENCES

Aagaard P. (2003). Training-induced changes in neural function. *Exerc Sport Sci Rev* **31,** 61-67.

Aagaard P, Andersen JL, Dyhre-Poulsen P, Leffers AM, Wagner A, Magnusson SP, Halkjaer-Kristensen J & Simonsen EB. (2001). A mechanism for increased contractile strength of human pennate muscle in response to strength training: changes in muscle architecture. *J Physiol* **534,** 613-623.

Adam A & De Luca CJ. (2005). Firing rates of motor units in human vastus lateralis muscle during fatiguing isometric contractions. *J Appl Physiol (1985)* **99,** 268-280.

Adkins DL, Boychuk J, Remple MS & Kleim JA. (2006). Motor training induces experience-specific patterns of plasticity across motor cortex and spinal cord. *J Appl Physiol (1985)* **101,** 1776-1782.

Andreassen S & Arendt-Nielsen L. (1987). Muscle fibre conduction velocity in motor units of the human anterior tibial muscle: a new size principle parameter. *J Physiol* **391,** 561-571.

Barbero M, Merletti R & Rainoldi A. (2012). *Atlas of muscle innervation zones : understanding surface electromyography and its applications*. Springer, Milan ; New York.

Bartko JJ. (1966). The intraclass correlation coefficient as a measure of reliability. *Psychol Rep* **19,** 3-11.

Blok JH, van Dijk JP, Drost G, Zwarts MJ & Stegeman DF. (2002). A high-density multichannel surface electromyography system for the characterization of single motor units. *Rev Sci Instrum* **73,** 1887-1897.

Button KS, Ioannidis JP, Mokrysz C, Nosek BA, Flint J, Robinson ES & Munafo MR. (2013). Power failure: why small sample size undermines the reliability of neuroscience. *Nat Rev Neurosci* **14,** 365-376.

Carroll TJ, Selvanayagam VS, Riek S & Semmler JG. (2011). Neural adaptations to strength training: moving beyond transcranial magnetic stimulation and reflex studies. *Acta physiol* **202,** 119-140.

Castronovo AM, Negro F, Conforto S & Farina D. (2015). The proportion of common synaptic input to motor neurons increases with an increase in net excitatory input. *J Appl Physiol (1985)* **119,** 1337-1346.

Cescon C & Gazzoni M. (2010). Short term bed-rest reduces conduction velocity of individual motor units in leg muscles. *J Electromyogr Kinesiol* **20,** 860-867.

Cohen J. (1988). *Statistical power analysis for the behavioral sciences*. L. Erlbaum Associates, Hillsdale, N.J.

Dideriksen JL, Gallego JA, Holobar A, Rocon E, Pons JL & Farina D. (2015). One central oscillatory drive is compatible with experimental motor unit behaviour in essential and Parkinsonian tremor. *J Neural Eng* **12,** 046019.

Duchateau J, Semmler JG & Enoka RM. (2006). Training adaptations in the behavior of human motor units. *J Appl Physiol (1985)* **101,** 1766-1775.

Enoka RM. (1995). Morphological features and activation patterns of motor units. *J Clin Neurophysiol* **12,** 538-559.

Farina D, Holobar A, Gazzoni M, Zazula D, Merletti R & Enoka RM. (2009). Adjustments differ among low-threshold motor units during intermittent, isometric contractions. *J Neurophysiol* **101,** 350-359.

Farina D, Merletti R & Enoka RM. (2004). The extraction of neural strategies from the surface EMG. *J Appl Physiol (1985)* **96,** 1486-1495.

Farina D & Mesin L. (2005). Sensitivity of surface EMG-based conduction velocity estimates to local tissue in-homogeneities--influence of the number of channels and inter-channel distance. *J Neurosci Methods* **142,** 83-89.

Farina D, Muhammad W, Fortunato E, Meste O, Merletti R & Rix H. (2001). Estimation of single motor unit conduction velocity from surface electromyogram signals detected with linear electrode arrays. *Med Biol Eng Comput* **39,** 225-236.

Farina D, Negro F, Gazzoni M & Enoka RM. (2008). Detecting the unique representation of motor-unit action potentials in the surface electromyogram. *J Neurophysiol* **100,** 1223-1233.

Farina D, Negro F, Muceli S & Enoka RM. (2016). Principles of Motor Unit Physiology Evolve With Advances in Technology. *Physiology* **31,** 83-94.

Folland JP & Williams AG. (2007). The adaptations to strength training : morphological and neurological contributions to increased strength. *Sports Med* **37,** 145-168.

Gibala MJ, Little JP, van Essen M, Wilkin GP, Burgomaster KA, Safdar A, Raha S & Tarnopolsky MA. (2006). Short-term sprint interval versus traditional endurance training: similar initial adaptations in human skeletal muscle and exercise performance. *J Physiol* **575,** 901-911.

Gooch CL & Harati Y. (1997). Longitudinal tracking of the same single motor unit in amyotrophic lateral sclerosis. *Muscle Nerve* **20,** 511-513.

Green HJ, Barr DJ, Fowles JR, Sandiford SD & Ouyang J. (2004). Malleability of human skeletal muscle Na(+)-K(+)-ATPase pump with short-term training. *J Appl Physiol (1985)* **97,** 143-148.

Heroux ME & Gandevia SC. (2013). Human muscle fatigue, eccentric damage and coherence in the EMG. *Acta Physiol* **208,** 294-295.

Holobar A, Glaser V, Gallego JA, Dideriksen JL & Farina D. (2012). Non-invasive characterization of motor unit behaviour in pathological tremor. *J Neural Eng* **9,** 056011.

Holobar A, Minetto MA & Farina D. (2014). Accurate identification of motor unit discharge patterns from high-density surface EMG and validation with a novel signal-based performance metric. *J Neural Eng* **11,** 016008.

Holobar A & Zazula D. (2007). Multichannel blind source separation using convolution kernel compensation. *IEEE Trans Signal Process* **55,** 4487-4496.

Hyvarinen A & Oja E. (2000). Independent component analysis: algorithms and applications. *Neural Netw* **13,** 411-430.

Kamen G & Knight CA. (2004). Training-related adaptations in motor unit discharge rate in young and older adults. *J Gerontol A Biol Sci Med Sci* **59,** 1334-1338.

Laine CM, Martinez-Valdes E, Falla D, Mayer F & Farina D. (2015). Motor Neuron Pools of Synergistic Thigh Muscles Share Most of Their Synaptic Input. *J Neurosci* **35,** 12207-12216.

Li X, Holobar A, Gazzoni M, Merletti R, Rymer WZ & Zhou P. (2015). Examination of Poststroke Alteration in Motor Unit Firing Behavior Using High-Density Surface EMG Decomposition. *IEEE Trans Biomed Eng* **62,** 1242-1252.

Martinez-Valdes E, Laine CM, Falla D, Mayer F & Farina D. (2016). High-density surface electromyography provides reliable estimates of motor unit behavior. *Clin Neurophysiol* **127,** 2534-2541.

Masuda T, Miyano H & Sadoyama T. (1985). The position of innervation zones in the biceps brachii investigated by surface electromyography. *IEEE Trans Biomed Eng* **32,** 36-42.

McCarthy JP, Pozniak MA & Agre JC. (2002). Neuromuscular adaptations to concurrent strength and endurance training. *Med Sci Sports Exerc* **34,** 511-519.

Muceli S, Poppendieck W, Negro F, Yoshida K, Hoffmann KP, Butler JE, Gandevia SC & Farina D. (2015). Accurate and representative decoding of the neural drive to muscles in humans with multi-channel intramuscular thin-film electrodes. *J Physiol* **593,** 3789-3804.

Narici MV, Hoppeler H, Kayser B, Landoni L, Claassen H, Gavardi C, Conti M & Cerretelli P. (1996). Human quadriceps cross-sectional area, torque and neural activation during 6 months strength training. *Acta Physiol Scand* **157,** 175-186.

Natora M & Obermayer K. (2011). An Unsupervised and Drift-Adaptive Spike Detection Algorithm Based on Hybrid Blind Beamforming. *Eurasip J Adv Sig Pr*.

Negro F, Muceli S, Castronovo AM, Holobar A & Farina D. (2016). Multi-channel intramuscular and surface EMG decomposition by convolutive blind source separation. *J Neural Eng* **13,** 026027.

Piitulainen H, Holobar A & Avela J. (2012). Changes in motor unit characteristics after eccentric elbow flexor exercise. *Scand J Med Sci Sports* **22,** 418-429.

Pucci AR, Griffin L & Cafarelli E. (2006). Maximal motor unit firing rates during isometric resistance training in men. *Exp Physiol* **91,** 171-178.

Rich C & Cafarelli E. (2000). Submaximal motor unit firing rates after 8 wk of isometric resistance training. *Med Sci Sports Exerc* **32,** 190-196.

Selvanayagam VS, Riek S & Carroll TJ. (2011). Early neural responses to strength training. *J Appl Physiol (1985)* **111,** 367-375.

Tenan MS, Marti CN & Griffin L. (2014). Motor unit discharge rate is correlated within individuals: a case for multilevel model statistical analysis. *J Electromyogr Kinesiol* **24,** 917-922.

van Dijk JP, Schelhaas HJ, Van Schaik IN, Janssen HM, Stegeman DF & Zwarts MJ. (2010). Monitoring disease progression using high-density motor unit number estimation in amyotrophic lateral sclerosis. *Muscle Nerve* **42,** 239-244.

Vila-Cha C, Falla D, Correia MV & Farina D. (2012). Adjustments in motor unit properties during fatiguing contractions after training. *Med Sci Sports Exerc* **44,** 616-624.

Vila-Cha C, Falla D & Farina D. (2010). Motor unit behavior during submaximal contractions following six weeks of either endurance or strength training. *J Appl Physiol (1985)* **109,** 1455-1466.

Watanabe K, Gazzoni M, Holobar A, Miyamoto T, Fukuda K, Merletti R & Moritani T. (2013). Motor unit firing pattern of vastus lateralis muscle in type 2 diabetes mellitus patients. *Muscle Nerve* **48,** 806-813.

Weibull A, Flondell M, Rosen B & Bjorkman A. (2011). Cerebral and clinical effects of short-term hand immobilisation. *Eur J Neurosci* **33,** 699-704.

4.3. Study 3

DIFFERENTIAL MOTOR UNIT CHANGES AFTER ENDURANCE OR HIGH-INTENSITY INTERVAL TRAINING

E. Martinez-Valdes[1], D. Falla[2], F. Negro[3], F. Mayer[1], D. Farina[4]

Affiliations

1. Department of Sports Medicine and Sports Orthopaedics, University of Potsdam, Potsdam, Germany.

2. Centre of Precision Rehabilitation for Spinal Pain (CPR Spine), School of Sport, Exercise and Rehabilitation Sciences, College of Life and Environmental Sciences, University of Birmingham, Birmingham, United Kingdom.

3. Department of Clinical and Experimental Sciences, Università degli Studi di Brescia, Brescia, Italy.

4. Department of Bioengineering, Imperial College London, Royal School of Mines, London, United Kingdom.

Reference

Martinez-Valdes E, Falla D, Negro F, Mayer F & Farina D. (2017). Differential Motor Unit Changes after Endurance or High-Intensity Interval Training. Medicine and science in sports and exercise 49, 1126-1136.

4.3.1. ABSTRACT

Purpose: Using a novel technique of high-density surface electromyography (HDEMG) decomposition and motor unit (MU) tracking, we compared changes in the properties of vastus medialis (VM) and vastus lateralis (VL) MUs following endurance (END) and high-intensity interval training (HIIT). **Methods:** Sixteen men were assigned to an END or HIIT group (n=8 each) and performed six training sessions over 14 days. Each session consisted of 8-12×60s intervals at 100% peak power output (PPO) separated by 75s of recovery (HIIT) or 90-120min continuous cycling at ~65% VO_{2peak} (END). Pre and post intervention, participants performed: 1) incremental cycling to determine VO_{2peak} and PPO and 2) maximal (MVC), submaximal (10, 30, 50 and 70% MVC) and sustained (until task failure at 30% MVC) isometric knee extensions while HDEMG signals were recorded from the VM and VL. EMG signals were decomposed (submaximal contractions) into individual MUs by convolutive blind source separation. Finally, MUs were tracked across sessions by semi-blind source separation. **Results:** After training, END and HIIT improved VO_{2peak} similarly (by 5.0 and 6.7%, respectively). The HIIT group showed enhanced maximal knee extension torque by ~7% ($p=0.02$) and was accompanied by an increase in discharge rate for high-threshold MUs (≥50% knee extension MVC) ($p<0.05$). In contrast, the END group increased their time to task failure by ~17%, but showed no change in MU discharge rates ($p>0.05$). **Conclusions:** HIIT and END induce different adjustments in MU discharge rate despite similar improvements in cardiopulmonary fitness. Moreover, the changes induced by HIIT are specific for high-threshold motor units. For the first time we show that HIIT and END induce specific neuromuscular adaptations, possibly related to differences in exercise load intensity and training volume.

4.3.2. INTRODUCTION

High intensity interval training (HIIT) describes physical exercise that is characterized by brief, intermittent bursts of vigorous physical activity, interspersed by periods of rest or low-intensity exercise (Gibala *et al.*, 2012). Subjects perform short periods of training (from 30 seconds to 1 minute) at intensities from 90% of maximum heart rate and above, interspersed with a passive or active rest, achieving a maximum exercise volume of 10 to 20 min/session (30-60 min/week). In comparison to traditional high-volume endurance training (END), HIIT induces similar changes in a range of physiological (e.g., enhanced aerobic metabolism), performance (e.g., faster completion of a certain amount of work), and health-related markers (e.g., increased flow-mediated dilation) (Burgomaster *et al.*, 2005; Gibala *et al.*, 2006; Rakobowchuk *et al.*, 2008; Little *et al.*, 2010), but with a much lower time commitment. Therefore, HIIT is typically offered as an alternative to END. However, no study has evaluated the neuromuscular adaptations induced by HIIT. Since neuromuscular adaptations to training are highly specific and vary according to the training regime (Vila-Cha *et al.*, 2010), differences in neuromuscular adaptations to HIIT and END might be expected since the training protocols differ in load intensity and exercise volume.

Recordings of motor units provide a window to the central nervous system, allowing analysis of the way in which the central nervous system controls muscle force (Farina *et al.*, 2016). In one of the few studies assessing motor unit adaptations following training, Vila-Cha et al. (Vila-Cha *et al.*, 2010) observed different changes in low-threshold motor unit discharge rates (average discharge rate and discharge rate variability) between END and strength training. These findings suggested a specific adaptation in motor unit discharge rate according to the training regime applied. However, these differences could not be assessed for high threshold motor units due to previous technical limitations. Indeed, there is a lack of knowledge about changes in discharge rate of high threshold motor units (Duchateau *et al.*, 2006), since classic methods for electromyography (EMG) signal decomposition are limited to the identification of a few motor units concurrently, at low forces (Duchateau & Enoka, 2011). Nonetheless, high-density surface electromyography (HDEMG) has recently emerged as an alternative to overcome this limitation. The availability of many (tens) observation sites allows for automatic methods

of source separation to reliably identify a large number of motor units, for a wide range of forces (close to the maximum voluntary contraction, MVC, force) (Farina & Holobar, 2016; Martinez-Valdes *et al.*, 2016b; Negro *et al.*, 2016). Moreover, several observation channels can be used to track the same motor units across different sessions, therefore allowing longitudinal studies of the same motor units in humans over long periods of time (weeks) (Martinez-Valdes *et al.*, 2016c). This achievement has opened new possibilities to study the neuromuscular adaptions to training.

The purpose of the study was to evaluate, for the first time, changes in muscle activity and motor unit properties (discharge rate, discharge rate variability and recruitment threshold) of synergistic knee extensor muscles, following short-term low-volume HIIT and high-volume END training interventions, utilizing a novel technique of HDEMG motor unit tracking. It was hypothesized that, despite similar increases in cardiorespiratory fitness parameters (e.g., peak oxygen uptake, VO_{2peak} (McKay *et al.*, 2009)), these two training protocols will induce different changes in motor output (maximal strength, rate of torque development, time to task failure) that will be related to different adjustments in motor unit discharge rates. Moreover, we hypothesized that these adjustments will vary across the motor unit pool, with low-threshold motor units showing different changes compared to high threshold motor units, given the differences in load intensity and training volume between the two types of training.

4.3.3. METHODS

4.3.3.1. Participants

Eighteen healthy men (mean (SD) age: 29 (3) years, height: 178 (6) cm, mass: 79 (9) kg) participated. All subjects were physically active and took part in some form of recreational exercise at least two to three times per week (e.g. soccer, running, etc.). None of the subjects were engaged in regular training for a particular sporting event or competition. Exclusion criteria included any neuromuscular disorder as well as any current or previous history of knee pain and age < 18 or > 35 years. Participants were asked to avoid any strenuous activity 24 h prior to the measurements. Nine subjects were randomly assigned to a HIIT group and the other nine were assigned to an END group. A control

group was not implemented since we previously reported no changes in motor output and vasti muscles motor unit behavior, in control subjects measured in the space of two weeks (Martinez-Valdes *et al.*, 2016b). The ethics committee of the Universität Potsdam approved the study (approval number 26/2015), in accordance with the declaration of Helsinki (2004). All participants gave written, informed consent.

4.3.3.2. Experimental protocol

The experimental protocol consisted of baseline measurements (i.e., isometric knee extension torque, EMG recordings, peak oxygen uptake (VO_{2peak}) determination), a 2-week intervention of END or HIIT training and post-training measurements.

Baseline measurements (Torque and EMG measurements). The participant was seated in an isokinetic dynamometer (CON-TREX MJ, PHYSIOMED, Regensdorf, Switzerland), with the trunk reclined to 15° in an adjustable chair while the hip and distal thigh were secured to the chair. The rotational axis of the dynamometer was aligned with the lateral femoral epicondyle of the dominant leg and the lower leg was secured to the dynamometer lever arm above the lateral malleolus. Maximal and submaximal isometric knee extensions were exerted with the knee flexed to 90°. After placement of the surface electrodes (as described in *Data acquisition* below), subjects performed three maximal voluntary contractions (MVC) of knee extension each over a period of 5 s. These trials were separated by 2 min of rest. The highest MVC value was used as a reference for the definition of the submaximal torque levels. Five minutes of rest were provided after the MVC measurement. In each of the baseline and post-intervention sessions, the submaximal torques were expressed as a percent of the MVC measured during the same session. After the MVCs, the participants performed three maximal-ballistic isometric contractions, each separated by 30 s of rest. They were encouraged to exert their maximal torque as fast as possible in response to a visual signal shown on a computer monitor. Then, after 5 minutes of rest, and following a few familiarization trials at low torque levels (10 and 30% MVC), subjects performed submaximal isometric knee extension contractions at 10, 30, 50 and 70% MVC in a randomized order. The contractions at 10-30% were sustained for 20 s, while the contractions at 50 and 70% MVC lasted 15 and 10 s respectively. In each trial, the subjects received visual feedback of the torque applied by the leg to the dynamometer, which was displayed as a trapezoid (5 s ramps with hold-phase durations as specified

above). Each contraction level was performed twice per session and 2 minutes of rest were allowed after each contraction. The randomization order of these contractions was kept the same for each subject in the pre and post intervention sessions, to minimize the possible influence of cumulative fatigue in the results of the motor unit data when studying the training-induced adaptations. Finally, the subjects performed a further isometric knee extension contraction at 30% MVC, maintaining the torque level for as long as possible. Time to task failure was defined as the time instant when the subject exerted a force 10% MVC below the target force for an interval of time of 2 s (Castronovo *et al.*, 2015).

Then, 24 h after these measurements, the subjects returned to the laboratory to perform an incremental test to exhaustion on an electronically braked cycle ergometer (Lode Excalibur Sport V2.0, Groningen, the Netherlands). VO_{2peak} and the submaximal ventilation thresholds were determined using a gas analysis system (ZAN 600, Nspire Health, Oberthulba, Germany), which was calibrated before each test with known values of oxygen (O_2), carbon dioxide (CO_2), and volume. Following a 3-min warm-up at 30 W, the test began with the workload increasing by 6 W every 12 s until volitional exhaustion. The revolutions per minute were maintained between 80 and 90 throughout the incremental test and training sessions. The value used for VO_{2peak} corresponded to the highest value achieved over a 30 s collection period. Peak power output was defined as the maximal power (W) achieved at the end of the ramp VO_{2peak} cycle-ergometer test. Finally, the first ventilatory threshold (VT1) was identified by the ventilatory equivalent method, where VT1 corresponded to the power output and VO_2 value at which the ventilatory equivalent for O_2 (V_E/VO_2) exhibited a systematic increase without a concomitant increase in the ventilatory equivalent for CO_2 (V_E/VCO_2) (WASSERMAN, 2012). The respiratory compensation point (VT2) was identified by using the criterion of an increase in both V_E/VO_2 and V_E/VCO_2 and by using the first decrease in the end-tidal pressure of CO_2 ($PETCO_2$) as a confirmatory indicator (Wasserman, 2012).

Training Protocols. The training interventions were performed using two protocols that have shown similar improvements in cardio-respiratory fitness (VO_{2peak}) and aerobic capacity, despite differences in total training volume and intensity (Gibala *et al.*, 2006; Little *et al.*, 2010). The training protocol commenced approximately 72 h after the incremental test and consisted of six training sessions over 14 days. Each session was

performed on Mondays, Wednesdays, and Fridays. An investigator of the study (E.M-V) supervised all training sessions. For the END group, training consisted of 90-120 min of continuous cycling at 65% of VO_{2peak} using a protocol described previously (Gibala *et al.*, 2006). The duration of exercise increased from 90 min during sessions 1 and 2 to 105 min during sessions 3 and 4, and finally to 120 min during sessions 5 and 6. For the HIIT group, training consisted of 60 s bouts of high-intensity cycling at 100% peak power output as described previously (Little *et al.*, 2010). These bouts were interspersed by 75 s of cycling at 30 W for recovery (Little *et al.*, 2010). Participants completed 8 high-intensity intervals during sessions 1 and 2, 10 intervals during sessions 3 and 4, and 12 intervals on the final two sessions. A warm-up period of 3 min at 30 W was performed each session prior to training.

In summary, the HIIT group performed the exercise at an intensity of ~335 W, with a total training commitment of 8-12 min per session (18-27 min including recovery). The total training commitment for HIIT over the two weeks was 60 min (135 min including recovery), reaching a total exercise volume of ~1205 kJ (~1375 kJ including recovery). In contrast, the END group performed the exercise at an intensity of ~165 W, with a total training commitment of 90-120 min per session. The total training commitment for END over the two weeks was 630 min, achieving a total exercise volume of ~6250 kJ.

Post-training measurements. The post-training sessions (torque, EMG recordings and incremental test) were identical to the baseline-testing procedures and were performed approximately 72 h post training.

4.3.3.3. Data Acquisition

EMG signals were acquired from the vastus medialis (VM), vastus lateralis (VL) and biceps femoris (BF) muscles during maximal and submaximal isometric contractions as described above. For the VM and VL, surface EMG signals were recorded in monopolar derivation with a two-dimensional (2D) adhesive grid (SPES Medica, Salerno, Italy) of 13 × 5 equally spaced electrodes (each of 1 mm diameter, with an inter-electrode distance of 8 mm), with one electrode absent from the upper right corner. The electrode grids were positioned as described previously (Laine *et al.*, 2015; Martinez-Valdes *et al.*, 2016b). EMG signals were initially recorded during a brief voluntary contraction during which a linear non-adhesive electrode array was moved over the skin to detect the location of the

innervation zone and tendon regions (Martinez-Valdes *et al.*, 2016a). After skin preparation (shaving, abrasion and water), the electrode cavities of the grids were filled with conductive paste (SPES Medica, Salerno, Italy) and the grids positioned between the proximal and distal tendons of the VL and VM muscles with the electrode columns (comprising 13 electrodes) oriented along the muscle fibers. Reference electrodes were positioned over the malleoli and patella of the dominant leg. Signals from the BF were recorded in bipolar mode with Ag-AgCl electrodes (Ambu Neuroline 720, Ballerup, Denmark; conductive area 28 mm^2) and were positioned according to guidelines (Barbero *et al.*, 2012). The location of the electrodes was marked on the skin of the participants using a surgical pen (subjects were instructed to re-mark the electrode zone daily). Also, the position of the electrodes was further reported on a transparent sheet by using anatomical landmarks. These procedures allowed a similar electrode positioning across sessions.

Torque and EMG signals were sampled at 2048 Hz, converted to digital data by a 12-bit analogue to digital converter (EMG-USB 2, 256-channel EMG amplifier, OT Bioelettronica, Torino, Italy, 3dB, bandwidth 10-500 Hz). EMG signals were amplified by a factor of 2000, 1000, 500, 500 and 500 for the 10, 30, 50, 70 and 100% MVC contractions, respectively. Data were stored on a computer hard disk and analyzed in Matlab offline (The Mathworks Inc., Natick, Massachusetts, USA). Finally, before decomposition, the 64-monopolar EMG channels were re-referenced offline to form 59 bi-polar channels using the difference between the adjacent electrodes in the direction of the muscle fibers.

4.3.3.4. Signal analysis

Torque. The torque signal was low-pass filtered offline at 15 Hz. The coefficient of variation (CoV) of torque (SD torque/mean torque) was calculated from the stable-torque region during the submaximal contractions. Rate of torque development (RTD) was calculated from the ballistic contractions as the maximum slope of the torque-time curve (Δtorque/Δtime) as presented previously (Vila-Cha *et al.*, 2010). Briefly, for RTD calculation, the torque signal that was originally sampled at 2048 Hz was low pass filtered at 15 Hz and then resampled at 30 Hz, the peak slope was detected from the derivative of this torque signal. The onset of torque during the ballistic contractions was defined as the

time instant when torque exceeded 7.5 Nm (Aagaard *et al.*, 2002).

Interference EMG. The average rectified values (ARV) obtained from submaximal, maximal and explosive contractions, were averaged over all channels of the electrode grid to increase its repeatability between pre-post intervention trials (Gallina *et al.*, 2016). During the submaximal isometric contractions, the ARV was computed from the HDEMG and bipolar (for BF) signals in intervals of 1 s. These values were extracted from the stable-torque region of the contractions (e.g., hold-phase of 20 seconds at 30% MVC). ARVs of the maximal (MVC) contractions were analyzed in a time window of 250 ms centered at the peak EMG activity. During the explosive contractions, ARV was calculated in a 50 ms interval centered at the time instant of the maximal slope in torque (Vila-Cha *et al.*, 2010). Finally, co-activation was quantified as the average of VM and VL ARV divided by the BF ARV (33).

Motor unit analysis. The EMG signals recorded during the submaximal isometric contractions (from 10 to 70% MVC) were decomposed offline with a method that has been extensively validated (Negro *et al.*, 2016). The signals were decomposed throughout the whole duration of the submaximal contractions and the discharge times of the identified motor units were converted in binary spike trains (Martinez-Valdes *et al.*, 2016b). The mean discharge rate and discharge rate variability (coefficient of variation of the inter-spike-interval, CoV_{isi}, see below for details), were calculated during the stable plateau torque region. Recruitment thresholds for each motor unit were defined as the knee extension torque (Nm) at the times when the motor unit began discharging action potentials. Discharge times that were separated from the next by > 200 ms were excluded from the estimation of recruitment thresholds to avoid aligning the thresholds with noise-generated discharges. Only motor units with a coefficient of variation for the inter-spike interval (CoV_{isi}) <30% which satisfied the constrains described in (Negro *et al.*, 2016), during the stable torque portion of the contraction were considered for further analysis. Finally, discharges that were separated from the next by <33.3 ms or >200 ms (30 and 5 Hz, respectively) were excluded from the mean discharge rate and CoV_{isi} estimates because these discharges are likely due to decomposition errors (Martinez-Valdes *et al.*, 2016b). A representative schematic summarizing the HDEMG recordings and motor unit decomposition procedures can be found in **Figure 11**.

Motor unit tracking. A motor unit tracking procedure was applied using a method that has been recently presented (Martinez-Valdes *et al.*, 2016c). The motor unit identification and tracking method is an extension of the convolutive blind source separation technique described by Negro et al. (Negro *et al.*, 2016) and it was adapted to extract motor units with multi-channel action potential shapes maximally similar across sessions. After the full blind HDEMG decomposition was performed on the baseline recording session, we applied a semi-blind separation procedure on the post-training session, focusing on finding only the sources that had de-whitened projection vectors (original multichannel filters or motor unit action potential profiles) similar to the ones extracted from session 1. The normalized cross-correlation between the extended projection vectors was used as a measure of similarity. For each motor unit identified in the pre-intervention trial, we ran the semi-blind algorithm on the post-intervention trial until a motor unit with normalized cross-correlation >0.8 was found. The algorithm maximized the probability to find the matched motor units across different trials (Martinez-Valdes *et al.*, 2016c). In this study, we used an extension factor of 16 for the decomposition iteration and 50 samples for computing the similarity measures between de-whitened projection vectors (motor unit action potential profiles). These parameters have been validated in (Martinez-Valdes *et al.*, 2016c).

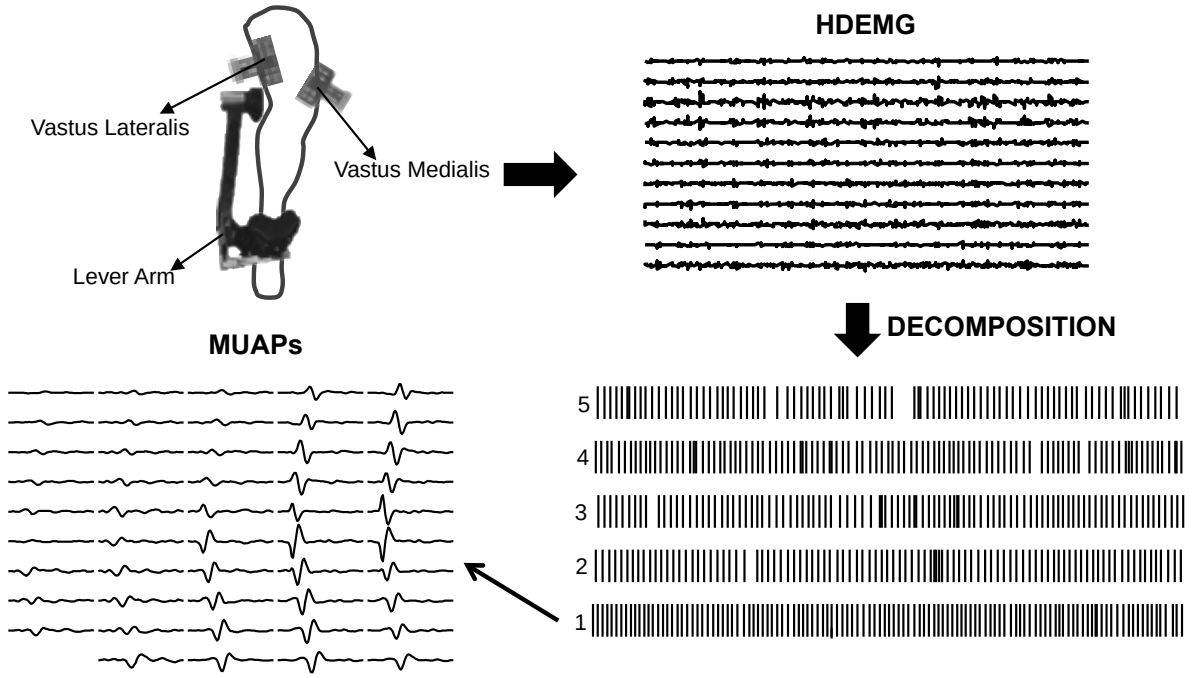

Figure 11. Schematic summarizing high density surface EMG (HDEMG) recordings and motor unit decomposition. A) Two HDEMG electrodes (64 channels each) were positioned over the vastus medialis and vastus lateralis muscles. HDEMG activity was recorded during the production of isometric knee extension force. On the upper right corner of the figure, EMG activity from 1 column of the vastus medialis HDEMG electrode (11channels) is shown. HDEMG data was then decomposed to reveal the firings of 5 individual motor units, which are represented as innervation pulse trains (horizontal bars). The firings from motor unit number 1 were used to trigger surface EMG signals that are presented as motor unit action potentials (MUAPs) across the whole electrode grid (49 double differential channels).

4.3.3.5. Statistical Analysis

Before comparisons, all variables were tested for normality using the Shapiro-Wilk test. The assumption of sphericity was checked by Mauchley's test and, if violated, the Greenhouse-Geisser correction was made to the degrees of freedom. Statistical significance was set at $p < 0.05$. Results are expressed as mean and standard deviation (SD) unless stated otherwise.

The effects of the two training programs on peak torque (MVC), RTD, time to task failure, CoV of torque and co-activation, as well as cardiopulmonary fitness parameters (VO_{2peak}, peak power output, VT1 and VT2) were assessed with a two-way repeated measures analysis of variance (ANOVA) with factors group (END and HIIT) and time (pre and post). Changes in ARV parameters during MVC, RTD and the submaximal contractions as well as mean discharge rate and CoV_{isi}, were evaluated with three-way repeated measures ANOVA with factors group (END and HIIT), time (pre and post) and

muscle (VM and VL) at each torque level (10, 30, 50 and 70% MVC) independently. Pairwise comparisons were made with the Student-Newman-Keuls post hoc test when ANOVA was significant. A four-way repeated measures ANOVA was performed [(factors: group, time, muscle and torque level (10, 30, 50, 70% MVC)] to check whether the recruitment thresholds (knee extension torque at which motor units began discharging action potentials) of the identified motor units, at each submaximal MVC level, increased with torque and also to evaluate if this parameter changed after the intervention. The intra-class correlation coefficient ($ICC_{2,1}$) was also computed in each of the groups (HIIT and END) at all submaximal torque levels, in order to check the consistency of the recruitment thresholds from the motor units tracked between pre and post training sessions. Finally, the partial eta-squared (η_p^2) for ANOVA was used to examine the effect size of changes in all the aforementioned parameters after the training intervention. A η_p^2 less than 0.06 was classified as "small", 0.07-0.14 as "moderate", and greater than 0.14 as "large" (Cohen, 1988).

4.3.4. RESULTS

The two groups initially consisted of 9 subjects each; however, 1 subject from the END group and 1 subject from the HIIT group did not complete the full training protocol and were excluded from the analysis. Therefore, results are presented for 8 participants in the END group (mean (SD) age: 29 (2) years, height: 177 (6) cm, mass: 77 (8) kg) and 8 participants in the HIIT group (mean (SD) age: 29 (3) years, height: 177 (7) cm, mass: 79 (7) kg). No differences were observed between groups for age, height and weight ($P > 0.51$). Moreover, there were no differences between the groups for any of the motor output (peak torque, time to task failure, rate of torque development and CoV of torque), cardiopulmonary fitness (VO_{2peak}, peak power output and submaximal ventilation thresholds) or electrophysiological (surface EMG amplitude, vasti-BF co-activation, motor unit discharge rate, CoV_{isi} and recruitment threshold) parameters assessed during the baseline sessions (prior to training) ($P > 0.32$ in all cases).

4.3.4.1. Cardiorespiratory fitness

Table 10 summarizes cardiorespiratory fitness changes assessed pre and post intervention for the HIIT and END protocols. Overall, all the variables changed similarly in both groups and none of the parameters showed a between-group interaction effect (P > 0.56). VO_{2peak} increased after training by 6.7 (4.1)% and 5.0 (7.8)% in HIIT and END group, respectively (main effect for time; p=0.001, η_p^2= 0.54). Peak power output also increased by 7.4 (3.3)% in HIIT and by 6.3 (3.0)% in END (main effect for time; p<0.001, η_p^2= 0.88). Regarding the submaximal ventilation thresholds, HIIT and END training only induced a significant increase of VT2 work intensity (W) of 9.1 (8.3)% and 9.0 (8.2)% in HIIT and END, respectively (main effect for time; p<0.001, η_p^2= 0.58). Further results for the cardiorespiratory fitness parameters and post-hoc tests can be found in **Table 10**

Table 10. Training response for aerobic parameters assessed during incremental cycling in the HIIT and END training groups

	HIIT			END		
Parameter	Pre	Post	P-value	Pre	Post	P-value
VO_{2peak} (ml/kg/min)	44.2 (7.1)	47.5 (8.0)*	0.02	44.9 (6.3)	47.2 (4.9)*	0.03
Peak power output (W)	334.8 (57.8)	360.3 (53.1)*	<0.001	339.6 (62.5)	361.5 (58.3)*	<0.001
VT1 (ml/kg/min)	28.0 (6.9)	32.5 (7.8)	0.14	28.7 (6.6)	32.0 (4.9)	0.17
VT1 (W)	198.5 (38.9)	222.4 (43.6)	0.07	196.8 (40.5)	227.5 (36.3)	0.05
VT 2 (ml/kg/min)	38.0 (6.0)	41.2 (6.8)	0.07	38.4 (6.9)	41.4 (5.9)	0.10
VT2 (W)	267.8 (39.3)	295.0 (35.4)*	0.03	269.3 (53.3)	294.0 (41.4)*	0.01

Values are means (SD). VT1, first ventilatory threshold; VT2, second ventilatory threshold or respiratory compensation point. Pre, pre-training; Post, post-training. There were no significant differences for any variable between HIIT and END (no interaction effects P>0.05).*Significant difference from Pre (P<0.05), according to post hoc analysis (Student-Newman-Keuls test).

4.3.4.2. Motor output

HIIT and END training induced specific changes in motor performance after the intervention **(Fig. 12)**. Two weeks of HIIT produced a significant increase in peak torque (MVC) of 6.7 (6.6)% that contrasted to the response of END, which showed similar peak torques across pre and post testing sessions (interaction: time × group; p=0.01, η_p^2= 0.38). On the contrary, END showed a significant increase in time to task failure of 16.9% (14.4)

that contrasted to the response of HIIT, which showed similar times to task failure across testing sessions (interaction: time x group; p=0.01, η_p^2= 0.33). Neither HIIT nor END induced any significant change in RTD (interaction: time × group; p=0.09, η_p^2= 0.087). Finally, CoV of torque increased significantly from 2.2 (0.4)% to 2.5 (0.6)% after training for the submaximal contractions at 10% MVC in the HIIT group (interaction: time × group; p=0.033, η_p^2= 0.28) **(Fig. 12)**. Conversely, CoV of torque at the other force levels (30, 50 and 70% MVC) showed no significant changes after the intervention for either group (P > 0.25) **(Fig. 13)**.

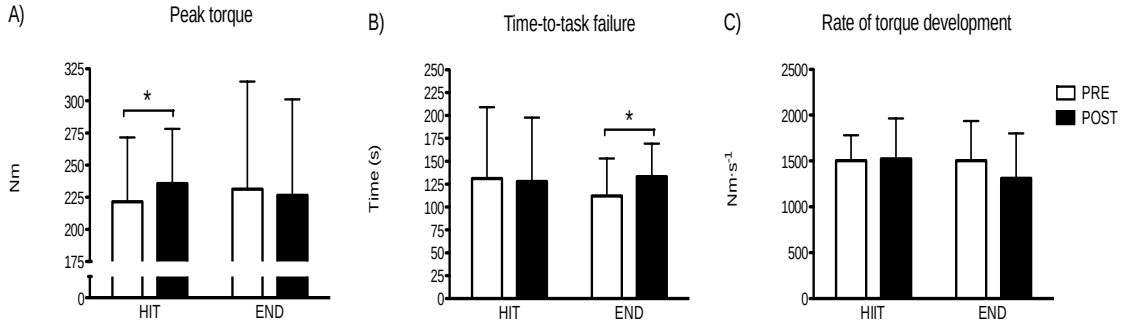

Figure 12. Results show changes [mean (SD)] in motor performance across the 2-wk training intervention. A: peak torque assessed during isometric maximal voluntary contractions (MVC). B: time to task failure assessed during sustained isometric contractions at 30% MVC. C: rate of force development during maximal explosive contractions (maximum slope). Bars represent the mean of each group. *P<0.05.

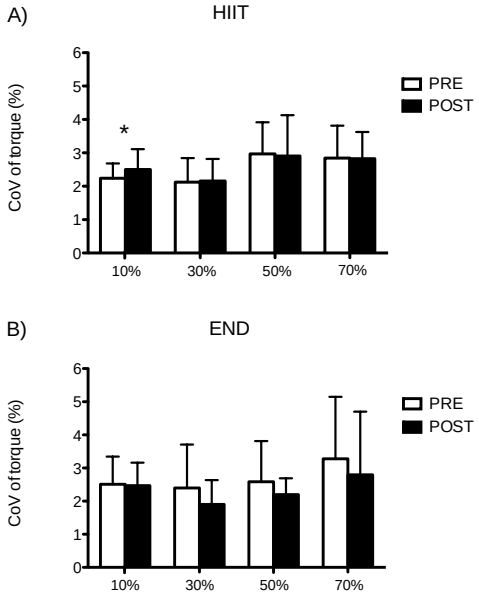

Figure 13. Values are means (SD) of the coefficient of variation of torque (CoV torque) at 10, 30, 50 and 70% of the maximum voluntary contraction (MVC). A: CoV force values for the high intensity interval-training group (HIIT). B: CoV force values for the endurance (END) group. *P<0.05.

4.3.4.3. Surface EMG

Figure 14 shows the EMG amplitude (ARV) of the VM and VL during submaximal (10, 30, 50 and 70% MVC), maximal (MVC) and ballistic isometric knee extension contractions for each testing session (pre-post). Overall, both vasti muscles showed similar changes of EMG amplitude over the training period (interaction: time × muscle; P > 0.15 for all isometric contractions). Regarding submaximal contractions (**Fig. 14a and 14b**), EMG amplitude at 10 and 30% MVC did not change after the intervention for any training group or muscle (VM, VL) (P > 0.14). However, the ARV of VM and VL during the 50% MVC contractions increased significantly for HIIT [11.4 (7.6)% and 11.3 (5.2)% increase in VM and VL, respectively] but not for END (interaction: time × group; P=0.007, η_p^2= 0.44). These differences were maintained at 70% MVC (interaction: time × group; P=0.02, η_p^2= 0.35), where ARV from the HIIT group increased by 13.0 (10.9)% and 14.1 (10.6)% in VM and VL, respectively. A similar result was observed for ARV during the maximal contractions (**Fig. 14c**), since VM and VL activity only increased in the HIIT group by 17.3 (12.6)% and 14.1 (10.2)%, respectively (interaction: time × group; P=0.001, η_p^2= 0.55). Neither HIIT nor END training induced any significant change in ARV during the ballistic contractions (**Fig. 14d**) (P > 0.16). Finally, the amount of vasti-BF co-activation did not differ across sessions in either group (P > 0.50 for all isometric contractions).

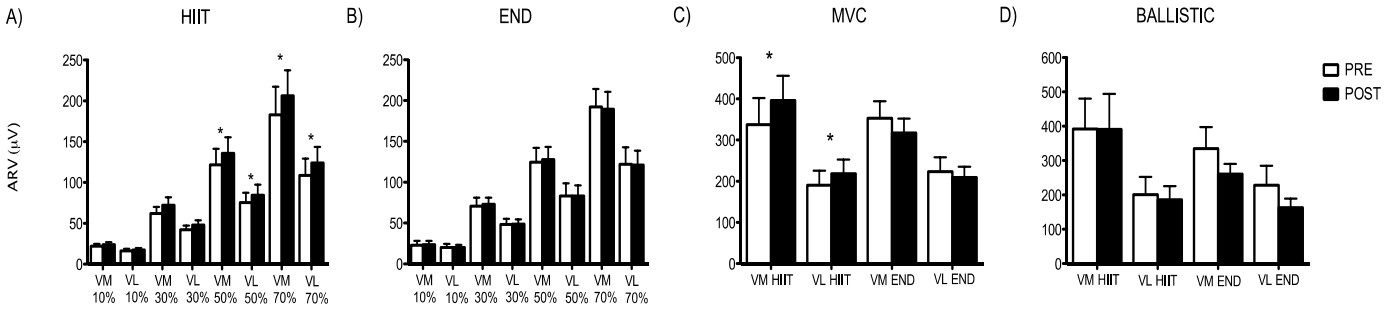

Figure 14. Values are means (SE) for the average rectified value (ARV) of the vastus medialis (VM) and vastus lateralis (VL) obtained during submaximal [10, 30, 50 and 70% of the maximum voluntary contraction (MVC)], maximal (MVC) and explosive isometric knee extension contractions before and after training (pre-post). A: high intensity interval training (HIIT) submaximal ARVs. B: endurance (END) training submaximal ARVs. C: ARV values during MVC for HIIT and END. D: ARV values during explosive contractions for HIIT and END. ARV was assessed during a time interval of 50 ms centered at the time instant of the maximum slope. *P<0.05.

4.3.4.4. Motor unit decomposition and tracking

The total number of decomposed motor units across the different torque levels and sessions was between [mean (range)] 134 (116 - 154) and 122 (95 – 141) for VM and VL, respectively. An example of the motor unit tracking procedure is reported in **Figure 15.** Figure 14a shows three motor units of the VM muscle that were identified at 70% MVC can be seen in the upper left corner. A de-whitened projection vector (motor unit action potential profile) from motor unit 1 (MU 1 PRE, blue) was extracted. This vector was then used to find a source that was maximally similar after the intervention (MU 1 POST, red). Finally, both projection vectors were visually inspected and matched by cross-correlation in order to confirm that the automatic tracking was correct (cross correlation between both projected vectors was 0.86, Figure 15a, right). This procedure was then repeated for motor units 2 and 3 (not shown in the figure). Figure 15b shows instantaneous discharge rates during the stable force part of the isometric contraction at 70% MVC (motor unit firings were low-pass filtered at 2 Hz) from the same 3 tracked motor units presented in Figure 15a PRE (left) and POST (right) HIIT. A clear increase from 19.0 (1.7) to 22.0 (2.1) pps was observed for these units after the intervention (see *Motor unit properties* results). Following this procedure, the number of tracked motor units across pre and post intervention testing sessions varied between 60 (46 - 69) and 50 (33 - 74) for VM and VL, respectively (across all submaximal force levels, in all 16 subjects). Therefore, 44.8 (39.5 – 50.9)% and 41.0 (33.7 – 49.7)% of motor units from those identified by decomposition could be tracked across sessions (average number of tracked motor units per subject was 4 (1) and 3 (1), for the VM and VL, respectively). The cross correlation values from the projecting vectors of the tracked motor units (from VM and VL) ranged between 0.80 and 0.96 (average: 0.86).

4.3.4.5. Motor unit properties

Figure 16 depicts the mean motor unit discharge rate for the VM and VL during the submaximal contractions at 10, 30, 50 and 70% MVC. No differences in the mean motor unit discharge rate were observed between the VM and VL in each testing session (interaction: time × muscle; $P > 0.30$ for all submaximal contractions). However, VM showed significantly greater mean motor unit discharge rates at 50 and 70% MVC (effect:

muscle; P=0.006, η_p^2= 0.45 and P=0.016, η_p^2= 0.37, at 50 and 70% MVC, respectively). For the contractions at 10 and 30% MVC (low threshold motor units, Fig. 16a), the average discharge rate for both vasti muscles was not influenced by either training (interaction: time × group; P=0.30 and 0.1, at 10 and 30% MVC, respectively). However, at both 50 and 70% MVC (high threshold motor units, Fig. 16b) the VM and VL increased their discharge rates (by 8.5 (9.0) and 9.5 (7.1)% at 50% MVC and by 12.1 (7.6) and 9.5 (6.6)% at 70% MVC in VM and VL, respectively) in the HIIT group but not in the END group (interaction: time × group; P=0.036, η_p^2= 0.29 and P=0.015, η_p^2= 0.38, at 50 and 70% MVC, respectively). The recruitment thresholds of the identified motor units increased with torque (effect: torque; P<0.001, η_p^2= 0.88), similarly for both muscles (interaction: torque x muscle; P=0.2, η_p^2= 0.12) and did not change after the intervention (interaction: time x group x torque; P=0.16, η_p^2= 0.14). These results are confirmed by the high ICCs found for the recruitment thresholds pre and post intervention at all force levels (average ICCs of 0.90 and 0.95 for HIIT and END, respectively) **(Fig. 17).** Finally, neither training induced change in CoV_{isi} **(Table 11)**.

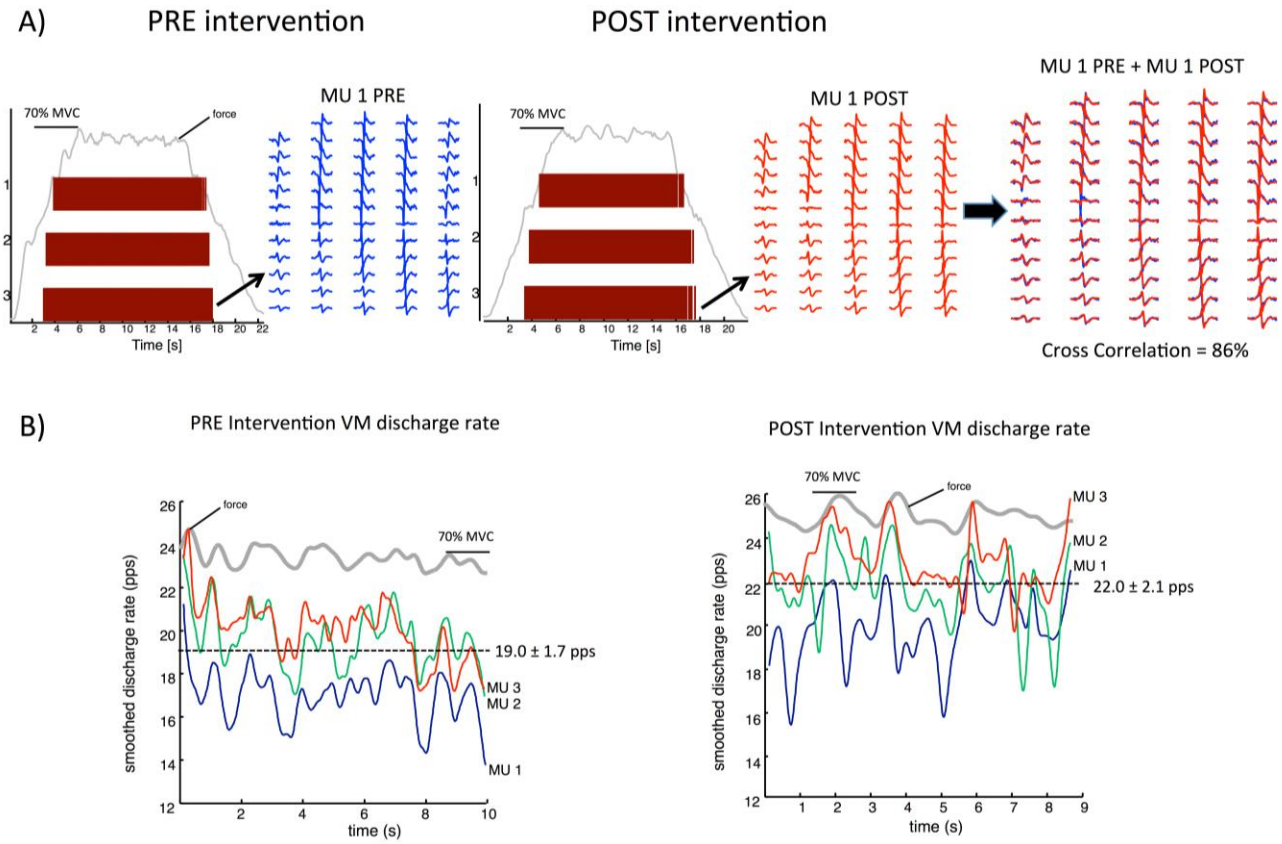

Figure 15. Procedure for motor unit tracking from one representative subject in the HIIT group. A) Three vastus medialis (VM) motor unit spike trains decomposed with convolutive blind source separation at 70% of the maximum voluntary contraction (MVC) before (PRE) the intervention can be seen in the left half of the figure. A de-whitened projection vector (motor unit action potential shapes across the electrode grid in 59 single differential channels) from the first motor unit is shown in blue. Semi-blind source separation was applied after the intervention to extract the source that was maximally similar to the projecting vector of motor unit one (center half of the figure, red). Finally, these two projecting vectors were compared by cross-correlation (right half of the figure), and were regarded as the same motor unit since they had a cross correlation of 86%. This procedure was repeated for motor units 2 and 3 (not shown). B) Instantaneous firing rates (motor unit firings were low pass filtered at 2Hz) from the same three motor units presented in A, during the stable force region before (PRE, left half of the figure) and after (POST, right half of the figure) the intervention. Note the increase in firing rates from 19 (1.7) pulses per second (pps) to 22.0 (2.1) pps.

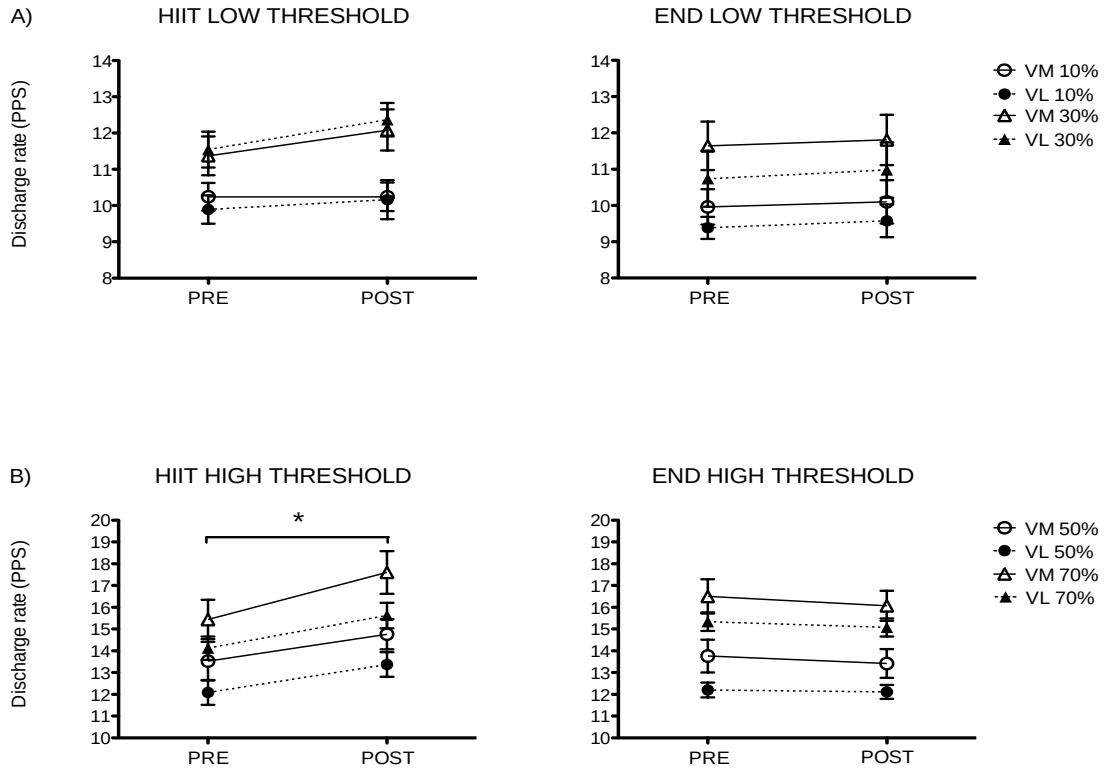

Figure 16. Values are means (SE) for motor unit discharge rates (in pulses per second, PPS) of the vastus medialis (VM) and vastus lateralis (VL) obtained during submaximal [10, 30, 50 and 70% of the maximum voluntary contraction (MVC)] contractions. A: Low threshold motor units discharge rate results (10 and 30% MVC) of endurance (END) and high intensity interval training (HIIT). B: High threshold motor unit discharge rate results (50 and 70% MVC) of END and HIIT. *P<0.05.

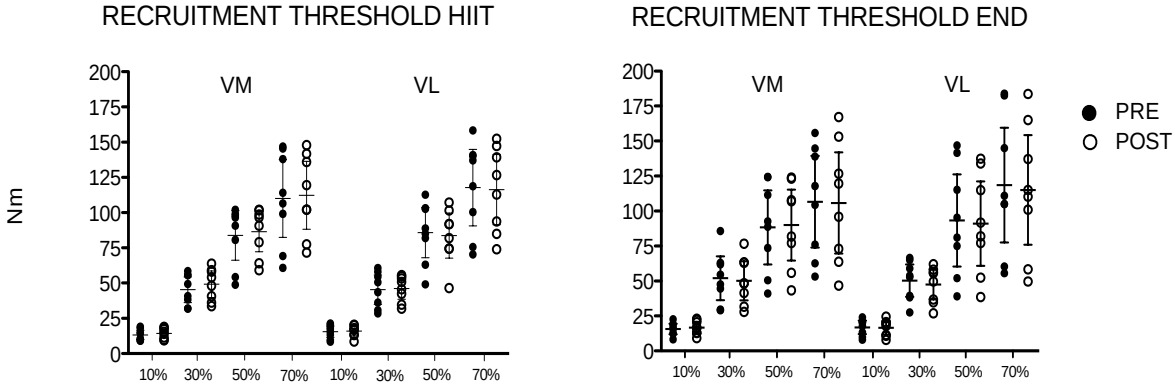

Figure 17. Motor unit recruitment threshold individual values (whiskers represent the 95% confidence interval) for vastus medialis (VM) and vastus lateralis (VL), before (PRE, filled circles) and after (POST, open circles) high intensity interval training (HIIT) and endurance training (END) at all force levels (10, 30, 50 and 70% MVC).

Table 11. Coefficient of variation for inter-spike interval (CoV_{isi})% for motor units identified for each group, muscle, load and session

	HIIT				END			
	PRE		POST		PRE		POST	
Torque level %MVC	VM	VL	VM	VL	VM	VL	VM	VL
10%	16.8 (1.4)	17.7 (2.9)	16.9 (3.7)	18.9 (5.8)	18.8 (1.9)	15.9 (3.4)	18.6 (3.4)	16.2 (4.5)
30%	20.5 (4.1)	24.4 (5.5)	21.2 (2.6)	23.0 (5.2)	24.4 (5.5)	23.2 (6.1)	22.9 (5.3)	24.2 (7.7)
50%	25.4 (3.6)	27.1 (6.9)	26.3 (4.2)	28.2 (4.4)	26.5 (4.5)	21.5 (5.2)	26.5 (3.6)	22.8 (6.6)
70%	28.3 (7.3)	29.0 (4.2)	27.3 (5.2)	29.8 (3.2)	27.4 (4.8)	27.5 (4.8)	27.2 (4.2)	26.1 (6.8)

Coefficient of variation for the inter-spike interval (CoV_{isi}) of motor units from each group, muscle [vastus medialis (VM) and vastus lateralis (VL)], force level [10, 30, 50 and 70% of the maximum voluntary contraction (MVC)], and session (pre and post).

4.3.5. DISCUSSION

This is the first study to show that HIIT and END training elicit distinct adjustments in motor output and motor unit behavior despite similar changes in cardio-respiratory fitness. HIIT determined an increase in MVC peak torque, with an increase in EMG amplitude and motor unit discharge rate at the highest force levels (from 50% MVC and above). Conversely, END induced an increase in time to task failure for a sustained contraction at 30% MVC and no changes in isometric knee extension strength or motor unit discharge rate. Taken together, these findings suggest that HIIT and END induce specific neuromuscular adaptations, which likely relate to their differences in exercise intensity and training volume.

4.3.5.1. Training protocols and motor output

Previous studies have reported that HIIT can be used as an alternative to endurance training. Studies comparing short-term low-volume HIIT and high-volume END have found similar physiological adaptations in aerobic metabolism (Gibala *et al.*, 2006; Little *et al.*, 2010), exercise performance (Gibala *et al.*, 2006; McKay *et al.*, 2009) and cardiorespiratory fitness (McKay *et al.*, 2009; Gibala *et al.*, 2012), despite large differences in exercise volume and exercise intensity. Therefore, we used previously validated protocols that differed in both time commitment and intensity, but were known to induce similar metabolic and cardiorespiratory fitness adaptations (Gibala *et al.*, 2006; Little *et al.*,

2010). These protocols were selected in order to verify whether similar adaptations were also observed at the neuromuscular level, despite the divergent nature of both training regimes (HIIT: low-volume, high-load vs. END: high-volume, low-load). As expected, the two trainings resulted in a similar increase in VO_{2peak}, peak power output and submaximal ventilation thresholds (Table 10), in agreement with previous reports (McKay *et al.*, 2009; Gibala *et al.*, 2012). However, HIIT and END induced different changes in motor performance that can be related to their different training characteristics. Currently there are no other studies that have detailed changes in neuromuscular performance following HIIT. In the only study that examined changes in muscle function, the authors did not observe changes in isometric knee extension strength after a 4-week HIIT intervention (de Oliveira *et al.*, 2015), in contrast with our results. However, the training consisted of lower loads (average peak power output of 236 W vs. 335 W, in the current study). Moreover, peak power output was estimated with a stepwise incremental cycling protocol with relatively long steps of 3 min, which is known to underestimate the peak power (Zuniga *et al.*, 2012). The current results suggest that HIIT training must be performed at the maximum (or supra maximum) power output achieved during an incremental ramp test in order to induce a significant increase in knee extensor strength. Indeed, the repetitive muscle activity at high loads was presumably responsible for the increase in MVC peak torque after HIIT.

Previous studies have also reported a significant increase in isometric knee extension endurance time (time to task failure) during low-level submaximal contractions after an END training intervention (Vila-Cha *et al.*, 2010; Vila-Cha *et al.*, 2012). For instance, Vila-Cha et al. (Vila-Cha *et al.*, 2010) observed a 30% increase in time to task failure after a 6-week END cycling intervention. In the same study, the authors did not find any increase in time to task failure following strength training. These results are comparable to our findings. Again, these different adaptations are presumably due to the differences in training volume and exercise intensity between the two interventions (HIIT: short periods of activity at high intensity vs. END: long periods of activity at moderate intensity).

Even though HIIT was associated with increased MVC peak torque, no change in RTD was observed (Fig. 12c). Small to moderate increases in knee extensor strength

(approximately 7% in the current study) are not typically associated with increased RTD. Both Vila-Cha et al. (Vila-Cha *et al.*, 2010) and Aagaard et al. (Aagaard *et al.*, 2002) only observed an increase in RTD after the isometric knee extension strength (following resistance training) increased by 18% and 17%, respectively. Nevertheless, it is possible that more ballistic HIIT protocols, such as the Wingate-based sprint interval training, may induce changes in RTD.

4.3.5.2. Maximal and submaximal contractions and global EMG parameters

Changes of VM and VL EMG amplitude showed similar behavior in the HIIT and END groups at the lowest torque levels (10 and 30% MVC), where no significant change in EMG amplitude was observed. However, only HIIT showed a significant increase in EMG amplitude for both vasti muscles in contractions at 50, 70 and 100% MVC (Fig. 14). Previous studies have documented that both increases in muscle cross sectional area and neural factors are responsible for increases in maximal muscle strength (Duchateau *et al.*, 2006). Since changes in muscle-fiber architecture have not been documented after only two weeks of training, the surface EMG results in the current study strongly suggest that the observed changes in maximal isometric muscle torque after HIIT are mainly of neural origin. Increased agonist muscle activation and decreased antagonist activation have been suggested as important factors influencing increases in muscle strength (Duchateau *et al.*, 2006). However, we did not identify changes in vasti/BF co-activation (at all torque levels). Therefore, the increased maximal torque was presumably due to factors that also influenced the EMG-torque relation in the agonist, such as changes in motor unit discharge rates or peripheral factors (e.g., muscle fiber conduction velocity), as also shown in a recent study (Vila-Cha *et al.*, 2010). These early adaptations likely involve changes in supraspinal excitability, spinal pathways or changes in the membrane properties in the motoneurons (Duchateau *et al.*, 2006). Nevertheless, the exact nature of these early neural adaptations is not yet known (Duchateau *et al.*, 2006). Regarding the submaximal contractions, the observed changes in surface EMG amplitude in HIIT were markedly greater among the highest contraction levels (Fig. 14a), which ultimately suggest a preferential change in the discharge rates of high threshold motor units *(see Submaximal contractions and motor unit properties).* Indeed, it is likely that the high loads placed on the subjects during HIIT increased the activity of these units. In support of this

observation, Vila-Cha et al. (Vila-Cha *et al.*, 2010) previously reported an increase in EMG amplitude at 30 and 100% MVC, but not at 10% MVC, after 3 weeks of resistance training. However, this earlier work also showed an increase of EMG amplitude at 10 and 30% MVC after 3 weeks of END training. Since a decrease in motor unit discharge rate was simultaneously observed after END training, this result was interpreted as an increase of motor unit recruitment at these force levels, although EMG amplitude depends on multiple influencing factors (Farina *et al.*, 2004, 2014). In this study, we attempted to limit the variability in EMG amplitude estimates by averaging across all electrodes of the grid (Gallina *et al.*, 2016; Martinez-Valdes *et al.*, 2016b).

4.3.5.3. Submaximal contractions and motor unit properties

In accordance with the surface EMG results, the HIIT and END groups showed similar motor unit discharge rates pre-and post-training for VM and VL at 10 and 30% MVC. However, only HIIT induced an increase in motor unit discharge rate at 50 and 70% MVC, which is also in agreement with surface EMG results (Fig. 16). Together, these findings suggest that changes in motor unit discharge rate are not only specific to the training protocol, but also to the size (Henneman *et al.*, 1965) and threshold of the motor units recruited during the exercise. Indeed, the main differences between HIIT and END are the volume of training and the loads at which the subjects perform the exercise. Even though we did not measure motor unit recruitment during cycling (this is not technically possible), the HIIT protocol, that involved short exercise bouts at the maximal power output, likely required the recruitment of most motor units (Vollestad & Blom, 1985; Krustrup *et al.*, 2004) whereas the END training, that was performed at a much lower load, likely involved lower threshold units with greater aerobic capacity (Vollestad & Blom, 1985; Krustrup *et al.*, 2004). In accordance with size-specific adjustments in motor units, Kamen and Knight (Kamen & Knight, 2004) previously observed an increase in VL discharge rates at 100% MVC, but not at 10 or 50% MVC, after 6 weeks of resistance training involving maximal knee-extension isometric contractions. For END, we did not find training-induced changes in motor unit discharge rates in the torque range investigated (Fig. 16). This observation is in accordance with Mettler et al. (Mettler & Griffin, 2016) but contrasts with the results of Vila-Cha et al. (Vila-Cha *et al.*, 2010). However, the latter study differed with respect to ours for training intensity (50 to 75% of heart rate reserve vs.

65% VO_{2peak}), volume (60 to 150 min/week vs. 285 to 345 min/week) and duration (3 to 6 weeks vs. two weeks) (Vila-Cha *et al.*, 2010). Collectively, these findings suggest that END would lead to either maintained or decreased discharge rates, since MVC torque is not expected to change after this type of training (Glowacki *et al.*, 2004). Maintained or decreased motor unit discharge rates after END training interventions (at the same relative torque level) are thought to be important factors for longer times to task failure during submaximal, isometric fatiguing contractions (Vila-Cha *et al.*, 2010; Vila-Cha *et al.*, 2012; Mettler & Griffin, 2016).

The tracking technique applied in this study allowed for the first time to compare individual motor unit recruitment thresholds before and after training. The Recruitment thresholds of the tracked motor units were similar before and after the intervention for both muscles and groups (Fig. 17), suggesting that the observed changes in discharge rate after HIIT were mainly due to an increased neural drive to the muscle, and not to changes in intrinsic motor neuron properties. Previous studies documenting changes in motor unit discharge rates have used unmatched population samples to infer adaptations to a particular motor unit pool (Kamen & Knight, 2004; Pucci *et al.*, 2006; Vila-Cha *et al.*, 2010; Stock & Thompson, 2014; Mettler & Griffin, 2016). However, these previous approaches are limited by the possibility of comparing different motor units, with different recruitment thresholds, in the pre and post training sessions. Conversely, we could record and follow the same motor units across sessions, providing an accurate interpretation of changes in discharge rate and recruitment threshold. Finally, no change in discharge rate variability (CoV_{isi}) was observed for any of the groups after the intervention, despite that there was a significant increase in CoV of torque for the HIIT group at 10% MVC. A recent study showed that 6 weeks of resistance training increases force/torque steadiness (reduction in CoV of force/torque) and reduces motor unit discharge rate variability (CoV_{isi}) in submaximal contractions at 20 and 30% MVC (Vila-Cha & Falla, 2016). However, an increase in force steadiness following resistance training has not been observed in all studies (Beck *et al.*, 2011) and the association between enhanced force steadiness and the reduction of CoV_{isi} is poor (Negro *et al.*, 2009). Therefore, the increase in CoV of torque at 10% MVC for the HIIT group in the present study could be related to other factors rather than an increase in CoV_{isi}. Although the high loads performed during HIIT might have

induced a reduction in the accuracy to maintain the required steadiness at low torque levels, torque steadiness remained similar at all torque levels following END training despite of the low to moderate loads used for this type of training. Therefore, the observations of training-induced changes in torque steadiness require further investigation.

4.3.5.4. Methodological implications

In this study, for the very first time, we applied motor unit tracking across sessions to study training interventions (Martinez-Valdes *et al.*, 2016a; Negro *et al.*, 2016a). With this approach, all differences in motor unit discharge rate between END and HIIT groups had a large effect size and showed a clear intervention effect. Previous investigations of this type but without motor unit tracking have shown contradicting results (Kamen & Knight, 2004; Vila-Cha *et al.*, 2010; Stock & Thompson, 2014; Mettler & Griffin, 2016). Some studies have even failed to report an effect in discharge rates despite clear increases in muscle strength and surface EMG amplitude (Pucci *et al.*, 2006). We suggest that these changes could have been masked because of the low number of identified motor units (usually low-threshold) and the un-matched motor units across sessions. Accordingly, we have previously shown that the effect size in longitudinal investigations is substantially increased with our technique (Martinez-Valdes *et al.*, 2016a; Negro *et al.*, 2016a), which opens new possibilities for further research.

4.3.5.5. Conclusion

Two weeks of HIIT and END showed similar improvement in cardiorespiratory fitness but different adjustments in motor unit behavior. HIIT enhanced maximum torque output and was accompanied by an increase in motor unit discharge rate at the highest torque levels (50 and 70% MVC). In contrast, END increased the time to task failure, but did not influence motor unit discharge rates. These findings reveal that HIIT and END induce differential adaptations among low and high threshold motor units. The study also shows the first results on training-induced changes in motor unit discharge rate by tracking the same individual units before and after training. This methodology may open new perspectives in the study of neural adaptations to training.

4.3.6. REFERENCES

Aagaard P, Simonsen EB, Andersen JL, Magnusson P & Dyhre-Poulsen P. (2002). Increased rate of force development and neural drive of human skeletal muscle following resistance training. *Journal of applied physiology* **93,** 1318-1326.

Barbero M, Merletti R & Rainoldi A. (2012). *Atlas of muscle innervation zones : understanding surface electromyography and its applications*. Springer, Milan ; New York.

Beck TW, DeFreitas JM, Stock MS & Dillon MA. (2011). Effects of Resistance Training on Force Steadiness and Common Drive. *Muscle & nerve* **43,** 245-250.

Burgomaster KA, Hughes SC, Heigenhauser GJ, Bradwell SN & Gibala MJ. (2005). Six sessions of sprint interval training increases muscle oxidative potential and cycle endurance capacity in humans. *Journal of applied physiology* **98,** 1985-1990.

Castronovo AM, Negro F, Conforto S & Farina D. (2015). The proportion of common synaptic input to motor neurons increases with an increase in net excitatory input. *Journal of applied physiology* **119,** 1337-1346.

Cohen J. (1988). *Statistical power analysis for the behavioral sciences*. L. Erlbaum Associates, Hillsdale, N.J.

de Oliveira MF, Caputo F, Corvino RB & Denadai BS. (2015). Short-term low-intensity blood flow restricted interval training improves both aerobic fitness and muscle strength. *Scandinavian journal of medicine & science in sports*.

Duchateau J & Enoka RM. (2011). Human motor unit recordings: origins and insight into the integrated motor system. *Brain research* **1409,** 42-61.

Duchateau J, Semmler JG & Enoka RM. (2006). Training adaptations in the behavior of human motor units. *Journal of applied physiology* **101,** 1766-1775.

Farina D & Holobar A. (2016). Characterization of Human Motor Units From Surface EMG Decomposition. *P Ieee* **104,** 353-373.

Farina D, Merletti R & Enoka RM. (2004). The extraction of neural strategies from the surface EMG. *Journal of applied physiology* **96,** 1486-1495.

Farina D, Merletti R & Enoka RM. (2014). The Extraction of Neural Strategies from the Surface Emg: An Update. *Journal of applied physiology***,** jap 00162 02014.

Farina D, Negro F, Muceli S & Enoka RM. (2016). Principles of Motor Unit Physiology Evolve With Advances in Technology. *Physiology* **31,** 83-94.

Gallina A, Pollock CL, Vieira TM, Ivanova TD & Garland SJ. (2016). Between-day reliability of triceps surae responses to standing perturbations in people post-stroke and healthy controls: A high-density surface EMG investigation. *Gait & posture* **44,** 103-109.

Gibala MJ, Little JP, Macdonald MJ & Hawley JA. (2012). Physiological adaptations to low-volume, high-intensity interval training in health and disease. *The Journal of physiology* **590,** 1077-1084.

Gibala MJ, Little JP, van Essen M, Wilkin GP, Burgomaster KA, Safdar A, Raha S & Tarnopolsky MA. (2006). Short-term sprint interval versus traditional endurance training: similar initial

adaptations in human skeletal muscle and exercise performance. *The Journal of physiology* **575,** 901-911.

Glowacki SP, Martin SE, Maurer A, Baek W, Green JS & Crouse SF. (2004). Effects of resistance, endurance, and concurrent exercise on training outcomes in men. *Medicine and science in sports and exercise* **36,** 2119-2127.

Henneman E, Somjen G & Carpenter DO. (1965). Excitability and inhibitability of motoneurons of different sizes. *Journal of neurophysiology* **28,** 599-620.

Kamen G & Knight CA. (2004). Training-related adaptations in motor unit discharge rate in young and older adults. *The journals of gerontology Series A, Biological sciences and medical sciences* **59,** 1334-1338.

Krustrup P, Soderlund K, Mohr M & Bangsbo J. (2004). The slow component of oxygen uptake during intense, sub-maximal exercise in man is associated with additional fibre recruitment. *Pflugers Archiv : European journal of physiology* **447,** 855-866.

Laine CM, Martinez-Valdes E, Falla D, Mayer F & Farina D. (2015). Motor Neuron Pools of Synergistic Thigh Muscles Share Most of Their Synaptic Input. *The Journal of neuroscience : the official journal of the Society for Neuroscience* **35,** 12207-12216.

Little JP, Safdar A, Wilkin GP, Tarnopolsky MA & Gibala MJ. (2010). A practical model of low-volume high-intensity interval training induces mitochondrial biogenesis in human skeletal muscle: potential mechanisms. *The Journal of physiology* **588,** 1011-1022.

Martinez-Valdes E, Guzman-Venegas RA, Silvestre RA, Macdonald JH, Falla D, Araneda OF & Haichelis D. (2016a). Electromyographic adjustments during continuous and intermittent incremental fatiguing cycling. *Scandinavian journal of medicine & science in sports* **26,** 1273-1282.

Martinez-Valdes E, Laine CM, Falla D, Mayer F & Farina D. (2016b). High-density surface electromyography provides reliable estimates of motor unit behavior. *Clinical neurophysiology : official journal of the International Federation of Clinical Neurophysiology* **127,** 2534-2541.

Martinez-Valdes E, Negro F, Laine CM, Falla D, Mayer F & Farina D. (2016c). Tracking motor units longitudinally across experimental sessions with high-density surface electromyography. *The Journal of physiology*.

McKay BR, Paterson DH & Kowalchuk JM. (2009). Effect of short-term high-intensity interval training vs. continuous training on O2 uptake kinetics, muscle deoxygenation, and exercise performance. *Journal of applied physiology* **107,** 128-138.

Mettler JA & Griffin L. (2016). Muscular endurance training and motor unit firing patterns during fatigue. *Experimental brain research* **234,** 267-276.

Negro F, Holobar A & Farina D. (2009). Fluctuations in isometric muscle force can be described by one linear projection of low-frequency components of motor unit discharge rates. *The Journal of physiology* **587,** 5925-5938.

Negro F, Muceli S, Castronovo AM, Holobar A & Farina D. (2016). Multi-channel intramuscular and surface EMG decomposition by convolutive blind source separation. *Journal of neural engineering* **13,** 026027.

Pucci AR, Griffin L & Cafarelli E. (2006). Maximal motor unit firing rates during isometric resistance training in men. *Experimental physiology* **91,** 171-178.

Rakobowchuk M, Tanguay S, Burgomaster KA, Howarth KR, Gibala MJ & MacDonald MJ. (2008). Sprint interval and traditional endurance training induce similar improvements in peripheral arterial stiffness and flow-mediated dilation in healthy humans. *American journal of physiology Regulatory, integrative and comparative physiology* **295,** R236-242.

Stock MS & Thompson BJ. (2014). Effects of barbell deadlift training on submaximal motor unit firing rates for the vastus lateralis and rectus femoris. *PloS one* **9,** e115567.

Vila-Cha C & Falla D. (2016). Strength training, but not endurance training, reduces motor unit discharge rate variability. *Journal of electromyography and kinesiology : official journal of the International Society of Electrophysiological Kinesiology* **26,** 88-93.

Vila-Cha C, Falla D, Correia MV & Farina D. (2012). Adjustments in motor unit properties during fatiguing contractions after training. *Medicine and science in sports and exercise* **44,** 616-624.

Vila-Cha C, Falla D & Farina D. (2010). Motor unit behavior during submaximal contractions following six weeks of either endurance or strength training. *Journal of applied physiology* **109,** 1455-1466.

Vollestad NK & Blom PC. (1985). Effect of varying exercise intensity on glycogen depletion in human muscle fibres. *Acta physiologica Scandinavica* **125,** 395-405.

Wasserman K. (2012). *Principles of exercise testing and interpretation : including pathophysiology and clinical applications*. Wolters Kluwer Health/Lippincott Williams & Wilkins, Philadelphia.

Zuniga JM, Housh TJ, Camic CL, Bergstrom HC, Traylor DA, Schmidt RJ & Johnson GO. (2012). Metabolic parameters for ramp versus step incremental cycle ergometer tests. *Applied physiology, nutrition, and metabolism = Physiologie appliquee, nutrition et metabolisme* **37,** 1110-1117.

4.4. Study 4

MOTOR NEURON POOLS OF SYNERGISTIC THIGH MUSCLES SHARE MOST OF THEIR SYNAPTIC INPUT

C.M. Laine[1], E. Martinez-Valdes[2], D. Falla[1,3], F. Mayer[2], D. Farina[1]

Affiliations

1. Department of Neurorehabilitation Engineering,
   Bernstein Focus Neurotechnology Göttingen (BFNT),
   Bernstein Centre for Computational Neuroscience (BCCN),
   University Medical Center Göttingen,
   Georg-August University Göttingen, Germany

2. Department of Sports Medicine and Sports Orthopaedics,
   University of Potsdam

3. Pain Clinic,
   Center for Anesthesiology, Emergency and Intensive Care Medicine,
   University Hospital Göttingen.

Reference

Laine CM, Martinez-Valdes E, Falla D, Mayer F & Farina D. (2015). Motor Neuron Pools of Synergistic Thigh Muscles Share Most of Their Synaptic Input. The Journal of neuroscience : the official journal of the Society for Neuroscience ***35,*** *12207-12216.*

4.4.1. ABSTRACT

Neural control of synergist muscles is not well understood. Presumably, each muscle in a synergistic group receives some unique neural drive and some drive which is also shared in common with other muscles in the group. In this investigation, we sought to characterize the strength, frequency spectrum, and force dependence of the neural drive to the human vastus lateralis and vastus medialis muscles during the production of isometric knee extension forces at 10% and 30% of maximum voluntary effort. High-density surface electromyography (EMG) recordings were decomposed into motor unit action potentials in order to examine the neural drive to each muscle. Motor unit coherence analysis was used to characterize the total neural drive to each muscle as well as the drive shared between muscles. Using a novel approach based on partial coherence analysis, we were also able to specifically study the neural drive unique to each muscle (not shared). The results showed that the majority of neural drive to the vasti muscles was a cross-muscle drive characterized by a force-dependent strength and bandwidth. Muscle-specific neural drive was at low frequencies (< 5 Hz) and relatively weak. Frequencies of neural drive associated with afferent feedback (6-12 Hz) and with descending cortical input (~20 Hz) were almost entirely shared by the two muscles, while low frequency (< 5 Hz) drive comprised shared (primary) and muscle-specific (secondary) components. This study is the first to directly investigate the extent of shared vs. independent control of synergist muscles at the motor neuron level.

4.4.2. INTRODUCTION

It has long been suspected that actions involving multiple muscles are controlled through a simplified set of high-level commands, the fingerprints of which can be observed as coordinated activity among muscles, i.e., 'muscle synergies' (for reviews see: Tresch and Jarc, 2009; Bizzi and Cheung, 2013). There is an important controversy, however, as to whether such activity implies that multiple muscles are controlled together by shared neural input, or if it simply reflects the mechanical constraints of a given task (Tresch and Jarc, 2009; Kutch and Valero-Cuevas, 2012; Bizzi and Cheung, 2013). In several species, stimulation of cutaneous (Tresch *et al*., 1999), spinal (Giszter *et al*., 1993; Levine *et al*., 2014), or cortical (Graziano *et al*., 2002; Overduin *et al*., 2012, 2014) neurons produces coordinated muscle activities, strongly suggesting the construction of muscle synergies by the nervous system. However, many questions remain related to the usage of such circuitry in man, and in particular, the extent to which muscles of a synergy are driven by shared vs. independent inputs. The most common methods used to characterize muscle synergies in man cannot assess the distribution/delivery of neural drive to the activated muscles.

For decades, neuromuscular control signals have been investigated by examining correlated activity among motor units (Sears and Stagg, 1976; De Luca *et al*., 1982; Rosenberg *et al*., 1989; Farmer *et al*., 1993; Halliday *et al*., 1995), since this reflects their shared (and 'effective') neural drive (Farina and Negro, 2014; Farina *et al*., 2014). The strategy has not generally been applied to the analysis of groups of muscles. It has been exceedingly rare in past studies for both within-muscle and across-muscle motor unit correlations to be evaluated during execution of a motor task. Even with such measurements, it is not possible to determine the relative strength/proportion of neural drive that is unique to a given muscle vs. shared with other simultaneously activated muscles.

In this study, we have overcome these limitations to investigate a simple synergy. Specifically, we investigated two synergist muscles of the quadriceps, the vastus lateralis (VL) and vastus medialis (VM), during production of two isometric knee extension forces (10% and 30% of maximum voluntary effort). To comprehensively evaluate within-muscle and across-muscle neural drive, we used the well-established technique of motor

unit coherence analysis (Rosenberg *et al*., 1989; Farmer *et al*., 1993; Halliday *et al*., 1995; Amjad *et al*., 1997), which describes the frequency spectrum of neural input. We then applied a novel method based on partial coherence analysis to separate the total neural drive to each muscle into shared (cross-muscle) and unique (muscle-specific) components, as well as evaluate the relative strength of each.

Our overall hypothesis was that the two vasti muscles would be controlled primarily by a shared neural drive, with relatively little unique drive to each muscle. This prediction was motivated by the high degree of synchronized motor unit discharges (Mellor and Hodges, 2005) and firing rate fluctuations (Beck *et al*., 2012) across the two vasti muscles, which attain magnitudes similar to what has been reported for within-muscle motor unit correlations (De Luca *et al*., 2008; Beck *et al*., 2011).

The idea that multiple muscles can be controlled mainly through shared input is of great importance for understanding 'muscle synergies'. Our study represents the first direct test (and direct support) of this concept at the level of neural drive in man, for a simple task and synergy. We also present the most comprehensive characterization of neural drive to the vasti muscles to date.

4.4.3. METHODS

All procedures were approved by the Universitaetsmedizin Goettingen (ref # 24/1/14), and were conducted in accordance with the Declaration of Helsinki. Written consent was obtained from all study participants. Ten healthy adult males (mean (SD) age 27(4)) participated in the study, all free from musculoskeletal or neurological conditions affecting the lower extremities, and all without history of lower limb surgery.

4.4.3.1. Task

Participants were seated upright in the chair of a Biodex System 3 (Biodex Medical Systems Inc., Shirley, NY, USA), which enabled stable fixation of the torso, right thigh and lower leg. The knee was flexed at an angle of 90 degrees, and isometric knee extension force was exerted on a dynamometer fixed to the lower leg just above the lateral malleolus. Knee extension forces were quantified for each individual as a percentage of their maximum voluntary contraction (%MVC) level, established at the beginning of each recording session. During each recording session, the participants used visual feedback of

their exerted force (displayed on a computer screen) to maintain 20s contractions at 10% or 30 % MVC. Three contractions at each force level were accomplished per session, separated by at least 2 min, and in randomized order. Each individual participated in 3 sessions, resulting in a total of 9 contractions per force level for each subject.

4.4.3.2. Electromyography (EMG)

Surface EMG signals were recorded over the VM and VL of each subject using high-density, 64-channel surface EMG arrays (LISiN-OT Bioelettronica, Torino, Italy). Each electrode array consists of a 5 x 13 grid of electrodes (1mm diam., 8mm interelectrode distance), with one electrode absent from the upper right corner. The arrays were located centrally between the proximal and distal tendons of the muscles, with the long axis of each rectangular array aligned with the muscle fibers (Figure 2). The proper positioning of the electrodes was confirmed by moving a non-adhesive linear electrode array over the skin during a voluntary muscle contraction, allowing the innervation zone, tendon regions, and appropriate orientation angle to be determined (Masuda *et al*., 1985; Farina *et al*., 2001). Signals were amplified and recorded (sampling rate 2048 Hz) using an OT Bioelettronica USB2 amplifier and associated OT Biolab software (LISiN-OT Bioelettronica). The EMG data was processed and analyzed offline using Matlab (The Mathworks Inc., Natick, Massachusetts, USA). Prior to decomposition, the 64-monopolar EMG channels (referenced at the knee) were re-referenced offline to form 59 bipolar channels (i.e. using the difference between adjacent electrodes in the direction of the muscle fibers).

4.4.3.3.Motor unit decomposition

EMG signals were decomposed into single motor unit activity using an automatic blind source separation algorithm which has undergone extensive validation (Holobar and Zazula, 2004, 2007; Farina *et al*., 2008, 2009). The algorithm reconstructs signals as outputs of a convolutive mixing model. In this model, spike trains represent the motor unit activity, whereas the motor unit action potential (MUAP) shapes are treated as mixing coefficients. The model can account for arbitrary differences in MUAP shapes observed from different EMG channels (see Holobar and Farina, 2014 for review). The method is fundamentally different from common template-matching procedures, which are typically used for decomposing multi-unit signals recorded from a single spatial location.

Since the decomposition algorithm is automatic, each output spike train must be evaluated for quality prior to use. Only units whose firing rates were stable over the entire contraction (no pauses > 500 ms) were utilized in further analysis. Also, motor units were discarded if the coefficient of variation of their inter-spike-intervals was > 30%, as this would indicate a high number of erroneously classified or missed action potentials (Holobar *et al*., 2014). Mean discharge rates were required to fall between 5 and 30 Hz (Enoka and Fuglevand, 2001). Additionally, a signal-based performance metric called pulse-to-noise ratio (PNR), was used to test the accuracy of the decomposed units. PNR is an indicator of the mean square error between the true discharge pattern of each identified unit and its estimation, where units with PNR > 30dB, exhibit a sensitivity > 90% and a false alarm rate < 2% (Holobar *et al*., 2014). For the present study, only motor units with a PNR > 30dB were used.

For further analysis, the activity of each motor unit was expressed as a binary spike train in which each time sample (sampling frequency = 2048 Hz) was assigned either a 0 or 1, depending on whether the particular time sample marked the beginning of a motor unit action potential. Trials in which fewer than 3 motor units were decomposed were excluded from further analysis. This left a total of 80 trials for each force level, spread over 9 subjects.

4.4.3.4. Motor unit coherence analysis

Much of the input to a motor neuron pool is widely distributed, and it can be argued that this 'shared' or 'common' input is the effective neural drive to muscles (Farina *et al*., 2014). Because this neural drive entrains the activity of the motor unit population, it can be characterized by examining correlated/synchronized activity between pairs of motor units. For example, simultaneous (within a few ms) firing between two units occurs more often than expected by chance when premotor axons branch onto both motor neurons (Sears and Stagg, 1976). On a longer time scale, motor units show concurrent fluctuations in their firing rates, also termed 'common drive' (De Luca *et al*., 1982). A more complete picture can be obtained by extending correlation procedures into the frequency domain using coherence analysis (Rosenberg *et al*., 1989). This method provides the most comprehensive description of common input (Myers *et al*., 2004; Negro and Farina, 2012) in use, and is especially popular because different frequencies of neural drive can be

attributed to different sources of input, for example, the stretch reflex loop (e.g. Erimaki and Christakos, 1999, 2008; Christakos *et al*., 2006), or the motor cortex (e.g. Farmer *et al*., 1993, 1997; Conway *et al*., 1995; Salenius *et al*., 1997; Brown *et al*., 1998).

In derivation, coherence analysis is a frequency domain extension of Pearson's product moment correlation. The coherence calculated at a given frequency represents the linear correlation between the two signals at that frequency, with a value of 0 representing no correlation and a value of 1 representing perfect correlation. For interpretation, it is important to note that coherence is primarily a measure of phase locking, with signal power being a less important factor. This is ideal for measuring motor unit synchronization because the power spectra of single motor unit spike trains are not themselves very informative, as they tend to be dominated by their mean firing rates, and do not faithfully reflect the frequency content of their neural input (Negro and Farina, 2012).

To assess the frequency content of common synaptic input to the motor units within each muscle, we calculated the pooled coherence (Amjad *et al*., 1997) between all unique pairs of simultaneously active motor unit spike trains. The method essentially concatenates all unique pairs of spike trains into two long trains, which are then subjected to coherence analysis. The mathematical details of this procedure are described at the end of this section. To characterize unique drive to each muscle we conducted a novel type of pooled partial coherence analysis. Partial coherence evaluates synchrony between two signals after statistically removing any components which are also synchronous with a third 'reference' signal (Halliday *et al*., 1995, 1999; Rosenberg *et al*., 1998; Ward *et al*., 2013). The remaining 'residual' coherence profile has the same interpretation as standard coherence. In the present case, the 'reference' signal was the sum of all motor unit spike trains recorded from one muscle, repeated to reach the length of the concatenated motor unit spike trains derived from the other muscle. Using this technique, any activity in the reference muscle which was synchronous with the motor units of the other muscle is removed from their coherence, leaving a pooled residual coherence profile that reflects only the muscle-specific portion of the neural drive. Finally, to understand the extent to which cross-muscle neural drive reflected fluctuations in knee extension force, we calculated the partial motor unit coherence across muscles using force as the reference

signal. The residual cross-muscle motor unit coherence in this case represents the cross-muscle drive which is uncorrelated with knee extension force. **Figure 18** depicts a graphical representation of the above logic, and how each method of coherence analysis relates to a specific type of neural drive. **Figure 19** shows an example of motor unit decomposition and subsequent coherence analysis for a single trial.

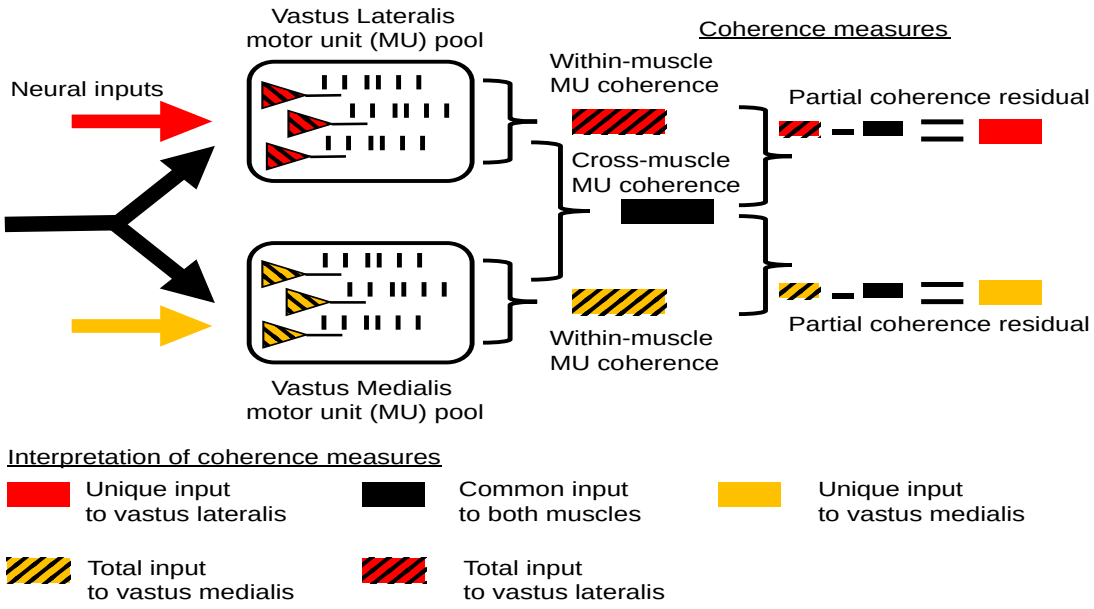

Figure 18. General methods. The motor units of the vastus lateralis and vastus medialis muscles are shown here as receiving a mixture of shared (black) and unique (yellow, red) neural command signals. Both sources of input are assumed to be widely distributed, and would therefore synchronize/entrain the activities of each targeted motor unit population. In this study, we characterized such synchronous activity among motor units in the frequency domain using coherence analysis. The technique reveals the frequency spectrum of synchronous activity between the spike trains of simultaneously active motor units. When coherence analysis is conducted on pairs of motor units recorded from the same muscle, the resulting spectrum describes the total common input to that muscle. The total input includes contributions from both muscle-specific and shared (cross-muscle) sources of drive. For this reason, the blocks representing within-muscle coherence are colored with stripes representing both the shared and unique sources of input influencing motor unit behavior. When coherence analysis is conducted using motor units recorded from different muscles, the common input to both muscles is revealed. This input does not include muscle-specific components and is therefore represented in the diagram using a single color (black). We then used partial coherence analysis to reveal the unique input to each muscle. The technique of calculating partial coherence involves removing any coherence between two signals which could be explained by a common third signal. The resulting 'residual' coherence therefore describes the correlation between two signals that is independent of the third signal. In this study, the method was used to remove any components of within-muscle coherence which could be explained by activity in the other muscle. We were therefore able to assess the strength of unique/independent drive to each muscle, and determine the relative contribution of cross-muscle drive to the total within-muscle coherence.

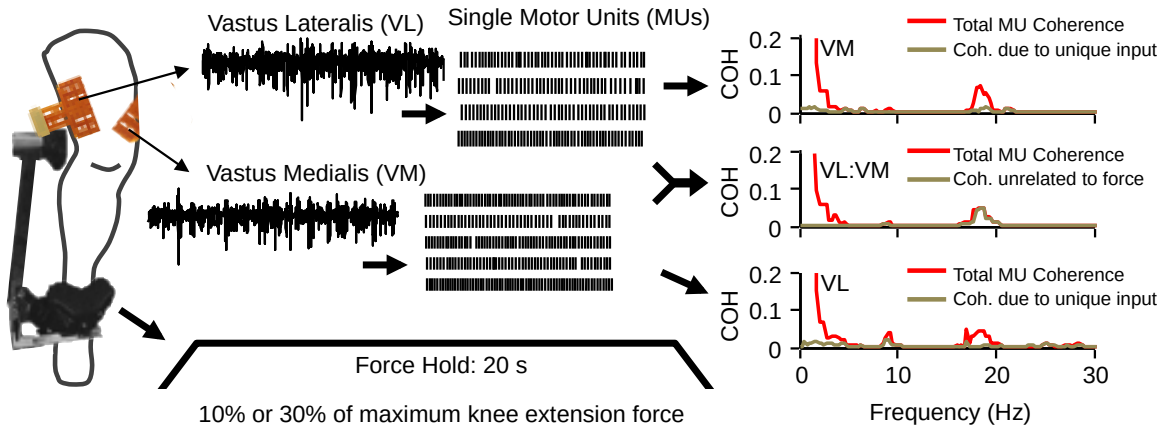

Figure 19. Recordings and data analysis. High-density surface EMG signals (64 channels) were recorded from the vastus lateralis and vastus medialis muscles of healthy participants during production of isometric knee extension force (10% and 30% of maximum force). The EMG signals were then decomposed to reveal the firing activities of single motor units. A schematic representation of the task and motor unit recording methodology is shown in the left half of the figure. A total of 80 trials (20 s each) were recorded across 9 subjects. For each trial, neural drive to the vasti muscles was characterized using the decomposed motor unit data. First, the pooled coherence between all concurrently active pairs of single motor units was derived for each muscle. The red traces in the top and bottom right panels show this analysis for a single trial at 30% maximum force. Motor unit coherence reveals the frequency content of neural drive to each muscle. The major component occurred in the 1-5 Hz range for both muscles, with smaller peaks present at ~10 Hz (mainly in the vastus lateralis in this trial) and just below 20 Hz. In addition, the pooled coherence of motor units recorded from opposite muscles was calculated to derive the frequency content of cross-muscle neural drive (red trace, middle right panel). The profile of cross-muscle coherence appears very similar to that observed within each muscle. The brown traces in the top and bottom right panels show a 'residual' coherence representing the within-muscle motor unit coherence that remains after removing any components that can be explained by cross-muscle neural drive. The residual therefore represents the frequency content of independent (muscle-specific) neural drive. In the trial depicted, the greatly reduced magnitudes of the brown (residual) coherence traces in comparison with the red traces suggest that majority of within-muscle motor unit coherence stems from cross-muscle drive. The brown trace in the middle right panel represents a similar analysis in which the effects of knee extension force are removed from the cross-muscle motor unit coherence. The residual in this case characterizes the frequency content of any cross-muscle drive that is uncorrelated with total knee extension force. In this trial, cross-muscle neural drive above about 5 Hz (especially near 20 Hz) appears to be uncorrelated with force, while lower frequencies are highly correlated with force.

4.4.3.5. Mathematical procedures

Coherence analysis:

As previously described, each signal was first divided into consecutive time segments, 3s in duration. The FFT was then calculated for each segment using the spectrogram function in Matlab, specifying that time segments be non-overlapping and weighted by a rectangular window function. For each frequency, the complex values obtained across N time segments were used to derive the auto spectra and cross spectra of the signals x and y (xx, yy, and xy, respectively) as follows:

xx = $\sum_{i=1}^{i=N} X_i \cdot conj(X_i)$

yy = $\sum_{i=1}^{i=N} Y_i \cdot conj(Y_i)$

xy = $\sum_{i=1}^{i=N} X_i \cdot conj(Y_i)$

where conj () refers to the complex conjugate of X_i or Y_i.

The magnitude squared coherence (typically referred to as 'coherence') for each frequency was then calculated as follows:

CohXY = $| xy |^2 / (xx \cdot yy)$

Each coherence profile was then smoothed in the frequency domain using a 3-point (0.5 Hz) running median. To assess the frequency content of the neural drive shared by both muscles, we repeated the same procedure using all combinations of motor unit pairs recorded from different muscles.

Partial coherence analysis:

To calculate partial coherence, we first derived the auto spectra for the reference signal z as described for x and y above. Then, the cross spectra of signal z with signal x were calculated as below:

xz = $\sum_{i=1}^{i=N} X_i \cdot conj(Z_i)$

zx = $\sum_{i=1}^{i=N} Z_i \cdot conj(X_i)$

The cross spectra yz and zy were calculated similarly. From these, the cross and auto spectra between x and y accounting for signal z were calculated as follows:

xx_z = $xx - (xz \cdot zx)/zz$

yy_z = $yy - (yz \cdot zy)/zz$

xy_z = $xy - (xz \cdot zy)/zz$

Finally, the residual coherence between x and y after accounting for signal z can was calculated as:

CohXY_z = $| xy \_z|^2 / (xx\_z \cdot yy\_z)$

In this study, we were interested in removing the effects of shared drive from the total drive to a given muscle. Therefore, the signals x and y represent the concatenated pairs of motor unit spike trains recorded from one muscle, while the reference signal was formed from the summation of all individual motor unit spike trains recorded simultaneously from the other muscle. The reference signal, as a composite spike train, will strongly reflect the activity which is common to all units. The reference signal was repeated to reach the length of the concatenated spike trains. In this way, each unique pair of units from a given trial was referenced to the same signal within the pooled partial coherence analysis.

4.4.3.6. Statistical comparisons

For each coherence profile, a 95% confidence level (CL) can be derived (Carter, 1987; Rosenberg *et al*., 1989) as follows:

$$CL = 1 - 0.05^{\wedge}(1/(N-1))$$

Where N is the number of data segments used to calculate the coherence profile. For residual coherence profiles, the "N-1" in the above equation is replaced by "N-2". We then calculated the proportion of total trials showing significant coherence at each frequency. Under the assumption that no true motor unit coherence exists at a given frequency, the use of a 95% confidence level will result in a false positive rate of about 5%. Therefore, a binomial test was used to determine if the proportion of trials showing significant coherence exceeded the expected error rate. The test provided a conservative evaluation of the relevant frequency content of neural drive within and between muscles.

To compare the strength/frequency content of neural drive between force levels, we first converted the coherence values at each frequency to standard Z-scores as follows:

$$COH\_zscore = [\operatorname{atanh}(\sqrt{COH}) / \sqrt{(1/ (2N))}] - bias$$

Where N is the number of segments used to calculate coherence (COH), and the bias is derived empirically as the mean COH_zscore calculated between 250 and 500 Hz, since this frequency band should contain no actual coherence (Baker *et al*., 2003). This

conversion was necessary prior to statistical testing since it sets coherence values on an interval (and ratio) scale and accounts for any differences in the number of units used in each pooled coherence calculation. To test differences in coherence at a given frequency across force levels, a randomization test on medians was used. In this test, the median difference in coherence across conditions was first calculated and then compared against a set of 10,000 median differences that had been derived after randomly shuffling the force level designations of each paired trial (80 pairs in total). By paired trials, we mean that the Nth 10% MVC contraction recorded for a given subject was always compared with the Nth 30% MVC contraction for the same subject. In the randomization test, the sign of their difference was randomly assigned in each of the 10,000 iterations. Shuffling paired trials controlled for any cross-subject or over-time effects that might complicate the statistics. The final p-value was calculated directly as the proportion of shuffled median-differences exceeding the original in absolute magnitude. This test was ideal for our purposes because it makes no assumptions concerning distribution shapes or the partitioning of variance across subjects and trials. The test was run on every frequency which showed a significant degree of coherence across the population (according to the binomial test) in at least one of the conditions being compared. In this way, we limited analysis to frequencies which were consistently present in the neural drive to the muscles.

Finally, we estimated the relative proportion of total within-muscle motor unit coherence not explainable by shared (cross-muscle) neural drive. To do this, we calculated the total area of significant coherence for each coherence profile and its associated residual coherence profile. The area of significant coherence was the summation, across all frequencies, of COH_zscores > 1.65. The ratio of significant coherence area (residual/total) was calculated for each trial and averaged per subject. This analysis yielded a per-subject estimate of the proportion of total common input that was unique to each muscle.

4.4.4. RESULTS

4.4.4.1. Motor unit decomposition

After exclusion of any trials where either muscle had fewer than 3 motor units decomposed for either force level, a total data set of 80 trials from across 9 subjects was

available for further analysis. A total of 9 contractions per force level were analyzed from each of the first 8 subjects, while 8 trials were analyzed from subject 9. Subject 10 had too few units decomposed at the 10%MVC level to be included in further analysis. From the VL recordings, the mean (SD) number of motor units decomposed was 7.5 (2.3) for 10% MVC trials and 7 (3.2) for 30% MVC trials. The mean (SD) firing rates for these units was 8.8 (1.0) Hz at 10% MVC and 10.7 (1.6) Hz at 30% MVC. From the VM, an average of 7.7 (2.8) units were decomposed at 10% MVC and 7.5 (3.5) units at 30% MVC. The mean (SD) firing rates of VM motor units were 9 (0.9) Hz and 10.9 (1.6) Hz for 10 and 30% MVC, respectively.

4.4.4.2. Motor unit coherence within and between muscles

Figure 20, A and B depicts the percent of trials which showed significant coherence at each frequency for the VL and VM, respectively. Proportions greater than the marked 95% confidence level indicate that coherence was observed more often than expected by chance. The figures indicate which frequencies were consistently components of the overall drive to each muscle, for each force level. Below the x-axis of each plot are the results of a randomization test comparing the magnitude of coherence between the two force levels. The black bars represent frequencies at which the coherence differed significantly. For convenience of interpretation, the p-value for significance in this test was set to 0.01, which allows each bar to represent a 1 Hz bin (5 frequency samples). The overall coherence profiles are similar between both muscles, with the main features of neural drive comprising a 1-5 Hz component, a ~10 Hz component, and a ~20 Hz component, the latter two occurring only at 30% MVC. Comparing across force levels, differences in coherence occurred at frequencies above 5 Hz, and were particularly strong in the VM (both ~10 and ~20 Hz components showing strong force-dependence).

Figure 20, C and D depicts the percent of trials having significant coherence after statistically removing the common cross-muscle signal from the total within-muscle motor unit coherence. The resulting residual coherence reflects the unique, 'muscle-specific' drive to a given muscle. In general, only a 1-5 Hz component of muscle-specific drive appeared to exist for either muscle. A small peak at 18 Hz was present for the VM (30% MVC), although this was weak in terms of strength, bandwidth, and consistency. There

was no difference in muscle-specific drive to the VL across force levels, while for the VM, there were some small differences, primarily under 3 Hz.

Panels E and F (Figure 20) show the results of a randomization test comparing the magnitudes of total coherence to residual (muscle-specific) coherence at 30% MVC (top) and 10% MVC (bottom). At 30% MVC, the muscle-specific component was significantly smaller than the total coherence, at nearly every frequency where it existed, and in both muscles. The same was true for 10% MVC.

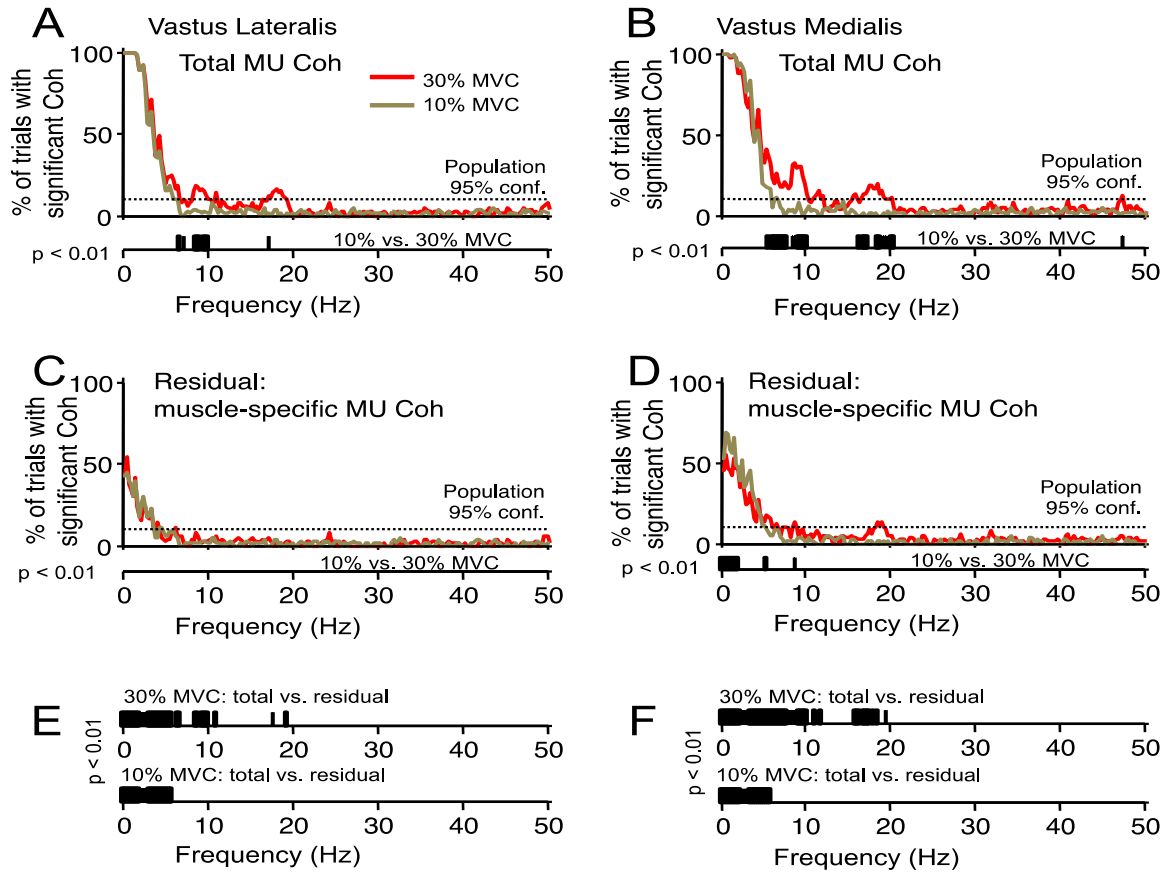

Figure 20. Total within-muscle motor unit coherence and muscle-specific motor unit coherence for the vasti muscles. Panels A and B show the proportion of trials (80 total) in which significant within-muscle motor unit coherence was observed for the vastus lateralis and vastus medialis, respectively. The red traces show results for muscle contractions held at 30% maximum voluntary contraction force (%MVC) while the brown traces show the results for 10% MVC. The dashed horizontal line indicates the highest proportion that could have been observed simply due to chance. Below the x-axis of each plot are the results of a randomization test comparing the coherence values observed at 10% MVC to 30% MVC. The black bars indicate frequencies at which a significant difference existed between coherence magnitudes measured across trials at each force level. The significance level has been set to 0.01, to correct for multiple comparisons and thus allow each bar to represent a frequency bin of 1 Hz. Panels C and D represent the same analysis as in A and B, but after removing the effects of cross-muscle drive on within-muscle coherence. The residuals shown therefore represent the frequency content of muscle-specific neural drive. Panels E and F show the results of a randomization test comparing the magnitude of total within-muscle coherence to the residual (muscle-specific) coherence at 30% MVC (top) and 10% MVC (bottom). Both muscles show similar profiles of total within-muscle coherence, with the primary component of each occurring below 5 Hz, but extending further to include components near 10 and 20 Hz when force increases from 10% MVC to 30% MVC. The magnitude of coherence below 5 Hz appeared not to change with force, in contrast to higher frequency components which did show force-dependence. Muscle-specific coherence was weaker, limited primarily to frequencies less than 5 Hz, and was not highly dependent on force.

Figure 21 depicts the percent of trials showing significant cross-muscle motor unit coherence. In this case, residual coherences represent the remaining coherence after subtracting any components which are correlated with force. Figure 20A shows that the cross-muscle coherence contained essentially the same frequency content as within-muscle coherence, again with frequencies above ~5 Hz showing significant force-dependence. Panel B shows that the component of cross-muscle drive not correlated with temporal fluctuations in force depended on the overall force level. At 30% MVC, frequencies > ~8Hz form significant components of the residual coherence, meaning that cross-muscle drive at this force level was not faithfully translated into force. Panel C shows a clear reduction in low frequency cross-muscle coherence after removing any components synchronized with force fluctuations. At 10% MVC, essentially every frequency under 6 Hz was reduced, while at 30% MVC all frequencies under 10 Hz were reduced. The effects above 10 Hz at 30% MVC were less consistent.

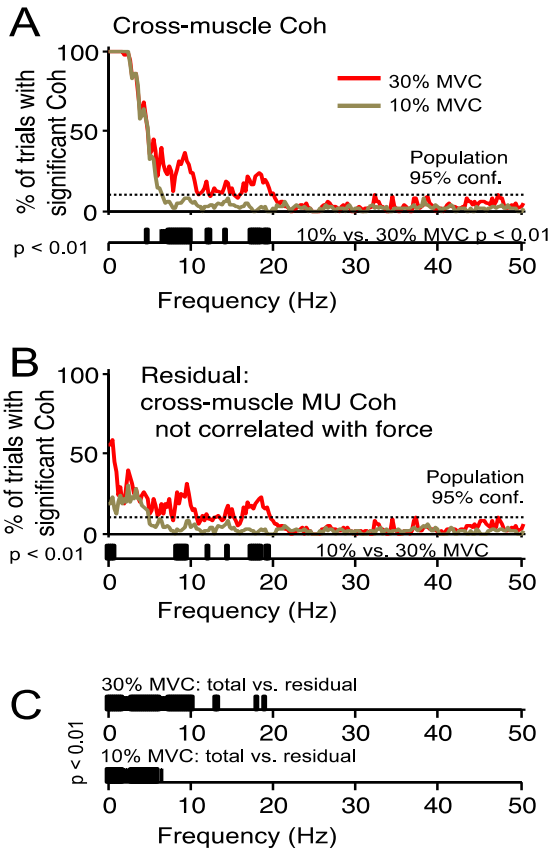

Figure 21. Cross-muscle coherence and its reflection in knee extension force. Panel A shows the proportion of trials having significant cross-muscle motor unit coherence. As before, red traces show results for 30% MVC force, and brown traces show results for 10% MVC. The overall frequency content of cross-muscle drive was very similar to the with-muscle drive, with a primary component from 1-5 Hz which extended to include components near 10 and 20 Hz at 30% MVC. Below the x-axis of panel A, the results of a randomization test show that neural drive above ~5 Hz showed clear force-dependence, whereas the lowest frequencies (under ~5 Hz) did not. Panel B shows the same analysis as in A, but after 'removing' any components of cross-muscle coherence that were synchronized with knee extension force. The residual coherence represents the cross-muscle drive which does not become translated into force fluctuations. Again, frequencies in the 10-20 Hz range were force-dependent while frequency components less than 5 Hz generally were not. Panel C shows the comparison of total to residual coherence at each force level. The removal of force from cross-muscle coherence greatly reduced its magnitude at nearly every frequency under 10 Hz where coherence was consistently observed. The reduction of higher frequency (10-20 Hz) coherence was less pronounced.

4.4.4.3. The contribution of muscle-specific drive to the total (within-muscle) coherence

For each muscle and force level, the area of significant within-muscle motor unit coherence was calculated before and after removing the effects of cross-muscle drive. The residual coherence represents the unique, 'muscle-specific' drive. In **Figure 22**, the ratio between the residual coherence area and the total within-muscle coherence area is shown

per subject for each muscle. The top row shows results for 30%MVC contractions and the bottom shows results for 10% MVC contractions. The bar heights represent the mean proportion calculated across the trials completed by each subject while the error bars represent the standard deviation across repeated trials. These error bars show the approximate consistency of this measure across different trials, and are not intended for statistical comparisons. The proportion of total motor unit coherence explained by muscle-specific drive was low in all cases, with averages lower than 20% in the majority of subjects.

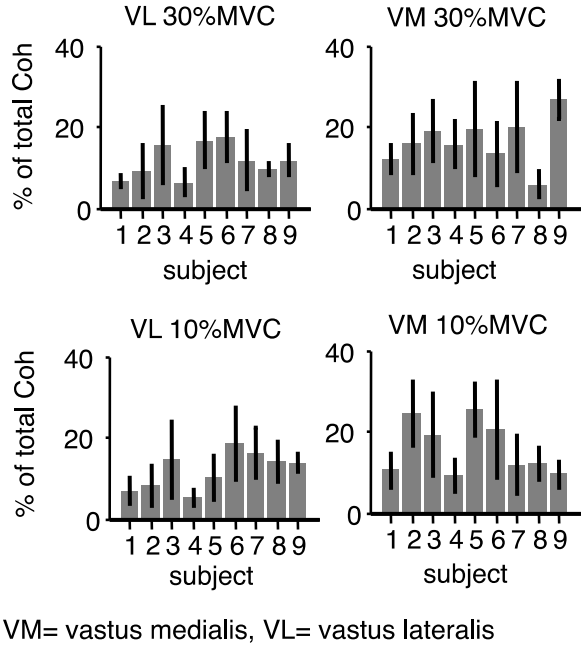

Figure 22. Proportion of total within-muscle coherence represented by muscle-specific drive. The proportion of total within-muscle motor unit coherence explained by independent drive to the vastus lateralis (left) or vastus medialis (right) is shown for each subject. Each bar represents the mean proportion calculated over all trials for a given subject. The error bars show the standard deviation of proportions calculated across trial replicates for each individual and indicate that the measure was relatively stable across trials and recording sessions. At knee extension forces of 30% MVC (top) and 10 % MVC (bottom), nearly all trials showed proportions of muscle-specific drive < 20 %. In other words, more than 80% of the unit-to-unit coherence measured in either muscle was due to cross-muscle drive.

4.4.4.4. Proportion of cross-muscle coherence unrelated to force

Figure 23 shows the proportion of cross-muscle coherence remaining after removing any components that were synchronous with force fluctuations over time. For both 30% MVC (top) and 10% MVC (bottom), the proportion of coherence unrelated to force was below 20% for all subjects. This implies that the cross- muscle neural drive is tightly coupled with the overall force.

4.4.5. DISCUSSION

In this study, we have characterized the frequency content and force-dependence of both shared (cross-muscle) and independent (muscle-specific) neural drive to the motor units of synergist muscles. Our findings lend direct neurophysiological support to the theory that synergistically-activated muscles are controlled primarily by a shared neural drive. Our study also represents the most comprehensive characterization of neural drive to the vasti muscles to date.

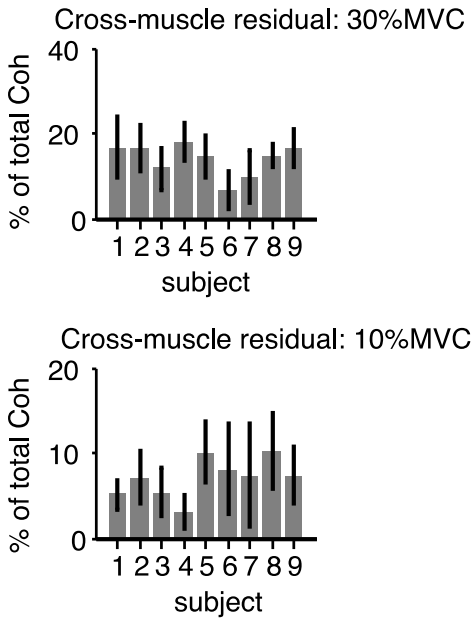

Figure 23. Proportion of cross-muscle coherence unrelated to knee extension force. The figure depicts the per-subject proportion of cross-muscle motor unit coherence which was uncorrelated with force. At both 30% MVC (top) and 10% MVC (bottom), the proportion is very low, suggesting that the majority (>80 %) of cross-muscle drive is related to force. As in Figure 5, the error bars show the standard deviation of proportions calculated across trial replicates for each individual.

The frequency content of neural drive to the VL and VM were very similar. At 10% MVC, the neural drive to either muscle spanned frequencies up to about 6 Hz, with significant coherence <3 Hz in most trials. In general, motor unit coherence at frequencies under 5 Hz reflects 'common drive', i.e., concurrent fluctuations in motor unit firing rates (De Luca *et al*., 1982; Myers *et al*., 2004). Common drive is of unknown physiological origin, but the lowest frequencies (<3 Hz) are unaffected by capsular stroke (Farmer *et al*., 1993) and are strengthened in cerebellar stroke (Sauvage *et al*., 2006). Common drive extends to antagonist muscle pairs if they are functionally linked (De Luca and Mambrito,

1987), and may depend on task context (Mochizuki *et al*., 2006; Laine *et al*., 2013, 2014) and proprioceptive input (De Luca *et al*., 2008; Laine *et al*., 2014).

At 10 % MVC, neural drive at frequencies > 6 Hz was not strongly reflected in the motor unit coherence of either muscle. When contraction force was increased to 30% MVC, a 6-12 Hz input (peak between 8 and 10 Hz) was observed, along with a new component in the beta band (~15-35 Hz), with a peak at 20 Hz. The neural drive in the 6-12 Hz frequency range is associated with physiological tremor, and may partly stem from oscillations of excitation around the Ia afferent feedback loop (Sutton and Sykes, 1967; Lippold, 1970; Hagbarth and Young, 1979; Young and Hagbarth, 1980; Erimaki and Christakos, 1999, 2008; Christakos *et al*., 2006). Higher frequency components in the neural drive (15-35 Hz) are most often considered to be of cortical origin (Farmer *et al*., 1993, 1997; Conway *et al*., 1995; Salenius *et al*., 1997; Brown *et al*., 1998). If these associations are true for the present scenario, it follows that afferent feedback and cortical drive were only strong enough to evoke significant motor unit coherence at force levels above 10% MVC. Of course, lack of significant coherence may not indicate complete absence of neural drive at high frequencies, given the variety of factors which can limit the sensitivity of coherence measures (Negro and Farina, 2012).

The cross-muscle motor unit coherence was nearly identical to the within-muscle motor unit coherence, in terms of both frequency content and force-dependence. The ~10 and ~20 Hz peaks in motor unit coherence at 30% MVC are particularly interesting, because they suggest that cross-muscle drive contains both Ia feedback and a descending cortical component. Surprisingly, our partial coherence analysis showed that these higher frequencies of coherence exclusively reflect cross-muscle drive, since the unique drive to either muscle contained no significant coherence above ~ 6 Hz. It is worth noting that if cortical drive is essentially a cross-muscle signal, then our findings directly support a core principle of the muscle synergy theory, namely, that cortical commands are of lower dimensionality than the muscles controlled.

We found that force fluctuations <6 Hz were well-synchronized with cross-muscle drive. For both force levels, the vast majority (>80%) of cross-muscle motor unit coherence was explainable by fluctuations in force. During visually-guided force control, low-frequency fluctuations in force reflect voluntary error corrections and involuntary

common firing rate modulation (common drive) among motor units (Sutton and Sykes, 1967; Allum *et al*., 1978; De Luca *et al*., 1982; Miall *et al*., 1993; Slifkin *et al*., 2000; Squeri *et al*., 2010). Due to the low pass filtering effects of muscle tissue, as well as the rest of the leg/ leg-fixation system, force fluctuations above ~5 Hz are extremely small and are negligible in terms of the overall force control (excluding the scenario of pathological tremor). As expected, cross-muscle drive above 10 Hz was not well correlated with force fluctuations.

The unique neural drive to each muscle appeared to be limited to the common drive (1-5 Hz) frequency range. In this study, 'muscle-specific' coherence reflects either an actual unique drive to one muscle, or a cross-muscle signal which has been obscured in one of the two muscles, for example due to noise. The 1-5 Hz drive to each vasti muscles consistently showed a muscle-specific component. Though relatively weak, its consistency suggests that it does represent a distinct source of 1-5 Hz drive. Regardless of the source, the magnitude of 1-5 Hz coherence was not strongly force-dependent. That said, the relation between coherence strength and neural drive strength may be somewhat complex and depends on many factors, including the physical distribution of axonal inputs, as well as the firing rates of the motor units in relation to the frequency of shared input (Negro and Farina, 2012).

We also observed a small component of muscle-specific drive to the VM at 18 Hz during 30% MVC contractions. The limited bandwidth (1 Hz) and consistency (2 more trials than expected by chance) of this input suggest that ~20 Hz cross-muscle drive was poorly reflected in the VL, making it appear unique to the VM. The VL itself did not show any muscle-specific input above 6 Hz.

In terms of proportions, we found that the within-muscle coherence attributable to muscle-specific drive was between 5% and 25% of the total within-muscle coherence, regardless of the force level or the muscle recorded from. This ratio was generally consistent across subjects, trials, and force levels. Although the detectable bandwidth of cross-muscle drive was larger at higher force levels, the global degree of within-muscle motor unit coherence attributable to cross-muscle drive was fairly stable. While increasing force resulted in a larger bandwidth of cross-muscle drive, the acquired high frequency

input had little influence on force, and as a result, the proportion of coherent activity not correlated with force was found to be larger at 30% MVC than at 10% MVC.

Because our findings support the theory that synergistically-activated muscles are controlled primarily by shared neural drive, it is important to further discuss how this result adds to previous literature supporting the notion of muscle synergies. There is ample evidence that synergies, or 'motor primitives' do have a neural origin (reviewed in Bizzi and Cheung, 2013). For example, they can be evoked and modified through afferent feedback in spinalized frog preparations (Tresch *et al*., 1999; Kargo and Giszter 2000a,b), they can be evoked through stimulation of spinal interneurons in frogs (Giszter *et al*., 1993) and mice (Levine et al., 2014), and they can be recruited by intracortical microstimulation in rhesus monkeys (Graziano *et al*., 2002; Overduin *et al*., 2012, 2014). In the frog, spinal interneurons involved in the organization of motor primitives have been extensively characterized (Hart and Giszter, 2010). That said, many questions remain unanswered, especially in the context of voluntary motor control in humans. For one, humans (and some higher primates) have direct cortico-motoneuronal cells which may have evolved specifically to free voluntary behavior from the constraints of spinal 'motor primitives' (Rathelot and Strick, 2009). Of course, these direct cortico-motoneuronal cells co-exist with the 'old' corticospinal track, where M1 cells project directly onto the spinal interneurons which may coordinate muscle activation (Rathelot and Strick, 2009). Regardless of the specific level at which 'motor primitives' may be prepared (spinal or cortical), it is not clear precisely how this signal is delivered to the targeted muscles. For example, multiple muscles could show fixed ratios of activation even if each muscle were to receive its own unique input and receive no shared/common drive. Alternatively, motor neurons of synergist muscles might share a low-frequency 'common drive' originating at the spinal level, but not higher frequency neural drive originating from the cortex. The precise circuitry of synergy formation is not well understood, and our results suggest that valuable information can be gained by approaching this problem from the motor neuron level.

It will require further research to fully understand how shared vs. muscle-specific drive to synergistically activated muscles changes in relation to task context or disease. For example, it is likely that characterization of synergistic muscle activation may yield

important information about plasticity and adaptation in the central nervous system following injury, for example, stroke (Gizzi *et al*., 2011). In addition, the theory of coherence and partial coherence contains many variations and extensions which have been previously described (Rosenberg *et al*., 1989, 1998), and which may be of particular benefit in studying coordination among larger sets of muscles. Importantly, our results provide the first neural support in man for the assumption that muscles can be controlled primarily through shared neural drive (Tresch and Jarc, 2009; Kutch and Valero-Cuevas, 2012; Bizzi and Cheung, 2013). Overall, our study has expanded the current understanding of vasti muscle activation and has introduced a new approach for investigating neural drive to multi-muscle systems.

4.4.6. REFERENCES

Allum JH, Dietz V, Freund HJ (1978) Neuronal mechanisms underlying physiological tremor. *J Neurophysiol* **41**:557–571.

Amjad AM, Halliday DM, Rosenberg JR, Conway BA (1997) An extended difference of coherence test for comparing and combining several independent coherence estimates: theory and application to the study of motor units and physiological tremor. *J Neurosci Meth* **73**:69–79.

Baker SN, Pinches EM, Lemon RN (2003) Synchronization in Monkey Motor Cortex During a Precision Grip Task. II. Effect of Oscillatory Activity on Corticospinal Output. *J Neurophysiol* **89**:1941–1953.

Beck TW, DeFreitas JM, Stock MS, Dillon MA (2011) Effects of resistance training on force steadiness and common drive. *Muscle & Nerve* **43**:245–250.

Beck TW, Stock MS, DeFreitas JM (2012) Effects of Fatigue on Intermuscular Common Drive to the Quadriceps Femoris. *Int J Neurosci* **122**:574–582.

Bizzi E, Cheung VCK (2013) The neural origin of muscle synergies. Front Comput Neurosci 7:51.

Brown P, Salenius S, Rothwell JC, Hari R (1998) Cortical Correlate of the Piper Rhythm in Humans. *J Neurophysiol* **80**:2911–2917.

Carter GC (1987) Coherence and time delay estimation. *Proceedings of the IEEE* **75**:236–255.

Christakos CN, Papadimitriou NA, Erimaki S (2006) Parallel Neuronal Mechanisms Underlying Physiological Force Tremor in Steady Muscle Contractions of Humans. *J Neurophysiol* **95**:53–66.

Conway BA, Halliday DM, Farmer SF, Shahani U, Maas P, Weir AI, Rosenberg JR (1995) Synchronization between motor cortex and spinal motoneuronal pool during the performance of a maintained motor task in man. *J Physiol* **489**:917–924.

De Luca CJ, Gonzalez-Cueto JA, Bonato P, Adam A (2008) Motor Unit Recruitment and Proprioceptive Feedback Decrease the Common Drive. *J Neurophysiol* **101**:1620–1628.

De Luca CJ, LeFever RS, McCue MP, Xenakis AP (1982) Control scheme governing concurrently active human motor units during voluntary contractions. *J Physiol* **329**:129–142.

De Luca CJ, Mambrito B (1987) Voluntary control of motor units in human antagonist muscles: coactivation and reciprocal activation. *J Neurophysiol* **58**:525–542.

Enoka RM, Fuglevand AJ (2001) Motor unit physiology: some unresolved issues. *Muscle & Nerve* **24**(1) 4-17.

Erimaki S, Christakos CN (1999) Occurrence of widespread motor-unit firing correlations in muscle contractions: their role in the generation of tremor and time-varying voluntary force. *J Neurophysiol* **82**:2839–2846.

Erimaki S, Christakos CN (2008) Coherent Motor Unit Rhythms in the 6-10 Hz Range During Time-Varying Voluntary Muscle Contractions: Neural Mechanism and Relation to Rhythmical Motor Control. *J Neurophysiol* **99**:473–483.

Farina D, Holobar A, Gazzoni M, Zazula D, Merletti R, Enoka RM (2009) Adjustments Differ Among Low-Threshold Motor Units During Intermittent, Isometric Contractions. *J Neurophysiol* **101**:350–359.

Farina D, Muhammad W, Fortunato E, Meste O, Merletti R, Rix H (2001) Estimation of single motor unit conduction velocity from surface electromyogram signals detected with linear electrode arrays. *Med Biol Eng Comput* **39**:225–236.

Farina D, Negro F (2014) Common Synaptic Input To Motor Neurons, Motor Unit Synchronization, And Force Control: *Exerc Sport Sci Rev* **43**:23–33.

Farina D, Negro F, Dideriksen JL (2014) The effective neural drive to muscles is the common synaptic input to motor neurons. *J Physiol* **592**(Pt 16):3427–3441.

Farina D, Negro F, Gazzoni M, Enoka RM (2008) Detecting the Unique Representation of Motor-Unit Action Potentials in the Surface Electromyogram. *J Neurophysiol* **100**:1223–1233.

Farmer SF, Bremner FD, Halliday DM, Rosenberg JR, Stephens JA (1993) The frequency content of common synaptic inputs to motoneurones studied during voluntary isometric contraction in man. *J Physiol* **470**:127–155.

Farmer SF, Halliday DM, Conway BA, Stephens JA, Rosenberg JR (1997) A review of recent applications of cross-correlation methodologies to human motor unit recording. *J Neurosci Meth* **74**:175–187.

Giszter SF, Mussa-Ivaldi FA, Bizzi E (1993) Convergent force fields organized in the frog's spinal cord. *J Neurosci* **13**(2):467-491.

Gizzi L, Nielsen JF, Felici F, Ivanenko YP, Farina D (2011) Impulses of activation but not motor modules are preserved in the locomotion of subacute stroke patients. *J Neurophysiol* **106**:202–210.

Graziano MSA, Taylor CSR, Moore T (2002) Complex movements evoked by microstimulation of precentral cortex. *Neuron* **34**:841–851.

Hagbarth K-E, Young RR (1979) Participation of the Stretch Reflex in Human Physiological Tremor. *Brain* **102**:509–526.

Halliday DM, Conway BA, Farmer SF, Rosenberg JR (1999) Load-Independent Contributions From Motor-Unit Synchronization to Human Physiological Tremor. *J Neurophysiol* **82**:664–675.

Halliday DM, Rosenberg JR, Amjad AM, Breeze P, Conway BA, Farmer SF (1995) A framework for the analysis of mixed time series/point process data—Theory and application to the study of physiological tremor, single motor unit discharges and electromyograms. *Prog Biophys Mol Biol* **64**:237–278.

Hart CB, Giszter SF (2010) A neural basis for motor primitives in the spinal cord. *J Neurosci* **30**:1322-1336.

Holobar A, Farina D (2014) Blind source identification from the multichannel surface electromyogram. *Physiol Meas* **35**:143-165.

Holobar A, Minetto MA, Farina D (2014) Accurate identification of motor unit discharge patterns from high-density surface EMG and validation with a novel signal-based performance metric. *J Neural Eng* **11**(1):016008.

Holobar A, Zazula D (2004) Correlation-based decomposition of surface electromyograms at low contraction forces. *Med Biol Eng Comput* **42**:487–495.

Holobar A, Zazula D (2007) Multichannel Blind Source Separation Using Convolution Kernel Compensation. *IEEE Trans Sig Proc* **55**:4487–4496.

Kargo WJ, Giszter SF (2000a) Rapid corrections of aimed movements by combination of force-field primitives. *J Neurosci* **20**:409-426.

Kargo WJ, Giszter SF (2000b) Afferent roles in hindlimb wiping reflex: free limb kinematics and motor patterns. *J Neurophysiol* **83**:1480-1501.

Kutch JJ, Valero-Cuevas FJ (2012) Challenges and New Approaches to Proving the Existence of Muscle Synergies of Neural Origin. *PLoS Comput Biol* **8**:e1002434.

Laine CM, Negro F, Farina D (2013) Neural correlates of task-related changes in physiological tremor. *J Neurophysiol* **110**:170–176.

Laine CM, Yavuz ŞU, Farina D (2014) Task-related changes in sensorimotor integration influence the common synaptic input to motor neurones. *Acta Physiol* **211**:229–239.

Levine AJ, Hinckley CA, Hilde KL, Driscoll SP, Poon TH, Montgomery JM, Pfaff SL (2014) Identification of a cellular node for motor control pathways. *Nat Neurosci* **17**:586-593.

Lippold OCJ (1970) Oscillation in the stretch reflex arc and the origin of the rhythmical, 8-12 c/s component of physiological tremor. *J Physiol* **206**:359–382.

Masuda T, Miyano H, Sadoyama T (1985) The position of innervation zones in the biceps brachii investigated by surface electromyography. *IEEE Trans Biomed Eng* **32**:36–42.

Mellor R, Hodges P (2005) Motor unit synchronization between medial and lateral vasti muscles. *Clin Neurophysiol* **116**:1585–1595.

Miall RC, Weir DJ, Stein JF (1993) Intermittency in human manual tracking tasks. *J Motor Behav* **25**:53–63.

Mochizuki G, Semmler JG, Ivanova TD, Garland SJ (2006) Low-frequency common modulation of soleus motor unit discharge is enhanced during postural control in humans. *Exp Brain Res* **175**:584–595.

Myers LJ, Erim Z, Lowery MM (2004). Time and frequency domain methods for quantifying common modulation of motor unit firing patterns. Journal of NeuroEngineering and Rehabilitation. *J Neuroeng Rehabil* **1**:2.

Negro F, Farina D (2012) Factors Influencing the Estimates of Correlation between Motor Unit Activities in Humans. *PLoS ONE* **7**:e44894.

Overduin SA, d'Avella A, Carmena JM, Bizzi E (2012) Microstimulation activates a handful of muscle synergies. *Neuron* **76**(6):1071-1077.

Overduin SA, d'Avella A, Carmena JM, Bizzi E (2014) Muscle synergies evoked by microstimulation are preferentially encoded during behavior. *Font Comput Neurosci* **8**(20): doi: 10.3389/fncom.2014.00020.

Rathelot JA, Strick PL (2009) Subdivisions of primary motor cortex based on cortico-motoneuronal cells. *PNAS* **106**(3):918-923.

Rosenberg JR, Amjad AM, Breeze P, Brillinger DR, Halliday DM (1989) The Fourier approach to the identification of functional coupling between neuronal spike trains. *Prog Biophys Mol Biol* **53**:1–31.

Rosenberg JR, Halliday DM, Breeze P, Conway BA (1998) Identification of patterns of neuronal connectivity—partial spectra, partial coherence, and neuronal interactions. *J Neurosci Meth* **83**:57–72.

Salenius S, Portin K, Kajola M, Salmelin R, Hari R (1997) Cortical control of human motoneuron firing during isometric contraction. *J Neurophysiol* **77**:3401–3405.

Sauvage C, Manto M, Adam A, Roark R, Jissendi P, De Luca CJ (2006) Ordered Motor-Unit Firing Behavior in Acute Cerebellar Stroke. *J Neurophysiol* **96**:2769–2774.

Sears TA, Stagg D (1976) Short-term synchronization of intercostal motoneurone activity. *J Physiol* **263**:357–381.

Slifkin AB, Vaillancourt DE, Newell KM (2000) Intermittency in the Control of Continuous Force Production. *J Neurophysiol* **84**:1708–1718.

Squeri V, Masia L, Casadio M, Morasso P, Vergaro E (2010) Force-Field Compensation in a Manual Tracking Task. *PLoS ONE* **5**:e11189.

Sutton GG, Sykes K (1967) The effect of withdrawal of visual presentation of errors upon the frequency spectrum of tremor in a manual task. *J Physiol* **190**:281–293.

Tresch MC, Jarc A (2009) The case for and against muscle synergies. *Curr Opin Neurobiol* **19**:601–607.

Tresch MC, Saltiel P, Bizzi E (1999) The construction of movement by the spinal cord. *Nat Neurosci* **2**:162-167.

Ward NJ, Farmer SF, Berthouze L, Halliday DM (2013) Rectification of EMG in low force contractions improves detection of motor unit coherence in the beta-frequency band. *J Neurophysiol* **110**:1744–1750.

Young RR, Hagbarth KE (1980) Physiological tremor enhanced by manoeuvres affecting the segmental stretch reflex. *J Neurol Neurosur Ps* **43**:248–256.

5. General conclusions and discussions

The main objective of this thesis was to compare the changes in motor unit behavior following END and HIIT by using novel surface EMG motor unit decomposition techniques. To accomplish this goal, a number of experiments were conducted to validate HDEMG as a tool to track changes in motor unit behavior after training. Therefore, this dissertation started with two studies showing the reliability and validity of HDEMG for training interventions, followed by one study comparing neuromuscular changes after two weeks of either END or HIIT. Finally, an additional study was implemented in order to understand the neural control of the synergistic muscles investigated during the training intervention. Each of the article's major findings, implications and potential limitations will be discussed.

5.1. Reliability and validity of HDEMG for the study of motor unit behavior

Before the emergence of HDEMG motor unit decomposition techniques, previous studies documenting changes in motor unit behavior after training mainly relied on intramuscular EMG recordings. These methods have high accuracy and are typically regarded as the "gold standard" of motor unit decomposition (Merletti & Farina, 2009). However, and due to their high selectivity, intramuscular EMG only allows the extraction of a few number of motor units during low contraction force levels (Holobar *et al.*, 2009). Moreover, it is almost impossible to relocate the electrode across sessions since once the skin is perforated, there is no way to predict where the electrode(s) will be placed in the muscle belly. Indeed, the problem of under sampling motor unit populations without even having the chance to track the same motor units across sessions has been considered as two of the major limitations of intramuscular EMG recordings for training studies (Carroll *et al.*, 2011). Consequently, there is a lack of studies monitoring changes in motor unit behavior after any type of training. The results of the few investigations available after resistance training show divergent changes in motor unit mean discharge rate and discharge rate variability (Rich & Cafarelli, 2000; Kamen & Knight, 2004; Pucci *et al.*, 2006; Vila-Cha *et al.*, 2010). It is very likely that the low reliability and lack of sensitivity of intramuscular EMG recordings were major factors influencing the results of motor unit

discharge rates after resistance training interventions. However, and quite surprisingly, there are no reliability studies for any motor unit variable extracted with intramuscular EMG recordings.

In study 1, a reliability study was performed. The most important variables extracted from HDEMG motor unit decomposition were analyzed at several force levels (10, 30, 50 and 70% of MVC force), with the aim to check if HDEMG motor unit data would show the required level of reliability for the planned training intervention (Study 3). Therefore, ten subject's VM and VL muscles were assessed during the production of isometric knee extension force across three different testing sessions (each session was separated by one week). Most of the variables studied (mean discharge rate, inter-spike interval, conduction velocity and motor unit action potential peak-to-peak amplitude) presented a high level of reliability across all force levels. Also, the number of extracted motor units was consistent across sessions and was higher than previous methods [average of 7 motor units vs. 4 (Vila-Cha *et al.*, 2010)]. Together, these results showed that HDEMG allowed decomposing a large and similar sample of motor units across sessions, which ultimately increased the consistency of motor unit parameters.

Since during study 1 experiments was possible to locate the HDEMG electrodes in a similar position across the different testing sessions (the skin of the participants was marked), we moved a step further and checked the possibility of tracking the same motor units longitudinally (study 2). For this purpose, a new automatic method that combined blind source separation techniques (Negro *et al.*, 2016a) and cross correlation of the motor unit action potentials (Maathuis *et al.*, 2008) was designed. This was possible due to the large amount of channels that HDEMG-based motor unit decomposition algorithms use to identify each of the motor unit action potentials (Farina *et al.*, 2008). In fact, the large number of HDEMG channels used in the present thesis (64 channels) allowed the tracking method to discriminate between different motor unit action potentials with great accuracy. Accordingly, a large number of VM and VL motor units (from 20% to 40% of the decomposed motor units) could be tracked across different trials in a wide range of contraction levels (from 10% up to 70% of the MVC force). Furthermore, the results showed that the tracked motor units presented even higher reliability and sensitivity compared to averaged population samples. Consequently, conduction velocity of tracked

motor units after a 2-week END training intervention presented an effect size that was almost two times higher compared to unmatched motor unit population samples. Taken together, these results suggest that motor unit tracking by HDEMG is the best method to monitor motor unit adaptations after training interventions and therefore, this was the chosen method for study 3.

5.2. Motor unit changes after HIIT and END

Previous research showed that END and HIIT induced similar metabolic and cardiopulmonary fitness adjustments despite of their differences in training volume and intensity (Gibala *et al.*, 2006; McKay *et al.*, 2009; Little *et al.*, 2010). Therefore, HIIT was offered as an attractive alternative to END since results from previous investigations suggested that HIIT physiological adaptations could be achieved with a much lower time commitment (Gibala *et al.*, 2012a). Despite that this could be appropriate for the enhancement of aerobic performance (e.g., increased maximal oxygen uptake), neural adaptations between both types of training were never examined. Therefore, a HIIT and END training intervention was performed using training protocols showing similar metabolic and cardiopulmonary fitness adaptations (Gibala *et al.*, 2006; Little *et al.*, 2010) despite their differences in load intensity and exercise volume. Since previous investigations have shown that the neural system adapts differently according to the training stimulus (e.g., load intensity, exercise volume and motor task) (Hakkinen & Komi, 1986; Morrissey *et al.*, 1995; Izquierdo *et al.*, 2002; Vila-Cha *et al.*, 2010; Penzer *et al.*, 2016), it was hypothesized that both types of training would show different adaptations among the motor unit population. Indeed, study 3 showed that six sessions of HIIT or END induced opposite adjustments in motor output and motor unit activity. The main findings were that HIIT increased muscle strength (isometric knee extension peak torque) while END increased the time to task failure during a low-force submaximal sustained contraction (30% MVC). These differences in motor output were also accompanied by increased vasti muscles discharge rate and surface EMG amplitude at the highest submaximal force levels (50 and 70% MVC) for HIIT but not for END. The specific changes in motor unit behavior observed in this study were quite interesting because they suggest a differential adaptation across the motor unit pool. The results suggest that these

differences are directly related to the type of training (END: low to moderate loads in long sessions vs. HIIT: high loads in short sessions), which likely favored the activation of motor units of different force thresholds (e.g., HIIT: preferential activation of high threshold motor units vs. END: preferential activation of low threshold motor units). Although there is some evidence that strength gains are induced by greater adaptation in type II fibers (Folland & Williams, 2007), there are currently no studies reporting a preferential adaptation of high threshold motor units when strength increases. Many studies have assumed that changes in motor unit behavior have been responsible for early strength gains since structural changes of the muscle fibers only happen after several weeks of training (approximately more than 10 weeks) [see (Folland & Williams, 2007) for review]. However, these early neural changes have been only explained by increases in surface EMG amplitude, which is a crude and indirect estimate of motor unit behavior (Farina *et al.*, 2004). On the contrary, the results in study 3 showed a clear adaptation of high threshold motor units in the HIIT group, since the same motor units were followed during the training intervention. Therefore, it is very likely that HIIT increased the knee extension peak torque due to changes in discharge rate among high threshold motor units. It is also very likely that HIIT increased maximal force due to increased motor unit recruitment, however, this could be only indirectly measured by increases in surface EMG amplitude in the present study.

5.3. Neural control of synergistic muscles

When a movement is performed, many muscles and motor units are simultaneously activated and coordinated. This poses a big challenge for the CNS since it has to control a large number of muscles, each of them comprising hundreds of motor units, around joints that possess many degrees of freedom, leading to a wide range of combinations of muscle patterns to produce the same movement. One way that the CNS can cope with this redundancy is by activating a large number of muscles synchronously rather than independently by a scheme called modular organization of movement or muscle synergies (Bizzi & Cheung, 2013; Bizzi & Ajemian, 2015). In this way, the CNS simplifies the control of movement since it just needs to select a small number of motor modules instead of activating many muscles individually to accomplish a particular motor task. Even

though this theory has been demonstrated in a number of studies [see (Bizzi & Cheung, 2013) for review], none of those investigations assessed the control of synergistic muscles at the motor unit level. Indeed, it is not known if synergistic muscles would also share their neural drive. Motor unit recordings are ideal to examine common synaptic inputs between muscles since fluctuations in motor unit discharge rates are closely related to muscle force oscillations (Farina *et al*., 2010). Thus, by using a new approach based on partial coherence, we could study the amount of "shared" and "independent" neural input received by the VM and VL muscles motor units during the production of isometric knee extension force. The results clearly showed that these synergistic muscles shared most of their neural drive since inter-muscular coherence was higher than intra-muscular coherence in both low (<5 Hz) and high frequencies (>5Hz). This implies that the CNS does not control each muscle separately as previously thought, but rather synchronously. These findings can be confirmed with the results of the training intervention since the vasti muscles motor unit behavioral properties changed similarly after HIIT and END. These results can be expected since both muscles were synergistically producing the necessary knee extension force during the cycling task (Wakeling & Horn, 2009; Hug *et al.*, 2010).

Previous investigations measuring the level of synchronization between muscles have used surface EMG amplitude fluctuations to study the presence of common inputs (Boonstra *et* al., 2008; Mohr *et al*., 2015). Thus, synchronous activity between muscles was studied through coherence analysis of the surface EMG (rectified or un-rectified signal). However, this approach could be questionable since surface EMG amplitude fluctuations are poorly correlated with force oscillations, since several phenomena such as amplitude cancellation, signal cross talk and noise may alter surface EMG estimates (Negro *et al*., 2009; Farina *et al*., 2010).

Therefore, the results of study 4 combined with the findings of study 3, provide the following conclusions: first, it is very likely that motor unit behavior and properties of synergistic muscles to change similarly after a training intervention [result which was also observed by (Vila-Cha *et al.*, 2010)] and second, surface EMG amplitude measures do not provide the accuracy of motor unit recordings to study common inputs between synergistic muscles. This criticism can be extended to studies that use surface EMG amplitude parameters [ARV or root mean square (RMS)] as an index of muscle activation. In fact,

there is a large number of studies aiming to compare the level of activation between the vasti muscles during several knee extension exercises (Mirzabeigi *et al.*, 1999; Edwards *et al.*, 2008; Slater & Hart, 2016). These investigations assumed that the vasti muscles are controlled independently and therefore tried to find exercises producing a similar level of VM and VL activation. However, the present results suggest that synergistic muscles still receive a greater amount of common synaptic input compared to independent synaptic inputs, even when amplitude measures suggest a different level of between-muscle activation.

6. Implications

High intensity interval training exists for more than 80 years but its popularity just increased during the last decade. This rise in popularity coincides with the vast amount of studies documenting similar improvements in aerobic performance compared to END exercise (Gibala *et al.*, 2006; Rakobowchuk *et al.*, 2008; McKay *et al.*, 2009; Little *et al.*, 2011a; Gibala *et al.*, 2012a), which has even led some authors to question the principle of training specificity (Hawley, 2008). However, the results of the present thesis suggest that the principle of training specificity holds between these two types of training at the neuromuscular level. This has strong implications for training prescription since each type of training will induce different functional adaptations in motor output. For instance, HIIT could be appropriate when aerobic performance gains need to be accompanied by an improvement in strength. In contrast, END training would be more appropriate when training goals involve increased resistance to fatigue during contractions at low force levels. Consequently, each of these adaptations should be adjusted according to the needs of patients, athletes and the general population.

The new method to track different motor units across different testing sessions has opened up new opportunities to study changes in motor unit behavior after training interventions that could not be accomplished before. This method will not only provide the chance to re-examine previous inconsistencies in motor unit behavior after training interventions, but would also allow researchers to answer new questions about motor unit behavior after a particular intervention in different populations (young, adult and elderly), in a wide range of force levels (from low to high-threshold motor units) and even after the progression of neuromuscular disorders.

Finally, the proposed motor unit correlation method based on partial coherence will allow examining the neural origin of muscle synergies by investigating the presence of shared synaptic inputs between a large number of muscles. These investigations would help to confirm if the observed shared synaptic input between the VM and VL is also found in other groups of muscles during the execution of different tasks.

7. Limitations and future work

Although the results of the present dissertation indicate that short-term END and HIIT induce distinct changes in motor unit behavior, it is not known if the magnitude of these changes would be maintained in longer training interventions. Future investigations with longer interventions would help to analyze the long-term neuromuscular effect of the training protocols analysed. Also, it is important to acknowledge that several types of HIIT exist. Therefore, comparison with other protocols should be conducted carefully. It would be of great interest to see the neuromuscular adaptations of other HIIT protocols with different work/rest ratios and intensities (e.g., sprint interval training vs. HIIT).

In the current study, the motor unit tracking procedure was only applied across sessions that were two and two and a half weeks apart, where changes in muscle structure were not expected. Future investigations are needed in order to confirm if it is possible to track the same motor unit over several weeks during interventions eliciting adaptations at the tissue level (e.g., fiber hypertrophy).

Finally, the current HDEMG motor unit decomposition method was only applied to isometric contractions due to limitations of the decomposition algorithm. It is not yet possible to extract single motor unit data from dynamic contractions since large variations in muscle fiber length can influence decomposition results. Even though clear differences in motor output and motor unit behavior between HIIT and END protocols were found, it would have been very interesting to analyze those changes during the cycling task or during dynamic knee extension exercises similar to cycling. A very recent study suggested the possibility of blind source separation motor unit decomposition algorithms to decompose motor units during controlled dynamic contractions (Farina & Holobar, 2016), however, this is still under development. Future studies should aim to validate HDEMG tools for dynamic contractions in order to study the motor unit behavior during functional tasks.

8. Summary

This thesis demonstrates that HIIT and END elicit different neuromuscular adaptations despite similar improvements in cardiopulmonary fitness. Overall, the results show that both types of training induce a differential adaptation among the motor unit population that might be related to their differences in load intensity and exercise volume. These results could be assessed with great accuracy due to the high reliability of HDEMG to monitor training adaptations and due to the unprecedented possibility to track individual motor units during the intervention. Finally, it could be demonstrated that the two synergistic muscles investigated during the intervention (VM and VL) shared most of their synaptic input, which provided an explanation for the similar changes in motor unit behavior found for both muscles after the training interventions.

9. References

Adrian ED & Bronk DW. (1929). The discharge of impulses in motor nerve fibres: Part II. The frequency of discharge in reflex and voluntary contractions. *J Physiol* **67,** i3-151.

Bizzi E & Ajemian R. (2015). A Hard Scientific Quest: Understanding Voluntary Movements. *Daedalus-Us* **144,** 83-95.

Bizzi E & Cheung VC. (2013). The neural origin of muscle synergies. *Frontiers in computational neuroscience* **7,** 51.

Brownson RC, Baker EA, Housemann RA, Brennan LK & Bacak SJ. (2001). Environmental and policy determinants of physical activity in the United States. *Am J Public Health* **91,** 1995-2003.

Boonstra TW, Daffertshofer A, van Ditshuizen JC, van den Heuvel MR, Hofman C, Willigenburg NW & Beek PJ. (2008). Fatigue-related changes in motor-unit synchronization of quadriceps muscles within and across legs. *Journal of electromyography and kinesiology : official journal of the International Society of Electrophysiological Kinesiology* **18,** 717-731.

Burgomaster KA, Heigenhauser GJ & Gibala MJ. (2006). Effect of short-term sprint interval training on human skeletal muscle carbohydrate metabolism during exercise and time-trial performance. *J Appl Physiol* **100,** 2041-2047.

Burgomaster KA, Howarth KR, Phillips SM, Rakobowchuk M, Macdonald MJ, McGee SL & Gibala MJ. (2008). Similar metabolic adaptations during exercise after low volume sprint interval and traditional endurance training in humans. *The Journal of physiology* **586,** 151-160.

Burgomaster KA, Hughes SC, Heigenhauser GJ, Bradwell SN & Gibala MJ. (2005). Six sessions of sprint interval training increases muscle oxidative potential and cycle endurance capacity in humans. *Journal of applied physiology* **98,** 1985-1990.

Carroll TJ, Selvanayagam VS, Riek S & Semmler JG. (2011). Neural adaptations to strength training: moving beyond transcranial magnetic stimulation and reflex studies. *Acta physiologica* **202,** 119-140.

Cescon C & Gazzoni M. (2010). Short term bed-rest reduces conduction velocity of individual motor units in leg muscles. *Journal of electromyography and kinesiology : official journal of the International Society of Electrophysiological Kinesiology* **20,** 860-867.

De Luca CJ & Hostage EC. (2010). Relationship between firing rate and recruitment threshold of motoneurons in voluntary isometric contractions. *J Neurophysiol* **104,** 1034-1046.

Dideriksen JL & Farina D. (2013). Motor unit recruitment by size does not provide functional advantages for motor performance. *The Journal of physiology* **591,** 6139-6156.

Duchateau J, Semmler JG & Enoka RM. (2006). Training adaptations in the behavior of human motor units. *J Appl Physiol* **101,** 1766-1775.

Edwards L, Dixon J, Kent JR, Hodgson D & Whittaker VJ. (2008). Effect of shoe heel height on vastus medialis and vastus lateralis electromyographic activity during sit to stand. *Journal of orthopaedic surgery and research* **3,** 2.

Enoka RM. (2015). *Neuromechanics of human movement*. Human Kinetics, Champaign, IL.

Farina D, Fosci M & Merletti R. (2002). Motor unit recruitment strategies investigated by surface EMG variables. *Journal of applied physiology* **92,** 235-247.

Farina D, Holobar A, Merletti R & Enoka RM. (2010). Decoding the neural drive to muscles from the surface electromyogram. *Clinical neurophysiology : official journal of the International Federation of Clinical Neurophysiology* **121,** 1616-1623.

Farina D & Holobar A. (2016). Characterization of Human Motor Units From Surface EMG Decomposition. *P Ieee* **104,** 353-373.

Farina D, Merletti R & Enoka RM. (2004). The extraction of neural strategies from the surface EMG. *Journal of applied physiology* **96,** 1486-1495.

Farina D, Muhammad W, Fortunato E, Meste O, Merletti R & Rix H. (2001). Estimation of single motor unit conduction velocity from surface electromyogram signals detected with linear electrode arrays. *Medical & biological engineering & computing* **39,** 225-236.

Farina D & Negro F. (2015). Common synaptic input to motor neurons, motor unit synchronization, and force control. *Exercise and sport sciences reviews* **43,** 23-33.

Farina D, Negro F & Dideriksen JL. (2014). The effective neural drive to muscles is the common synaptic input to motor neurons. *The Journal of physiology* **592,** 3427-3441.

Farina D, Negro F, Gazzoni M & Enoka RM. (2008). Detecting the unique representation of motor-unit action potentials in the surface electromyogram. *Journal of neurophysiology* **100,** 1223-1233.

Folland JP & Williams AG. (2007). The adaptations to strength training : morphological and neurological contributions to increased strength. *Sports medicine* **37,** 145-168.

Garber CE, Blissmer B, Deschenes MR, Franklin BA, Lamonte MJ, Lee IM, Nieman DC, Swain DP & American College of Sports M. (2011). American College of Sports Medicine position stand. Quantity and quality of exercise for developing and maintaining cardiorespiratory, musculoskeletal, and neuromotor fitness in apparently healthy adults: guidance for prescribing exercise. *Medicine and science in sports and exercise* **43,** 1334-1359.

Gibala MJ & Little JP. (2010). Just HIT it! A time-efficient exercise strategy to improve muscle insulin sensitivity. *J Physiol* **588,** 3341-3342.

Gibala MJ, Little JP, Macdonald MJ & Hawley JA. (2012). Physiological adaptations to low-volume, high-intensity interval training in health and disease. *The Journal of physiology* **590,** 1077-1084.

Gibala MJ, Little JP, van Essen M, Wilkin GP, Burgomaster KA, Safdar A, Raha S & Tarnopolsky MA. (2006). Short-term sprint interval versus traditional endurance training: similar initial adaptations in human skeletal muscle and exercise performance. *The Journal of physiology* **575,** 901-911.

Hakkinen K & Komi PV. (1986). Training-induced changes in neuromuscular performance under voluntary and reflex conditions. *European journal of applied physiology and occupational physiology* **55,** 147-155.

Hawley JA. (2008). Specificity of training adaptation: time for a rethink? *The Journal of physiology* **586,** 1-2.

Heckman CJ & Enoka RM. (2012). Motor unit. *Comprehensive Physiology* **2,** 2629-2682.

Henneman E, Somjen G & Carpenter DO. (1965). Excitability and inhibitability of motoneurons of different sizes. *Journal of neurophysiology* **28,** 599-620.

Holobar A, Farina D, Gazzoni M, Merletti R & Zazula D. (2009). Estimating motor unit discharge patterns from high-density surface electromyogram. *Clinical neurophysiology : official journal of the International Federation of Clinical Neurophysiology* **120,** 551-562.

Holobar A, Minetto MA & Farina D. (2014). Accurate identification of motor unit discharge patterns from high-density surface EMG and validation with a novel signal-based performance metric. *Journal of neural engineering* **11,** 016008.

Holobar A & Zazula D. (2007). Multichannel blind source separation using convolution kernel compensation. *Ieee T Signal Proces* **55,** 4487-4496.

Hug F, Turpin NA, Guevel A & Dorel S. (2010). Is interindividual variability of EMG patterns in trained cyclists related to different muscle synergies? *Journal of applied physiology* **108,** 1727-1736.

Izquierdo M, Hakkinen K, Gonzalez-Badillo JJ, Ibanez J & Gorostiaga EM. (2002). Effects of long-term training specificity on maximal strength and power of the upper and lower extremities in athletes from different sports. *European journal of applied physiology* **87,** 264-271.

Kamen G & Knight CA. (2004). Training-related adaptations in motor unit discharge rate in young and older adults. *The journals of gerontology Series A, Biological sciences and medical sciences* **59,** 1334-1338.

Kleine BU, van Dijk JP, Lapatki BG, Zwarts MJ & Stegeman DF. (2007). Using two-dimensional spatial information in decomposition of surface EMG signals. *J Electromyogr Kinesiol* **17,** 535-548.

Little JP, Gillen JB, Percival ME, Safdar A, Tarnopolsky MA, Punthakee Z, Jung ME & Gibala MJ. (2011). Low-volume high-intensity interval training reduces hyperglycemia and increases muscle mitochondrial capacity in patients with type 2 diabetes. *Journal of applied physiology* **111,** 1554-1560.

Little JP, Safdar A, Wilkin GP, Tarnopolsky MA & Gibala MJ. (2010). A practical model of low-volume high-intensity interval training induces mitochondrial biogenesis in human skeletal muscle: potential mechanisms. *The Journal of physiology* **588,** 1011-1022.

Maathuis EM, Drenthen J, van Dijk JP, Visser GH & Blok JH. (2008). Motor unit tracking with high-density surface EMG. *Journal of electromyography and kinesiology : official journal of the International Society of Electrophysiological Kinesiology* **18,** 920-930.

McKay BR, Paterson DH & Kowalchuk JM. (2009). Effect of short-term high-intensity interval training vs. continuous training on O2 uptake kinetics, muscle deoxygenation, and exercise performance. *Journal of applied physiology* **107,** 128-138.

Merletti R & Farina D. (2009). Analysis of intramuscular electromyogram signals. *Philosophical transactions Series A, Mathematical, physical, and engineering sciences* **367,** 357-368.

Merletti R, Holobar A & Farina D. (2008). Analysis of motor units with high-density surface electromyography. *Journal of electromyography and kinesiology : official journal of the International Society of Electrophysiological Kinesiology* **18,** 879-890.

Milner-Brown HS, Stein RB & Yemm R. (1973). The orderly recruitment of human motor units during voluntary isometric contractions. *The Journal of physiology* **230,** 359-370.

Mirzabeigi E, Jordan C, Gronley JK, Rockowitz NL & Perry J. (1999). Isolation of the vastus medialis oblique muscle during exercise. *The American journal of sports medicine* **27,** 50-53.

Mohr M, Nann M, von Tscharner V, Eskofier B & Nigg BM. (2015). Task-Dependent Intermuscular Motor Unit Synchronization between Medial and Lateral Vastii Muscles during Dynamic and Isometric Squats. *PloS one* **10,** e0142048.

Moritz CT, Barry BK, Pascoe MA & Enoka RM. (2005). Discharge rate variability influences the variation in force fluctuations across the working range of a hand muscle. *Journal of neurophysiology* **93,** 2449-2459.

Morrissey MC, Harman EA & Johnson MJ. (1995). Resistance training modes: specificity and effectiveness. *Medicine and science in sports and exercise* **27,** 648-660.

Negro F, Holobar A & Farina D. (2009). Fluctuations in isometric muscle force can be described by one linear projection of low-frequency components of motor unit discharge rates. *The Journal of physiology* **587,** 5925-5938.

Negro F, Muceli S, Castronovo AM, Holobar A & Farina D. (2016a). Multi-channel intramuscular and surface EMG decomposition by convolutive blind source separation. *Journal of neural engineering* **13,** 026027.

Negro F, Yavuz US & Farina D. (2016b). The human motor neuron pools receive a dominant slow-varying common synaptic input. *The Journal of physiology*.

Patten C, Kamen G & Rowland DM. (2001). Adaptations in maximal motor unit discharge rate to strength training in young and older adults. *Muscle & nerve* **24,** 542-550.

Pedersen BK & Saltin B. (2006). Evidence for prescribing exercise as therapy in chronic disease. *Scandinavian journal of medicine & science in sports* **16 Suppl 1,** 3-63.

Penzer F, Cabrol A, Baudry S & Duchateau J. (2016). Comparison of muscle activity and tissue oxygenation during strength training protocols that differ by their organisation, rest interval between sets, and volume. *European journal of applied physiology*.

Pucci AR, Griffin L & Cafarelli E. (2006). Maximal motor unit firing rates during isometric resistance training in men. *Experimental physiology* **91,** 171-178.

Rakobowchuk M, Tanguay S, Burgomaster KA, Howarth KR, Gibala MJ & MacDonald MJ. (2008). Sprint interval and traditional endurance training induce similar improvements in peripheral arterial stiffness and flow-mediated dilation in healthy humans. *American journal of physiology Regulatory, integrative and comparative physiology* **295,** R236-242.

Rich C & Cafarelli E. (2000). Submaximal motor unit firing rates after 8 wk of isometric resistance training. *Medicine and science in sports and exercise* **32,** 190-196.

Semmler JG, Sale MV, Meyer FG & Nordstrom MA. (2004). Motor-unit coherence and its relation with synchrony are influenced by training. *Journal of neurophysiology* **92,** 3320-3331.

Sherrington C. (1925). Remarks on some aspects of reflex inhibition *Proc R Soc Lond B Biol Sci***,** 19-45.

Slater LV & Hart JM. (2016). Muscle Activation Patterns During Different Squat Techniques. *Journal of strength and conditioning research / National Strength & Conditioning Association*.

Van Cutsem M, Duchateau J & Hainaut K. (1998). Changes in single motor unit behaviour contribute to the increase in contraction speed after dynamic training in humans. *The Journal of physiology* **513 (Pt 1),** 295-305.

Vila-Cha C & Falla D. (2016). Strength training, but not endurance training, reduces motor unit discharge rate variability. *Journal of electromyography and kinesiology : official journal of the International Society of Electrophysiological Kinesiology* **26,** 88-93.

Vila-Cha C, Falla D, Correia MV & Farina D. (2012). Adjustments in motor unit properties during fatiguing contractions after training. *Medicine and science in sports and exercise* **44,** 616-624.

Vila-Cha C, Falla D & Farina D. (2010). Motor unit behavior during submaximal contractions following six weeks of either endurance or strength training. *Journal of applied physiology* **109,** 1455-1466.

Wakeling JM & Horn T. (2009). Neuromechanics of muscle synergies during cycling. *Journal of neurophysiology* **101,** 843-854.

Author's contribution

The present thesis is designed as a cumulative dissertation. In this regard, four scientific articles have been prepared and submitted to peer-reviewed journals. Study 1 and study 4 have been already accepted and published, while studies 2 and 3 are currently in revision. According to the local doctoral degree regulations (§ 7 (4), sentence No. 2), significant contributions to the articles from the respective co-authors were acknowledged and finally confirmed by each co-author.

Name	Code	Affiliation	Signature
Dario Farina	DF	University of Göttingen	
Deborah L. Falla	DLF	University of Göttingen; University of Birmingham	
Christopher Laine	CL	University of Göttingen	
Francesco Negro	FN	University of Göttingen	
Frank Mayer	FM	University of Potsdam	
Eduardo Martinez-Valdes	EMV	University of Potsdam	

Study	Design	Data collection	Data analyses	Interpretation	Manuscript
Chap. 4.1.	**EMV**, CL, DLF, FM, DF	**EMV**, CL	**EMV**, CL	**EMV**, CL, DLF, FM, DF	**EMV**, CL, DLF, DF
Chap. 4.2.	**EMV**, CL, FN, DLF, FM, DF	**EMV**, CL	**EMV**, FN	**EMV**, FN, DF	**EMV**, FN, CL, DLF, FM, DF
Chap. 4.3.	**EMV**, DLF, FM, DF	**EMV**	**EMV,** FN	**EMV**, DLF, FN, FM	**EMV**, DLF, DF
Chap. 4.4.	EMV, **CL** DLF, FM, DF	EMV, **CL**	**CL**, EMV	**CL**, DF, EMV	**CL**, DF, EMV, DLF

First author is highlighted in bold

Appendix

List of figures

List of tables

Abbreviations

ANOVA: analysis of variance
ARV: average rectified value
BF: biceps femoris muscle
CKC: convolution kernel compensation
CNS: central nervous system
CoV: coefficient of variation
CoVisi: coefficient of variation for the inter-spike interval
EMG: electromyography
END: endurance training
ES: effect size
HDEMG: high-density surface electromyography
HIIT: high-intensity interval training
HR_{max}: maximum heart rate
ICC: intra-class correlation coefficient
ISI: inter-spike interval
MUAP: motor unit action potential
MVC: maximum voluntary contraction
$PETCO_2$: end-tidal pressure of carbon dioxide
$PETO_2$: end-tidal pressure of oxygen
PNR: pulse-to-noise ratio
PPS: pulses per second
p2p: peak to peak
RFD: rate of force development
SEM: standard error of the measurement
SIL: silhouette
V_E/VO_2: ventilatory equivalent of oxygen
V_E/VCO_2: ventilatory equivalent of carbon dioxide
VO_{2peak}: peak oxygen uptake
VL: vastus lateralis muscle
VM: vastus medialis muscle
VT1: first ventilatory threshold
VT2: second ventilatory threshold
W: watts
η_p^2: partial eta squared